

Cerebral Metabolism of Ethanol-Derived Acetate: A Metabolic Basis for Dependence?

by
Peter C. Nicholas

A dissertation submitted to the faculty of the University of North Carolina at Chapel Hill in partial fulfillment of the requirements for the degree of Doctor of Philosophy in the Department of Biomedical Engineering.

Chapel Hill
2006

Approved by:

Jeffrey M. Macdonald, Ph.D., Advisor

Fulton T. Crews, Ph.D., Reader

Thomas M. O'Connell, Ph.D., Committee Member

Carol N. Lucas, Ph.D., Committee Member

Oleg Favorov, Ph.D., Committee Member

© 2006
Peter C. Nicholas
ALL RIGHTS RESERVED

ABSTRACT

**PETER C. NICHOLAS: Cerebral Metabolism of Ethanol-Derived Acetate:
A Metabolic Basis for Dependence?.**
(Under the direction of Jeffrey M. Macdonald, Ph.D..)

Alcoholism is a tremendous health problem throughout the world. Ethanol is a unique drug that is consumed in large quantities for pharmacologic effect, reaching blood concentrations as high as 100mM. Ethanol is eliminated almost exclusively via oxidation to acetate in the liver, and nearly all of the ethanol-derived acetate is released into the blood where it travels to other organs, including the brain, for use as an energy source. Thus ethanol directly alters metabolism in the liver, and causes the production of large amounts of acetate which may serve as a substrate for brain, possibly contributing to intoxication and dependence.

This dissertation describes two separate approaches to study the metabolic effects of ethanol. First, ^1H NMR-based metabolomic analysis of endogenous metabolites revealed decreased lactate and alanine, and increased acetate and ketone bodies due to ethanol. These results provided new insights regarding the effect of ethanol on gluconeogenesis. In addition, we determined that ethyl glucuronide (EtG), a unique metabolite of ethanol, produces a characteristic NMR signal. EtG is formed within hours of ethanol dosing, and remains elevated during a 4 day binge exposure. The antioxidant BHT appears to reduce formation of EtG during a 4 day exposure to ethanol.

Our second approach used ^{13}C -enriched tracers along with ^{13}C NMR to measure brain metabolism of ethanol-derived acetate. Our hypothesis was that cerebral metabolism of acetate released from the liver during ethanol oxidation perturbs cerebral metabolism, and thereby contributes to neuroadaptation associated with alcohol dependence and withdrawal. Using a single dose of $[2\text{-}^{13}\text{C}]$ ethanol intragastrically, we found carbons derived from ethanol are rapidly incorporated into brain amino acids glutamate, glutamine, and GABA. Next, we investigated whether a 10 day exposure to ethanol would increase cerebral utilization of acetate. We found that acetate metabolism was not increased, most likely because transport into brain astrocytes was not increased. We did find, however, that ethanol induced significant changes in metabolism of GABA, and we speculate that this may reflect neuroadaptations that produce tolerance to ethanol.

ACKNOWLEDGMENTS

To the extent that this project was successful, I have numerous people to thank. I would like to begin by acknowledging my parents Joan and Peter Nicholas. From them I learned a sense of wonder at the miracles of the world we inhabit, to strive for excellence in every undertaking, and to trust in my own judgment and follow my own path. Without their sacrifices and support, this project would have been impossible. Next I would like to thank all scientific mentors I have had throughout my career, in particular Protik (Tiku) Majumder, David Fushman, and David Cowburn. I rely so heavily upon the lessons, advice, and day-to-day tricks I learned from them that I could hardly function without them. I wish to thank the UNC MD-PhD program, and in particular Dr. Eugene Orringer and Dr. Gil White for sage advice and unwavering support throughout my graduate experience. Thanks are also due to the UNC Bowles Center for Alcohol Studies, in particular Sharon Owens for administrative help, and Melissa Mann for help submitting manuscripts. Thanks to my friends and fellow students for advice and companionship during this arduous journey. In particular my brother, Matthew, provided insightful advice at all stages of this work, an ear to bend when things looked bleak, and even last-minute technical advice on typesetting this document. Thanks kiddo!

With regard to specific contributions, I gratefully acknowledge the skillful assistance of Daniel Kim for all of the animal work required in this project. In addition, I gratefully acknowledge Michael Gamcsik for his generosity with his time, expertise, and equipment that made HPLC analysis possible.

I would like to thank my co-mentors, Jeffrey Macdonald and Fulton Crews, each of whom took a bit of a risk in agreeing to work with me on this collaborative project that was on the outskirts of everyone's expertise. Jeff is one of the most generous people I have ever known, his knowledge of intermediary metabolism is phenomenal, and his enthusiasm for both lofty experimental goals as well as minute details was a tremendous asset. Dr Crews taught me many valuable lessons, perhaps the most important of which is that one should aim to optimize methods while making biological

discoveries, lest the project become a study of the instrument alone. He offered a wonderful combination of healthy skepticism, open-mindedness, timely and insightful advice, and candid assessments on every topic we discussed. Without the support of these two people, this work could not have happened. I also would like to acknowledge the contributions of the other members of my dissertation committee: Carol Lucas for advice on mathematical modeling, Oleg Favorov for input about statistical classification methods and his shared interest in astrocyte biology, Tom O’Connell for input on all things NMR.

Finally, and most of all, I would like to my wife Matilda. Without your help and encouragement, I would never even have started this project. A wise man once said that the only thing worse than being a graduate student is to be married to one; I thank you most of all for your patience throughout this process. I admire your organized and efficient nature, and maybe someday, when I have my robot army doing my experiments, I’ll be able to follow your example.

Contents

List of Figures	x
List of Tables	xii
1 Introduction and Background	1
1.1 Metabolomics	2
1.1.1 Analytical Methods for Metabolomics	3
1.1.2 Analytical Methods for Metabolomics: NMR	3
1.1.3 Analytical Methods for Metabolomics: MS	6
1.1.4 Multivariate Statistical Methods for Metabolomics	7
1.1.5 Metabolomics: Challenges	8
1.1.6 Beyond metabolomics: Fluxomics	9
1.2 ^{13}C NMR as a Biological Tool	10
1.3 Astrocyte biology	11
1.3.1 Astrocyte Morphology and Ultrastructure	11
1.3.2 Astrocyte Excitation and Ion Homestasis	13
1.3.3 Astrocyte-Neuron Interactions	14
1.3.4 Roles of Astrocytes in Behavior and Integrated Physiology of the Organism	17
1.4 Alcohol abuse and alcoholism	19
1.5 Ethanol Metabolism and Biodistribution	19
1.6 The Effect of Ethanol on Energy Metabolism	22
1.7 EtOH and brain	23
1.7.1 Ethanol Dependence and Withdrawal	24
1.7.2 Altered astrocyte function: A Potential Biochemical Basis for Dependence and Craving	25
1.7.3 Ethanol & Cerebral Metabolism: Availability of Acetate During Intoxication	26

1.7.4	Ethanol & Cerebral Metabolism: Cerebral Utilization of Acetate	27
1.8	Outline of Dissertation	28
1.8.1	Metabolomic Studies	28
1.8.2	^{13}C NMR Analysis of Brain Metabolism	28
2	Proton NMR Spectroscopic Determination of Ethanol-Induced Formation of Ethyl Glucuronide in Liver	29
2.1	Abstract	29
2.2	Introduction	30
2.3	Materials and Methods	31
2.3.1	Animals	31
2.3.2	Tissue Extraction and Sample Preparation	31
2.3.3	Enzymatic hydrolysis	31
2.3.4	NMR spectroscopy	32
2.3.5	EtG Standard	33
2.4	Results and Discussion	33
2.5	Acknowledgments	40
3	Integrated Multi-organ Analysis of the Effect of Ethanol on Liver, Brain and Serum Metabolites	41
3.1	Introduction	41
3.2	Methods and Materials	42
3.2.1	Animal Handling Procedures and Sample Collection	42
3.2.2	^1H NMR Spectroscopic Analysis	43
3.2.3	Data Reduction and Principle Components Analysis	44
3.2.4	Statistical Analysis	45
3.2.5	Biochemical Interpretation	45
3.3	Results	46
3.3.1	^1H Spectroscopic Analysis of Serum	46
3.3.2	^1H Spectroscopic Analysis of Liver	46
3.3.3	^1H Spectroscopic Analysis of Brain	52
3.3.4	PC Analysis of Liver NMR spectra	52
3.3.5	PC Analysis of Serum NMR Spectra	57
3.3.6	PC Analysis of Brain NMR Spectra	59
3.4	Discussion	59
3.4.1	Energy Metabolites in Liver and Serum	59

3.4.2	Energy Metabolites in Brain	63
3.4.3	Betaine Metabolism and Transmethylation	64
3.4.4	Brain Metabolites	64
3.4.5	Ethyl Glucuronide	65
3.4.6	PC Analysis	66
3.4.7	Conclusion	66
4	Cerebral Metabolism of Ethanol-Derived Acetate: A Metabolic Basis for Dependence?	68
4.1	Introduction	68
4.2	Methods	72
4.2.1	Chemicals	72
4.2.2	Animal Procedures	72
4.2.3	Tissue extraction	74
4.2.4	NMR and HPLC sample preparation	74
4.2.5	NMR spectroscopy	75
4.2.6	NMR spectral processing	75
4.2.7	HPLC analysis	76
4.2.8	Calculation of Fractional Enrichment from ^{13}C NMR data . . .	76
4.2.9	Calculation of Fractional Enrichment from ^1H NMR data	77
4.2.10	Model of Cerebral Metabolism and analysis	77
4.2.11	Statistical analysis	78
4.3	Results & Discussion	78
4.3.1	Animals and tissue extraction	78
4.3.2	Serum: availability of ^{13}C -acetate for brain metabolism	78
4.3.3	Serum: assessment of ^{13}C -labeling in molecules other than acetate	81
4.3.4	Brain Fractional Enrichment: Acetate and other potential sub- strates	83
4.3.5	Fractional Enrichment of Brain Amino Acids	84
4.3.6	Unequal labeling of Glutamine C2 and C3	90
4.3.7	Steady-state analysis	92
4.4	Conclusion	92
5	Conclusions and Future Directions	95
5.1	Future Studies on Ethanol and Pyruvate Metabolism in Liver	95
5.2	Future Studies of Ethanol-Induced Formation of Ethyl Glucuronide . .	96

5.3	Future Studies on Cerebral Metabolism of Ethanol-Derived Acetate . .	97
5.4	Cerebral Utilization of Glucose	97
5.5	Ethanol-GABA Interactions	99
5.6	The Future of Metabolomics	100
A	NMR Essentials	103
A.1	History of NMR	103
A.2	NMR as a spectroscopic method	104
A.3	Physics of Magnetic Resonance	105
A.3.1	Nuclear Spin and Nuclear Magnetism	105
A.3.2	Equation of Motion	105
A.3.3	Equilibrium Magnetization	106
A.3.4	Relaxation	107
A.4	Modern NMR methods	107
A.4.1	The Spectrometer	107
A.4.2	NMR processing	108
B	Essentials of Metabolism	109
B.1	Overview of the TCA cycle	109
B.2	Metabolite Structures	109
C	Mathematical description of principal components analysis	113
C.1	Covariance and the covariance matrix	113
	Bibliography	115

List of Figures

1.1	^1H Spectrum of Liver extract	4
1.2	Intepreting metabolomic data	9
1.3	Astrocytes Provide Metabolic Support for Neurons	15
1.4	Ethanol ingestion, absorption, and biodistribution	20
1.5	Significant routes for hepatic ethanol oxidation	21
1.6	Ethanol-Induced Lipogenesis	23
2.1	700MHz ^1H spectra of ethyl glucuronide in liver extracts.	32
2.2	Enzymatic hydrolysis of ethyl glucuronide by β -glucuronidase.	33
2.3	Control spectra for enzymatic hydrolysis of ethyl glucuronide	34
2.4	Control spectra for enzymatic hydrolysis of ethyl glucuronide	36
2.5	Identification of Signal from the EtG Anomeric Proton	37
2.6	Effect of Enzymatic Hydrolysis on Putative EtG Signals	38
2.7	Spectrum of EtG with assignments	39
3.1	700MHz proton spectra of serum	47
3.2	Effect of Ethanol on Serum Metabolites	48
3.3	700MHz ^1H Spectra of Liver Extracts	49
3.4	Effect of Ethanol on Selected Liver Metabolites	51
3.5	Quantification of Ethyl-Glucuronide in Liver	52
3.6	Assignment of Betaine and TMAO in ^1H NMR Spectra of Liver Extracts	53
3.7	Effect of BHT and Ethanol on Betaine Concentration in Liver	53

3.8	700MHz ^1H Spectra of Brain Extracts	54
3.9	PC Analysis of Binge and Single-Dose Liver ^1H NMR Data	55
3.10	PC Analysis of Binge and Single-Dose Livers Separately	56
3.11	PC Analysis of Serum and Brain NMR Data	58
3.12	Mechanism for Ethanol-Induced Perturbation of Liver Metabolism . . .	60
4.1	Model of ^{13}C -acetate metabolism in brain	70
4.2	Experimental Design: Acute Versus Chronic Ethanol Groups	73
4.3	700MHz ^1H Spectra of Serum After Dosing with ^{13}C Ethanol	79
4.4	Confirming glucose ^{13}C satellite peaks in 700MHz ^1H spectra	82
4.5	400MHz ^1H Spectra of Brain Extracts	86
4.6	100MHz ^1H -decoupled ^{13}C Spectra of Brain Extracts	87
5.1	Comparing Flux via PC and PDH Using 2- ^{13}C Glucose	98
5.2	Expected Results of the 2- ^{13}C Glucose Study	98
A.1	Precession in a magnetic field	106
B.1	TCA cycle	110

List of Tables

1.1	Subtypes of astrocytes in the mouse hippocampus	12
2.1	Assignment of the EtG Proton Spectrum	38
4.1	Serum Concentrations and Enrichments	80
4.2	Concentration and FE of lactate and acetate in brain	85
4.3	Brain ^{13}C FE of amino acids	89
4.4	^{13}C labeling ratios in brain amino acids	90
A.1	Spectroscopy modalities	104
A.2	NMR isotopes	105
B.1	Metabolite structures	112

Chapter 1

Introduction and Background

As befits a dissertation in Biomedical Engineering, the studies described herein involve the application of knowledge and techniques from the fields of physics, engineering, chemistry, biochemistry, and biology. While it is beyond the scope of this work to provide a complete account of all relevant aspects of these fields, the intent of this introductory chapter is to provide an overview of the methods employed, a review of the current literature, and the rationale for the work that is detailed in later chapters. Before embarking on this task, however, a few words about the disease of alcoholism are in order.

Alcoholism is a disease that produces enormous harm to both individual health and society as a whole. Ethyl alcohol (ethanol, abbreviated EtOH) is a unique drug that is (i) ubiquitous, (ii) legal to consume in most places, (iii) ingested in large quantities compared to other pharmacologic agents, and therefore, (iv) metabolized to acetate in the liver, producing sustained millimolar blood levels of this direct metabolite, (v) capable of damaging multiple organs, including liver and brain. Due to (iii) and (iv), it was natural to inquire about possible metabolic mechanisms for organ toxicity and alcohol addiction, leading to our initial metabolomic studies. Upon closer examination of the literature, a hypothesis involving brain metabolism of ethanol-derived acetate presented itself as an attractive problem for study. Using carbon-13 ethanol as a metabolic tracer, we monitored the brain's metabolism of ethanol-derived acetate and studied the effect of chronic ethanol ingestion on this process.

With these goals in mind, we turn to a description of NMR-based metabolomics.

1.1 Metabolomics

The emerging field of metabolomics represents an exciting new set of methods for the characterization of biochemical systems and their response to environmental factors such as diet and exposure to toxins. The approach involves quantification of small molecules, coupled with various pattern recognition methods to extract meaningful information from the large data sets. (The complement of small molecules within an organism is termed 'the metabolome', hence the name metabolomics.) The goal is to collect a relevant sample from the organism under study, obtain a 'metabolic fingerprint' using techniques from analytical chemistry, and to apply multivariate statistical techniques to large numbers of samples (Nicholson et al., 1999). The many potential applications of this technique include: (i) identification of inexpensive and non-invasive diagnostic tests for various diseases, (ii) diagnosis of individuals likely to metabolize medications differently than the population average, and (iii) in basic science studies, corroboration of genomic and proteomic data with measurements of endogenous metabolites that are substrates for the genes in question.

Perhaps the strongest argument in favor of the metabolomic approach to diagnosis or classification of individuals, as opposed to the search for individual 'biomarkers' (i.e. single molecules that are believed to be specific indicators of a particular disease or phenotype) is that unique molecules are rarely present at the stage in which a disease is preventable. For example, assays for Creatine Kinase Mb (CKMB) and cardiac isoforms of certain other enzymes are extremely powerful diagnostic tools for heart attacks, but only after one has occurred. There is presently no satisfactory biomarker for coronary artery disease. Cholesterol levels and blood pressure have some predictive power, but not enough to enable physicians to focus their efforts on preventing heart attacks in those patients in which they are imminent. Thus, patients with suggestive symptoms are referred for expensive and invasive tests in the form of cardiac catheterization. All the while, it is reasonable to hypothesize that biochemical differences exist between people who will eventually develop coronary artery disease and those who will remain healthy.

Taking a different approach to the problem, Brindle et al. analyzed blood plasma from patients undergoing cardiac catheterization. The investigators collected proton NMR spectra of the plasma and used a supervised classification method to construct a predictive model that enabled them to determine with impressive accuracy the presence and severity of coronary artery occlusion based only on analysis of a blood sample.

While there may be significant questions regarding the details of their methods (see §5.6), the results of this study illustrate the power of a metabolomic approach to predict the presence of a disease based on pattern recognition of the metabolic fingerprint, where no single "biomarker" is available.

With this tantalizing success in mind, we now delve into the details of the technique.

1.1.1 Analytical Methods for Metabolomics

Before discussing individual methods, it is useful to describe the attributes of an ideal metabolomic measurement technique. First, the technique would be quantitative, providing reliable, independent measurements of all metabolites in a sample. Preferably, the technique would allow simultaneous measurement of endogenous molecules and exogenous tracers (e.g. isotopes) to facilitate studies of metabolic flux. In addition, the technique would be capable of analyzing samples at a rate of one every few minutes or less, and would provide unambiguous data for which any post-processing would be entirely automated so that full human effort could be devoted to interpretation of results, rather than the generation of results from raw data. As we will see, the methods presently available are far from ideal, but each offers certain advantages and drawbacks.

1.1.2 Analytical Methods for Metabolomics: NMR

Nuclear magnetic resonance (NMR) spectroscopy is the preeminent tool for chemical structure elucidation. Though it has a lower sensitivity to detection than techniques such as mass spectrometry (MS) or liquid chromatography (LC), NMR spectroscopy (NMRS) has several key advantages for quantitative analysis in metabolomics, most notably its large dynamic range and minimal requirements for sample preparation.

In order to maintain the focus of this introductory chapter on the application of NMRS as a tool for the study of ethanol metabolism and brain function, a brief review of NMR physics, instrumentation, and associated issues is presented in Appendix A. Instead, this section presents some examples of the use of NMRS in metabolomics.

The first example is a 700MHz proton spectrum of an extract from rat liver tissue (Fig. 1.1A). The second panel (B) shows an expanded view of the relatively uncongested region between δ 0.9-2.0 ppm. Signals from several metabolites are clearly resolved, and the high signal-to-noise ratio of this data is evident. Signals are assigned on the basis of chemical shift (frequency), multiplicity and coupling constant. The integrated intensity of each signal is directly proportional to concentration. Thus, in

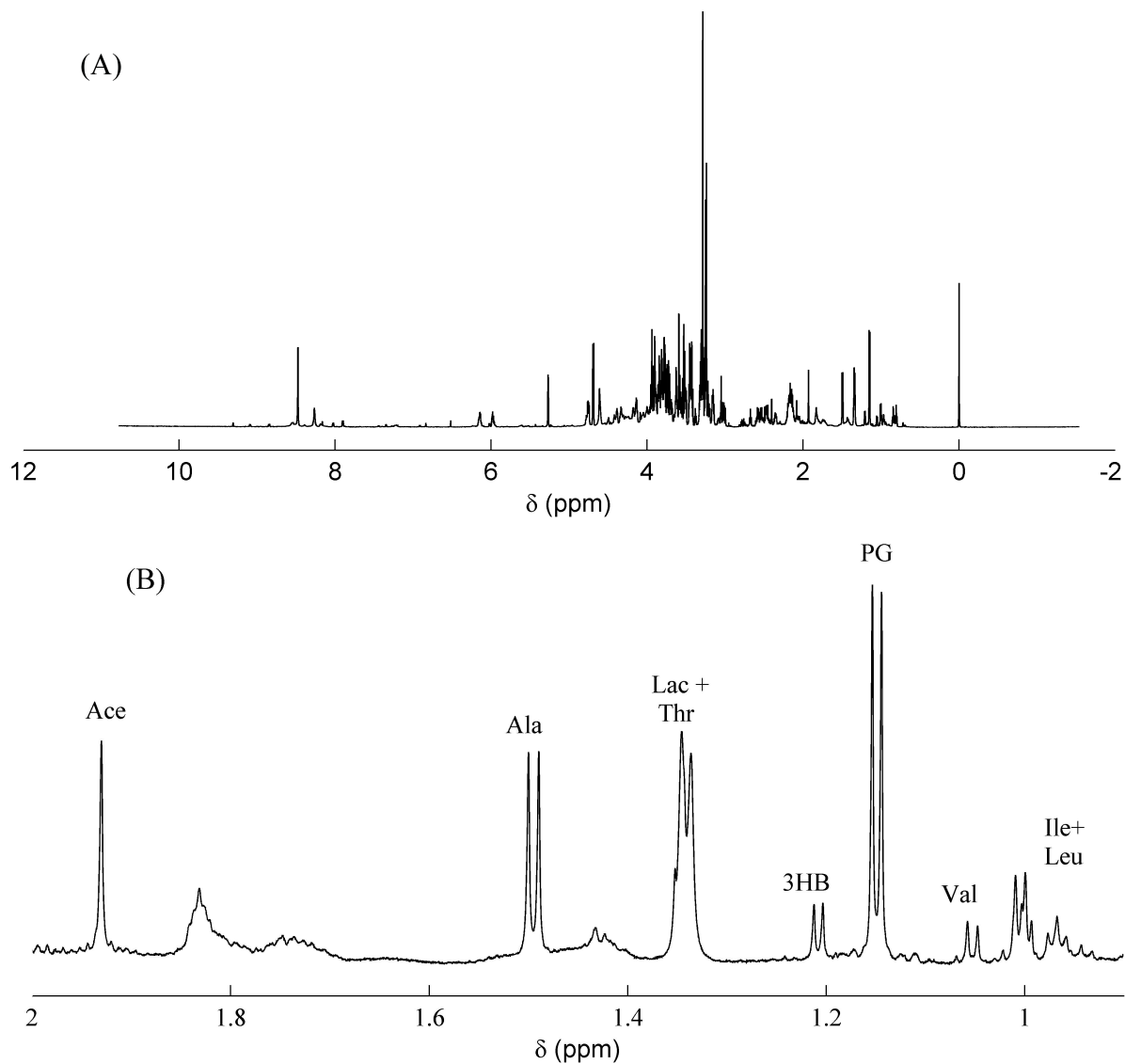


Figure 1.1: 700MHz proton spectrum of perchloric acid extract of liver. The lower panel (B) shows an expanded view of the signals from the methyl protons of several metabolites. Abbreviations: Ace, acetate; Ala, alanine, 3HB, beta-hydroxybutyrate; Ile, isoleucine; Leu, leucine; PG, propylene glycol; Thr, threonine; Val, Valine. Chemical structures for these molecules can be found in Appendix B.

theory, we can observe and quantify signals from every proton-containing molecule that was present in this animal's liver.

In practice, two issues limit our ability to quantify certain compounds: sensitivity and resolution/overlap. Using the most sensitive NMR spectrometer on campus at the present time, a 700MHz Varian Inova system with a cold probe installed, the detection threshold in a tissue extract is on the order of tens of μmol per kg tissue, depending on the number of chemically equivalent protons attached. (More protons produce greater signal, thus enabling the detection of smaller amounts of material.) However, to determine a 50% reduction in this compound with confidence, its basal level might need to be somewhat greater. Thus compounds that are present at very low concentrations will go undetected in NMR analysis using current methods.

A number of approaches could lower the detection threshold. If the signal of interest is large enough to be digitized, averaging more data will (eventually) yield adequate signal-to-noise for quantification. If solubility of the compounds is not limiting, samples may be pooled, and lyophilized extracts may be dissolved in smaller volumes of liquid and analyzed in special NMR tubes, thus increasing the concentration perhaps 2-10 fold. Removing salts from the sample might improve the ability to tune the cold probe, thus increasing the signal. However, even with great effort, the detection threshold will remain in the hundreds of nM range. If molecules at this concentration are of interest, one might consider concentrating the sample or isolating target molecules, but it might be sensible to select a different technique.

The problem of spectral overlap is even more vexing than low sensitivity, because it limits the quantification of compounds that are abundant enough to generate NMR signals. Even if a compound is present at millimolar concentrations, if its NMR signals overlap with those of other molecules, identification and unique quantification become difficult, or, in many cases, impossible. (In other words, if A and B overlap, it is possible to measure the sum A+B, but neither A nor B individually.)

Two methods can overcome the problem of overlapping NMR signals: (i) increase the spectral resolution by using a higher field spectrometer, or (ii) decrease the width of the signals by collapsing multiplets using a pulse sequence designed for this purpose (e.g. (Viant, 2003)). On the other hand, as we will see, it is sometimes possible to classify individuals based on pattern recognition techniques that treat spectra as abstract multivariate data without any knowledge of the underlying biochemical changes that produce differences in spectra between groups. Though this approach sometimes prevents insight into mechanisms responsible for disease, the ability to aid in certain di-

agnoses may be extremely valuable even in the absence of a mechanistic understanding of the processes that lead to disease.

As mentioned above, NMR spectroscopy offers impressive dynamic range. Modern spectrometers boast 20-bit ($2^{20} \sim 10^6$) effective dynamic range, with full linearity of response over this entire range. This figure applies to 'raw' metabolomic samples such as blood (serum and plasma) and urine. As we will see, the same is not true for mass spectrometry.

1.1.3 Analytical Methods for Metabolomics: MS

Mass spectrometry (MS), like NMR, is a mature analytical technique that has recently been applied to metabolomics. To be more precise, a family of hyphenated techniques such as gas chromatography (GC-MS), liquid chromatography (LC-MS), and others have been applied. In its most basic form, a mass spectrometer ionizes a sample, accelerates the charged particles, and measures the mass/charge (m/z) ratio for the ions. By measuring the mass of the parent ion precisely, the empirical formula can be inferred. Thus, we come to the first limitation of MS: it cannot easily distinguish between chemical isomers (Sumner et al., 2003). NMRS is inherently sensitive to chemical structure and therefore can distinguish many isomers easily. In addition, the ability of ^{13}C NMR spectroscopy to determine enrichment of each individual carbon atom within a given molecule provides a powerful tool for the analysis of metabolic flux. The great advantage of MS over NMR is the high sensitivity. Under ideal conditions, LC-MS and GC-MS can measure pico-molar (10^{-12}M), and femto-molar (10^{-15}M) concentrations, respectively – 10^6 to 10^9 times lower than NMR can measure. So why would one choose to use NMR? One answer lies in the phrase "under ideal conditions". Typical metabolomic samples are far from ideal: they contain many classes of molecules (proteins, lipids, glycoproteins, amino acids, sugars, nucleotides, etc.) in concentrations ranging from tens of millimolar down to a few molecules per mL. In order to make use of sensitivity that enables detection down to 10^{-15}M in a sample that contains some molecules at 10^{-2}M , a dynamic range of 10^{13} is required. In practice, the dynamic range of MS is closer to 10^2 - 10^4 , depending on the technique. The solution to this problem involves on the one hand extraction, dilution, derivatization and other forms of sample preparation, and on the other hand chromatographic separation to reduce the amount of material being exposed to the detector at any time. These techniques notwithstanding, issues such as differential ionization potential and competition or in-

teraction between various metabolites in a single sample create a situation in which it is very difficult to obtain quantitative data for a large set of samples.

Another reason to advocate the use of NMR rests on philosophical grounds: first, one might argue that if we want to understand metabolism, we need to accurately quantify all of the most abundant metabolites before delving into the analysis of femtomolar trace components. Second, the more manipulation of the sample before analysis, the greater the odds of introducing artifacts into the measurements. NMR is capable of analyzing any biofluid or tissue sample directly, or, more commonly, after adding 10-30% volume of D₂O for field lock. Thus, at the very least, we would argue, NMR data should be the first step in metabolomic analysis, with possible supplementation by MS data for those metabolites below the NMR detection limit. Recently Crockford et al. proposed a mathematical framework for integrating information obtained from the MS and NMR data (Crockford et al., 2006), and this complimentary use of the two techniques appears to be a very promising approach.

1.1.4 Multivariate Statistical Methods for Metabolomics

Having discussed the techniques used to acquire metabolomic data sets, we now turn our attention to the statistical analysis of that data. While many methods are available, principal components analysis (PC analysis, or PCA) has been used successfully in a number of NMR-based metabolomic studies. PCA is a simple and elegant method for reducing the dimensionality of multivariate data. Intuitively, the data for each subject can be envisioned as a single point in a multidimensional vector space, where the components of the vector are the measurements on that subject (e.g. concentrations of various metabolites). When data have been collected for many subjects, if there are differences in the metabolites between diseased and healthy individuals, then the points will cluster into different groups in this multidimensional space. Principal components analysis represents a basis transformation in which new basis vectors ("principal components") are constructed so that the first one lies along the direction of greatest variance in the data, the second is orthogonal to the first and lies in the direction of the most remaining variance, and so forth. Typically, the first several principal components (PCs) describe on the order of 90% of the total variance in a metabolomic data set. Provided that within a given data set the greatest source of variance is the metabolic perturbation between experimental groups and controls, plotting the data projected onto the new PCs very often allows 200-dimensional data to be visualized

in two or three dimensions, with clear separation of different groups. Moreover, the largest components of the first few PC vectors, by definition, are the elements of the data that explain the difference between groups. Thus PCA is simultaneously a tool for visualization as well as identification of the biochemical differences between groups. On the other hand, if plotting data projected onto the first few PCs does not show appreciable clustering of different groups, this result indicates that the largest source of variance within the data is not due to detectable biochemical differences between the groups. (Here the word "detectable" refers to the capabilities of the analytical method(s) selected.) If intra-group variance exceeds the between-group variance (i.e. the controls are more heterogeneous than any differences between the experimental group and controls), one must consider whether a meaningful biochemical difference exists, or if the null hypothesis may be correct. In the case that there is good reason to reject the null hypothesis, some of the methods named in the following section may be of use in focusing the analysis on whatever differences do exist between the control and experimental groups.

A mathematical description of PCA may be found in Appendix C.

Other techniques

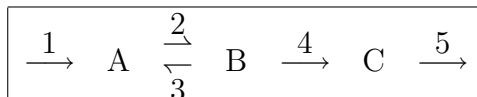
A detailed review of statistical methods for analysis of metabolomic data is beyond the scope of this dissertation. For completeness, the following alternative procedures deserve mention: partial least squares discriminant analysis (PLS-DA) (which is often used in conjunction with orthogonal signal correction (OSC) (Gavaghan et al., 2002)), and support vector machines (Joachims, 2002).

1.1.5 Metabolomics: Challenges

Generic Challenges

Though it is by no means unique to NMR-based metabolomics, the inability to quantify all constituents of the metabolome represents a serious stumbling block for the field. In general, measurement of the concentration of a small number of metabolite pools provides enough data for speculation, but not enough to draw conclusions. A trivial example serves to illustrate the point (Fig. 1.2).

In a pathway consisting of three metabolites, A, B, and C, if a metabolic perturbation increases B, decreases C, and leaves A unchanged, one can conclude that decreased flux through the pathway catalyzed by protein 4 is the most straightforward



Group	A	B	C	Conclusion
Normal	\leftrightarrow	\leftrightarrow	\leftrightarrow	normal
Experiment 1	\leftrightarrow	\uparrow	\downarrow	\downarrow 4
Experiment 2	N.D.	\uparrow	\downarrow	\downarrow 4
Experiment 3	N.D.	\uparrow	N.D.	\downarrow 4,5,3; \uparrow 1,2
Experiment 4	N.D.	N.D.	\downarrow	\downarrow 1,2,4; \uparrow 3,5
Experiment 5	\leftrightarrow	\uparrow	N.D.	\downarrow 4,5
Experiment 6	\leftrightarrow	N.D.	N.D.	normal

Figure 1.2: Difficulties of interpreting incomplete metabolomic data in a simple pathway with three metabolites A,B,C, and five fluxes catalyzed by proteins 1-5. N.D., indicates that the concentration was not determined in a given experiment. When all concentration data are available, the correct conclusion is self-evident (experiment 1). When data are missing, sometimes the correct interpretation can still be reached (experiment 2), but in other cases, the data support only vague conclusions (experiments 3,4,5) or incorrect conclusions (experiment 6).

explanation. If the same situation occurs, but experimental limitations preclude the measurement of A or B or C, it becomes more difficult to reach the correct conclusion. If B and C (the metabolites upstream and downstream, respectively, of the altered flux) can be measured (Experiment 2), then the correct conclusion is still obtained. On the other hand, if this does not occur, then the data provide the basis for testable hypotheses, but they do not support definitive conclusions regarding the activities of the five pathways. In the case where only one of the three metabolites could be detected (not an altogether uncommon scenario in NMR- or MS-based metabolomics), conclusions are either vague (Experiment 3,4) or incorrect (Experiment 6). The complexity of the biochemical pathways (branching, cycles, etc.) in a living system compounds the the problems illustrated by this trivial example. Thus a new approach involving the measurement of flux through various pathways has been proposed (see §1.1.6)

1.1.6 Beyond metabolomics: Fluxomics

As discussed in §1.1.5, interpreting data collected on a small fraction of the total number of metabolites in a given pathway is a serious problem for metabolomics. Quantitative analysis of *all* metabolites in a biological sample is a task of finite, but staggering, complexity. It seems unlikely that high-throughput methods analogous to those available

in the field of genomics will be forthcoming in the foreseeable future, in the sense that it will not be possible to receive a complete and accurate analysis of all metabolites in a sample within hours. The reason for this seemingly pessimistic view is as follows (Sumner et al., 2003). By comparison, the human genome project, one of the most daunting undertakings in history, involved the binary detection of only 4 structurally similar molecules in the absence of dynamic range limitations. The analysis of all metabolites in a sample is orders of magnitude more complex because, at a minimum, we would expect to obtain data about carbohydrates, amino acids, lipids, fatty acids, nucleotides, and sterols. The chemical properties of these molecules are so different that a single instrument is unlikely to provide satisfactory results for all of them in a single sample. Thus, for the present, we must either content ourselves with measuring a small fraction of the metabolome, or think differently about the problem. Since an important goal of metabolomic studies is the elucidation of mechanisms, as opposed to mere description of biochemical changes in various disease states, a new approach is required.

The use of tracers to measure flux through various pathways has been proposed as an alternative, complimentary approach to metabolomics . In addition to the arguments presented above, which rested primarily on the grounds that incomplete metabolomic data prevents definite conclusions about mechanisms for pathology, a separate case can be made for the "fluxomic" approach. Due to homeostatic mechanisms, organisms will resist changes in concentration of regulated metabolites until physiologic reserve is exhausted. Therefore, altered gene expression or enzyme function may precede measurable changes in concentration of metabolites (especially if it is not possible to measure all metabolites reliably). On the other hand, a technique capable of measuring metabolic flux may be much more sensitive in detecting a metabolic abnormality than one which relies on concentration.

There are two key problems with the fluxomic approach: first, it is difficult to select a single optimal tracer that will enable measurement of a useful number of fluxes. The second problem is that tracers are expensive, and time-resolved data are required to measure flux rates (although ratios of rates can be obtained from a single sample).

1.2 ^{13}C NMR as a Biological Tool

In order to fill the void in our understanding of biochemical mechanism left by concentration-only metabolomic studies, we turn to ^{13}C NMR-based measurements of metabolic flux. Carbon atoms form the backbone of nearly all important biomolecules (see Appendix

B). Naturally occurring samples contain a mixture of 98.9% ^{12}C and 1.1% ^{13}C , both of which are stable nuclei that do not undergo any form of radioactive decay. Because ^{12}C contains an even number of nucleons, this nucleus has zero spin, and thus no magnetic moment; therefore, it cannot be observed via NMR spectroscopy. However, the 1.1% ^{13}C present in naturally occurring molecules has spin 1/2 and is observable via NMR. Just as one may analyze complex mixtures of proton-containing biomolecules via ^1H NMRS, ^{13}C NMRS can analyze complex mixtures of any molecules that contain ^{13}C . The key difference, however, is that the investigator is free to select ^{13}C -enriched substrates based on knowledge of stereochemistry in the pathway of interest. Due to the high spectral resolution of ^{13}C NMR spectroscopy, individual carbon atoms within a molecule can be quantified independently. This data, when placed in the context of a suitable biochemical model allows the investigator to reconstruct the metabolic history of the carbons from the time they entered as the enriched tracer until they are analyzed in the metabolite of interest. It is possible to collect sequential *in vivo* ^{13}C NMR spectra, for example during the infusion of a tracer, and from this data to estimate the rates of many biochemical pathways.

1.3 Astrocyte biology

We now turn our attention from the field of metabolomics to focus on astrocytes. As we will see, these cells are potentially affected by chronic ethanol via a mechanism involving acetate metabolism. Before focusing on this hypothesis, I will present some background information on these fascinating and historically unappreciated cells.

Though long regarded as mere "brain glue", it has recently been appreciated that astrocytes may play vital roles in many brain functions (Volterra and Meldolesi, 2005). In addition to their traditional roles of providing scaffolds and metabolic support for neurons, recent studies demonstrate that astrocytes may act as local networks, integrating neuronal inputs and modulating synaptic transmission. In this capacity astrocytes may play critical roles in learning, memory, and higher-order cognitive functions.

1.3.1 Astrocyte Morphology and Ultrastructure

Limitations of classical staining techniques gave rise to the idea that multiple astrocytes might extend overlapping processes to cover multiple neurons. However, more recent techniques, such as the ability to microinject dye into a single astrocyte, reveal that

	GFAP expression	Input resistance	Membrane potential	Gap junction coupling	Glutamate	NG2 staining
Type 1	High	Low	Very neg.	Yes	High Uptake	Neg.
Type 2	Low	High	Less neg.	No	Low uptake AMPA-Rs	Neg.
Type 3	Low	High	Less neg.	No	Low uptake AMPA-Rs	Pos.

Table 1.1: Subtypes of astrocytes in the mouse hippocampus

astrocytes are far more organized, and that their processes show little overlap — each astrocyte has its own domain that encompasses up to thousands of synapses (Bushong et al., 2002). While a single astrocyte may envelop thousands of synapses, its interactions with these synapses can be controlled independently via microdomains including lamellipodia and filopodia (Volterra and Meldolesi, 2005). Thus the astrocyte itself may integrate signals and selectively modulate various synapses — these are exactly the characteristics one would expect of a communication hub. Moreover, astrocyte foot processes appear to be plastic, extending, retracting and reorganizing on timescales of minutes (Hirrlinger et al., 2004).

In addition to their role as integrators across networks of synapses, astrocytes serve as bridges between cerebral vessels and neurons (Volterra and Meldolesi, 2005). In light of their anatomical location and their ability to respond to neuronal activity, it has been suggested that astrocytes may regulate CNS blood flow via release of potassium in order to match perfusion to the metabolic demands of neuronal activity (Paulson and Newman, 1987). Other relevant molecules that astrocytes may release to modulate blood flow include epoxyeicosatrienoic acids (EETs), prostaglandins, and arachidonic acid (Koehler et al., 2006).

Astrocyte subtypes

With the rise in interest in astrocytes, it has become clear that they are not a homogeneous cell type. Within the mouse hippocampus alone, at least three types of astrocytes exist that differ in their expression of Glial fibrillary acidic protein (GFAP), proteoglycan NG2, and other properties (see Table 1.3.1) (Volterra and Meldolesi, 2005). The role and fate of NG2-positive cells remains unclear at this point — like astrocytes they make intimate contacts with neurons throughout the grey and white matter, have stellate morphology, and extend processes to synapses. However they possess the ability to

differentiate into oligodendrocytes, and may express different receptors and ion channels (Nishiyama et al., 2005). These NG2 cells share with NG2-negative astrocytes the ability to be stimulated by neural input via glutamate, ATP, and possibly other molecules (Butt et al., 2005). Yet NG2-positive cells are not the only histologic enigmas. On the basis of slightly different criteria, six subtypes of astrocytes have been identified in rat olfactory bulb (Bailey and Shipley, 1993). It seems very likely that within the category of cells deemed 'astrocytes', a great deal of morphologic and functional diversity has been overlooked.

Astrocyte receptors

Among others, astrocytes express AMPA receptors, metabotropic glutamate receptors (mGluRs), GABA_B receptors, and muscarinic acetylcholine receptors, various adrenergic receptors, and receptors for adenosine, dopamine, serotonin, histamine, opioids, substance P, and atrial natriuretic peptide (Porter and McCarthy, 1997).

1.3.2 Astrocyte Excitation and Ion Homeostasis

Astrocytes possess intrinsic oscillating Ca²⁺ currents during development (Parri and Crunelli, 2001), and afterwards. It has recently been appreciated that neuronal input via astrocytic mGluRs, GABA_B, and muscarinic ACh receptors can induce increases in astrocytic Ca²⁺, a form of astrocytic excitation (Newman, 2003). These Ca²⁺ increases can propagate in waves to neighboring astrocytes, covering distances of hundreds of μm (Cornell-Bell et al., 1990). The mechanisms for Ca²⁺-wave propagation are (a) diffusion of inositol trisphosphate (a second messenger for some mGluRs) through gap junctions and (b) release of ATP that functions as an extracellular messenger (Newman, 2001). In addition, neuronal input can modulate Ca²⁺ activity in astrocytes (Pasti et al., 1997). The exact significance of these Ca²⁺ waves is incompletely known, but they appear to play a role in physiologic modulation of synaptic activity by astrocytes (§1.3.3) and also in epilepsy (Tian et al., 2005; Petroff et al., 2002; Khurgel and Ivy, 1996).

Astrocytes, with their large network of cells connected via gap junctions, are critical buffers for extracellular K⁺ ions (Simard and Nedergaard, 2004). In addition to various potassium channels, astrocytes have Na/K ATPases that pump sodium out of the cell and potassium into the cell, thus maintaining Na⁺ gradients that are essential for glutamate removal (Anderson and Swanson, 2000), while removing K⁺ from the extracellular fluid to allow normal neuronal function.

1.3.3 Astrocyte-Neuron Interactions

Metabolic interactions between Astrocytes and Neurons

Astrocytes provide metabolic support for glutamatergic and GABAergic neurotransmission. (These are quantitatively the most important excitatory (Glu) and inhibitory (GABA) systems in the brain.) Astrocytic support (Fig. 1.3) is crucial because they possess two critical enzymes that neurons lack: glutamine synthase (GS) (Norenberg, 1979; Norenberg and Martinez-Hernandez, 1979), and pyruvate carboxylase (PC) (Yu et al., 1983; Shank et al., 1985). In particular, glutamatergic transmission relies upon the function of a glutamine-glutamate cycle in which neurons release glutamate, astrocytes remove it from the extracellular space and convert it to glutamine, and glutamine is returned to neurons for the resynthesis of neurotransmitter glutamate (Sibson et al., 1998). This cycle was first discovered by Benjamin and Quastel (Benjamin and Quastel, 1972), and subsequently confirmed in numerous studies (Pellerin and Magistretti, 1994; Shen et al., 1999; Sibson et al., 1997), though some debate exists regarding stoichiometry under various conditions, and which other substrates (if any) are shuttled between astrocytes and neurons (Sibson et al., 1998; Zwingmann and Leibfritz, 2003; Westergaard et al., 1995)

It is important to emphasize that neurons are completely dependent on astrocytes for the *de novo* synthesis of glutamate because neurons lack the anapleurotic enzyme pyruvate carboxylase (PC) (see Appendix B). Glutamate is a 5-carbon amino acid that does not cross the blood brain barrier (Hawkins et al., 1995), but which can be synthesized from glucose via the TCA cycle intermediate alpha-ketoglutarate (Hertz et al., 2000). Yet for every molecule of glutamate produced, a five carbon skeleton is lost from the TCA cycle. Without the activity of PC to replenish the carbon skeletons in the TCA cycle by synthesizing oxaloacetate from pyruvate, it would be impossible for net synthesis of glutamate to occur.

In addition to the synthesis of neurotransmitters, astrocytes are the primary cells responsible for synthesizing glutathione (GSH) within the CNS (Heales et al., 2004). Glutathione is a tripeptide (γ -glutamylcysteinylglycine) that functions as an antioxidant because of its ability to donate electrons, and it is therefore a neuroprotective compound (Hertz and Zielke, 2004); the lack of glutathione is itself neurotoxic (Jain et al., 1991). Astrocytes provide neurons with the GSH precursor L-cysteinylglycine through a somewhat convoluted mechanism that involves astrocytic synthesis and release of GSH, and extracellular cleavage of GSH to L-cysteinylglycine (Dringen et al.,

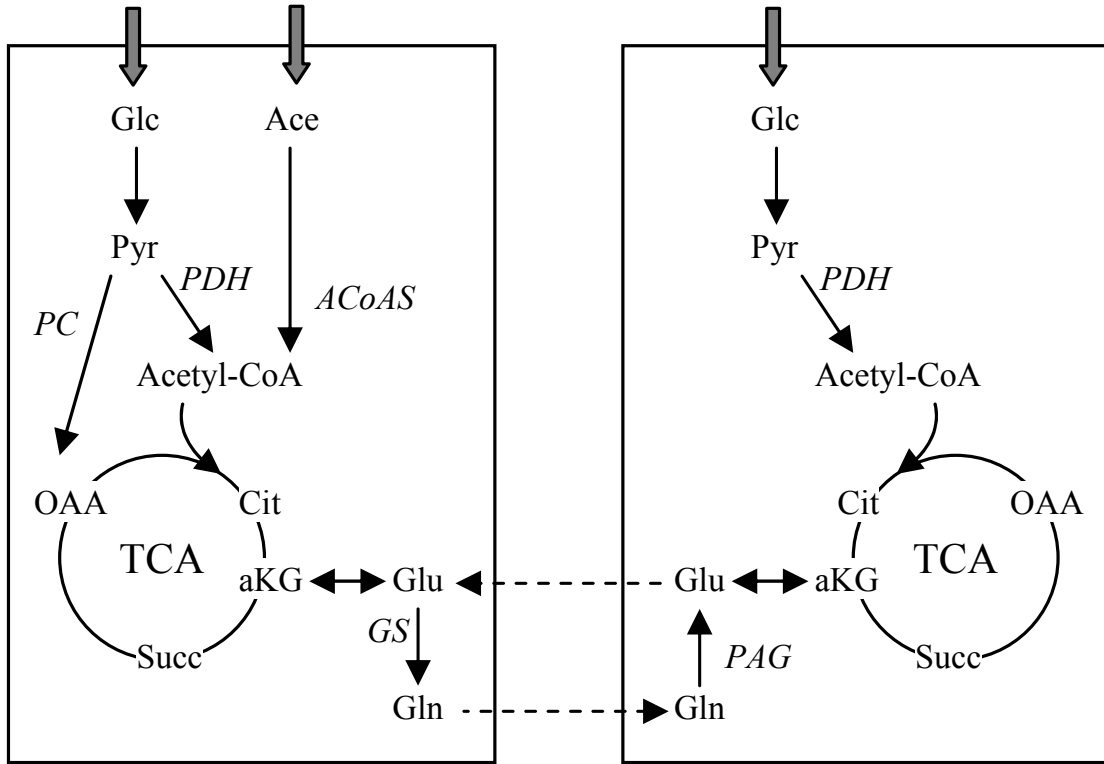


Figure 1.3: Astrocytes (left) possess the anapleurotic enzyme pyruvate carboxylase (PC) which enables them to replenish TCA cycle intermediates that are lost during net synthesis of glutamate. By contrast, neurons (right) express only pyruvate dehydrogenase, so that they can only form acetyl-CoA from pyruvate. Astrocytes also express glutamine synthetase (GS) that enables them to convert glutamate (an excitatory neurotransmitter) to glutamine that they release into the extracellular fluid for neurons to scavenge. Neurons form glutamate from precursor glutamine supplied by astrocytes, and they release it during neurotransmission. Astrocytes remove glutamate from the extracellular space, preventing excitotoxicity. Key: large grey arrows indicate ability to transport the specified molecule. Enzymes are italicized: ACoAS, acetyl-CoA synthetase; GS, glutamine synthetase; PAG, phosphate-activated glutaminase; PC, pyruvate carboxylase; PDH, pyruvate dehydrogenase. Metabolites: Ace, acetate; aKG, alpha-ketoglutarate; Cit, citrate; Glc, glucose; Gln, glutamine; Glu, glutamate; OAA, oxaloacetate; Pyr, pyruvate; Succ, succinate;

1999).

Signalling Between Astrocytes and Neurons: Gliotransmitters

Astrocytes possess their own repertoire of "gliotransmitters" that meet the criteria specified by Volterra: (1) synthesis and/or storage in astrocytes, (2) regulated release by physiological stimuli, (3) rapid (msec to sec) activation of responses in neighboring cells, and (4) a role in physiological processes — see Table 1 in (Volterra and Meldolesi, 2005). Among the molecules that meet these criteria are: Glutamate, ATP, Adenosine, D-Serine, various eicosanoids, TNF- α , and some peptide hormones.

Modulation of Synaptic Activity by Astrocytes

Astrocytes have at their disposal several means for modulating synaptic activity (Newman, 2003). Following signals from neurons that induce Ca^{2+} waves, several mechanisms allow astrocytes to modulate neuronal activity:

- **Glutamate Release by Astrocytes:**

Presynaptic neuronal activity can stimulate astrocytes to release glutamate, which can have either a stimulatory or inhibitory effect on neurons. If glutamate acts via postsynaptic mGluRs, the result is depression of both inhibitory and excitatory postsynaptic transmission. On the other hand, if glutamate acts via NMDA or AMPA receptors on pre- or post-synaptic neurons, the result is an increase in synaptic transmission. Thus in different contexts, glutamate release by astrocytes can have either a positive or negative neuromodulatory effect.

- **ATP Release by Astrocytes**

Muller cells (specialized retinal astrocytes) modulate synaptic activity via release of ATP. Like glutamate, ATP can have either an excitatory or inhibitory effect on neurotransmission. ATP can interact with P2X neuronal receptors to mediate a stimulatory effect. On the other hand, ATP can be cleaved to adenosine in the extracellular space, and adenosine can produce an inhibitory effect via adenosine A1 receptors through an increase in K^+ conductance.

- **Cofactor release**

Astrocytes are the sole source of D-serine, a necessary cofactor for NMDA receptor activation. NMDA receptor activation requires occupancy at both the glutamate site as well as a so-called "glycine" site for which D-serine appears to be the

endogenous ligand. Thus release of this cofactor by astrocytes provides a plausible mechanism for modulating synaptic activity.

- **Glutamate Transport**

As discussed above (§1.3.3), a glutamine-glutamate cycle operates between neurons and astrocytes. Moreover, astrocytes are entirely responsible for maintaining the low (3-4 M) extracellular concentration of glutamate through a process of co-transport with sodium and protons, followed by rapid conversion to glutamine (Danbolt, 2001). Thus, modulation of glutamate uptake provides a potential mechanism for astrocytes to influence synaptic transmission. On the other hand, as we will see in (§1.3.4), failure of astrocytes to supply precursor glutamine to neurons inhibits glutamate-dependent processes.

- **Extracellular Ions**

Astrocytes are also responsible for extracellular ionic homeostasis in the brain (Simard and Nedergaard, 2004). If they allow the extracellular K^+ levels to rise, the effect will be to depolarize neurons and increase synaptic transmission. (As discussed in §1.3.1, increasing extracellular potassium may be a form of communication between astrocytes and vascular smooth muscle.) On the other hand, if astrocytes allow H^+ levels to rise, the effect will be to block presynaptic Ca^{2+} channels and NMDA-Rs, thus decreasing synaptic transmission.

1.3.4 Roles of Astrocytes in Behavior and Integrated Physiology of the Organism

Clock genes and EEAT1/GLAST

A set of so-called "clock" genes named period 1,2,3 (Per1, Per2, Per3) plays a role in controlling diurnal rhythms. A "master clock" is located in the suprachiasmatic nuclei of the brain, and not surprisingly, the regulation is quite complex (Albrecht and Eichele, 2003). Nevertheless, knockout mice deficient in Per2 showed decreased expression of the glutamate transporter EEAT1 (GLAST) in astrocytes, leading to a hyperglutamatergic state in the brain (Spanagel et al., 2005; Yuferov et al., 2005). This finding suggests a connection between astrocytic glutamate transport and control of circadian rhythms.

Glutamatergic activity and learning

Due to their role in providing metabolic support for glutamatergic neurons (§1.3.3), normal astrocyte function is required for certain types of learning. Disruption of the supply of precursor glutamine through inhibition of either the astrocytic TCA cycle or glutamine synthase quickly abolishes glutamate release by neurons (Hertz and Zielke, 2004). Inhibition of the astrocytic TCA cycle by fluoroacetate in day-old chicks was shown to inhibit glutamate-dependent aversive learning, but injection of glutamate restored normal learning even in the presence of fluoroacetate (Hertz et al., 1996). Thus, to the extent that certain types of learning are dependent upon glutamatergic activity, astrocytic support of glutamatergic neurons is indispensable.

Glucose Homeostasis

As discussed in (§1.3.3) astrocytes may supply neurons with lactate derived from glucose. A recent study found that intraventricular injections of either glucose or L-lactate increased blood insulin and decreased blood glucose due to decreased hepatic glucose production (Lam et al., 2005). Moreover, neither injection of D-lactate (which cannot be converted to pyruvate within neurons), nor co-injection of L-lactate with the lactate dehydrogenase inhibitor, oxamate, caused similar changes, supporting the idea that neuronal metabolism of lactate to pyruvate is an essential step in this regulatory mechanism. Since inappropriately high production of glucose by the liver is at least partially responsible for diabetic hyperglycemia (Vaag et al., 1995; Taylor, 1999), it is possible that deficient astrocytic supply of L-lactate to neurons could be partially responsible for failure of homeostatic regulation of blood glucose in type II diabetes.

Oxytocin release and Lactation

During conditions that are associated with oxytocin and vasopressin release (childbirth, lactation, water deprivation), astrocytic processes, which normally provide dense coverage of neuronal elements, retract (Hirrlinger et al., 2004; Olier et al., 2004). In nursing rats, new axosomatic synapses appear after the astrocytic processes recede. These new synapses may play a role in synchronizing output from these neurons, helping them to secrete large amounts of hormone (Hatton, 1997). These changes reverse themselves after removal of the stimulus (i.e. weaning pups or correcting fluid balance) (Hatton, 1997). These findings suggest the intriguing possibility that one function of astrocytes is to inhibit the formation of inappropriate neural connections, and that the removal

of foot processes enables the formation of new connections in adult brain. Further, it suggests that reinstatement of normal astrocytic function may abolish the synchronous activity induced by the new synapses. Finally, it is appealing to speculate that cells that are involved in the hormonal regulation of fluid balance might also play a role in the perception of thirst, thus providing another possible link between astrocyte dysfunction and alcoholism.

1.4 Alcohol abuse and alcoholism

Ethanol not only damages multiple organ systems, causing significant morbidity and mortality, but the social and economic consequences of its abuse are staggering. While it is impossible to quantify the human cost, the estimated cost of alcohol abuse and alcoholism is more than \$100 billion annually in the US (Holland and Mushinski, 1999), and is similarly staggering elsewhere (Fenoglio et al., 2003; Devlin et al., 1997). Ethanol remains the third leading external cause of death in the United States, behind tobacco, and poor diet and inactivity (Mokdad et al., 2004; McGinnis and Foege, 1993). Withdrawal from ethanol can be deadly; those who survive carry a burden of neural sensitization that predisposes to craving and relapse (De Witte et al., 2003; Becker, 1996).

1.5 Ethanol Metabolism and Biodistribution

In humans, ethanol is typically consumed as a beverage. When ingested this way, it quickly reaches the stomach (Fig. 1.4). If the stomach is empty, the majority of the dose will be absorbed from the duodenum and jejunum into the blood of the hepatic portal system. On the other hand, solid food, if present in the stomach, will delay emptying of gastric contents, and up to 70% of the dose can be absorbed via the stomach itself, albeit at a slower rate (Eckardt et al., 1998). When transit time through the stomach is delayed by the presence of food, first-pass metabolism by gastric Alcohol Dehydrogenase (ADH, see below) occurs, though all but the smallest doses of ethanol will saturate the gastric ADH system. Thus in nearly all cases, ethanol will travel via the portal vein to the liver, where the vast majority of ethanol oxidation occurs. When ethanol is present in concentrations that saturate the liver's metabolic capacity, it will enter the systemic circulation, and distribute in total body water (Eckardt et al.,

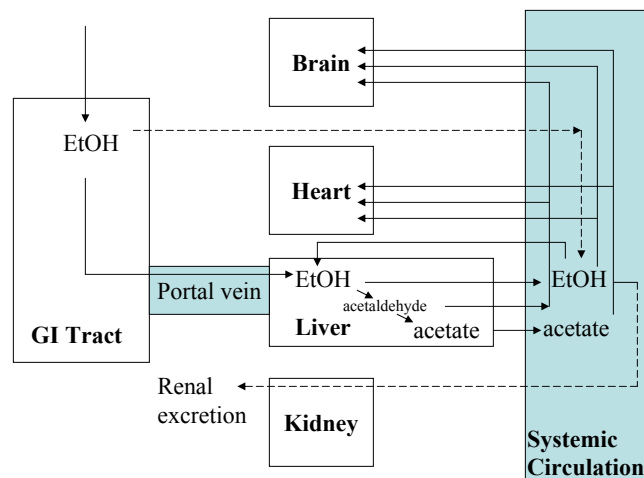


Figure 1.4: Ethanol ingestion, absorption, and biodistribution. Ethanol is absorbed from the the gastrointestinal tract into the portal vein (and to a lesser extent into the systemic circulation). First-pass metabolism of ethanol to acetaldehyde and acetate occurs primarily in the liver, and all three compounds are released into the circulation. Blood levels of ethanol range from 12mM for a 0.5g/kg dose to hundreds of mM in tolerant alcohol abusers; blood acetaldehyde levels are typically 0-2 μ M, and blood acetate is typically 1-2mM. The vast majority of a dose of ethanol is eliminated via hepatic oxidation to acetate; a small portion of ethanol is excreted renally, exhaled, and excreted in the sweat. Ninety percent of the acetate produced via ethanol oxidation is released into the blood where it travels to many organs and is used as a source of energy. A key hypothesis in this dissertation is that the brain adapts to this unusual energy source, and that resulting dependence on acetate as a substrate for cerebral metabolism is a component of dependence to ethanol.

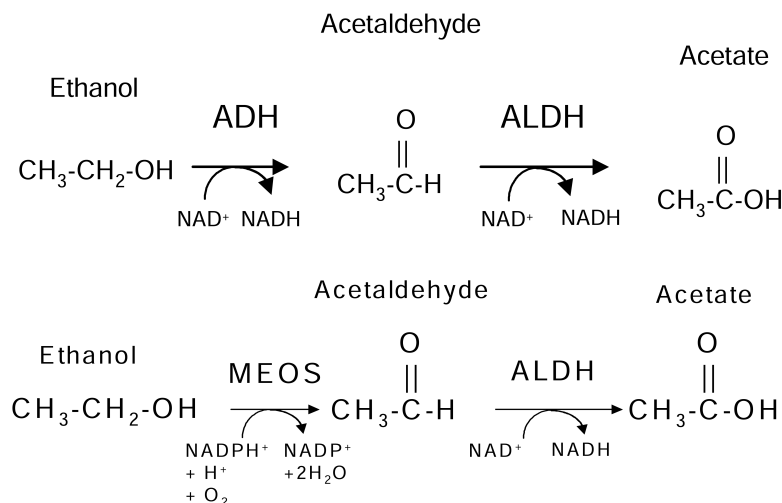


Figure 1.5: Significant routes for hepatic ethanol oxidation. The primary pathway for ethanol metabolism in naive animals involves the cytoplasmic Alcohol Dehydrogenase (ADH) and mitochondrial Aldehyde Dehydrogenase (ALDH). In ethanol-tolerant individuals, the inducible Microsomal Ethanol Oxidizing System (MEOS) can also contribute significantly.

1998). The 'classical' ethanol-oxidizing system involves two enzymes, cytosolic Alcohol Dehydrogenase (ADH) and intramitochondrial Aldehyde Dehydrogenase (ALDH).

The equilibrium of the ADH reaction at pH 7.3 favors the formation of ethanol, but the ALDH reaction is faster and irreversible. Thus, provided that NAD^+ may be regenerated in the mitochondria, the net reaction favors the oxidation of ethanol (Eckardt et al., 1998). Comparatively recent reports have shown the importance of the Microsomal Ethanol Oxidizing System (MEOS) which is comprised of various cytochrome P450 isoforms and distinguished from the ADH system on the basis that the MEOS is (i) oxygen and NADPH-dependent, rather than NAD^+ -dependent, and (ii) inducible (Lieber and DeCarli, 1970). In addition, a catalase system has been suggested to metabolize ethanol, although the quantitative significance of this pathway in vivo appears to be minimal (Lieber, 1999).

At high hepatic ethanol concentrations, a small amount of ethanol is eliminated via conjugation with activated UDP glucuronic acid (uridine-5'-diphospho- -glucuronic acid) in the presence of UDP glucuronyl transferase, forming ethyl glucuronide (EtG). Though it is certainly not a quantitatively important route for ethanol elimination (<0.5-1.5% of a dose of ethanol is excreted in urine as EtG (Wurst et al., 2002)), the slow release of EtG from the liver and subsequent storage in the hair, or elimination in the urine, make EtG a promising forensic marker of recent ethanol abuse (Droenner

et al., 2002)(Wurst et al., 2003). For completeness, it is worth mentioning that small amounts (<5% of a given dose) of ethanol may be eliminated by the kidneys, skin, and lungs (Norberg et al., 2003). Also, the brain has been suggested to possess some ability to oxidize ethanol, but reports have been inconsistent and at most the brain appears to have 0.1-1% of the ethanol-oxidizing capacity of the liver (Eckardt et al., 1998).

1.6 The Effect of Ethanol on Energy Metabolism

Much of the impact of ethanol metabolism on the liver can be understood in terms of the change in Oxidation-Reduction (redox) state. Oxidation of ethanol results in excess production of NADH (see §1.5), which drives the equilibrium of reactions that require reduced cofactors away from oxidation of other substrates. In particular, the increased NADH/NAD ratio drives a shift from oxaloacetate to malate in the TCA cycle, and may therefore slow the TCA cycle (Mayes, 2000). Thus products of ethanol metabolism (acetate, NADH, NADP) slow the oxidation of fatty acids (see Fig. 1.6). The result is increased esterification of fatty acids to form triacylglycerol, which is likely the basis for alcoholic fatty liver disease (Mayes, 2000). As we will see in chapter 3, *in vivo* ethanol metabolism impairs gluconeogenesis (though the situation can be a bit more complex in isolated liver). The simultaneous inhibition of glucose production and increased output of acetate, which can supply 2-carbon units for oxidative metabolism in the TCA cycle (§B.1), suggests that many tissues may adapt to increase metabolism of this unusual energy source.

In vertebrates, there is only a single enzyme through which acetate can participate in metabolism: acetate can enter the TCA cycle after being converted into Acetyl-CoA via Acetyl-CoA Synthetase (ACoAS) (EC 6.2.1.1) (see §B.1); thus, acetate lies only two reactions away from this hub of metabolism (Kanehisa et al., 2006). In addition, it is worth noting that a pair of acetyl-CoA molecules can condense to form acetoacetyl-CoA via Acetyl-CoA Acetyltransferase (ACoAT) (EC 2.3.1.9). From acetoacetyl-CoA, HMG-CoA Synthase (EC 2.3.3.10) catalyzes the formation of 3-Hydroxy-3-methylglutaryl-CoA (HMG-CoA) that represents a crossroads between the formation of ketone bodies and the synthesis of sterols.

In addition to the liver, which actually releases more than 90% of the acetate it produces during ethanol metabolism (Jucker et al., 1998), many tissues have the capacity to metabolize acetate. As we will see, acetate is a substrate for astrocytes in the brain (Waniewski and Martin, 1998; Zwingmann and Leibfritz, 2003). Acetyl-CoA

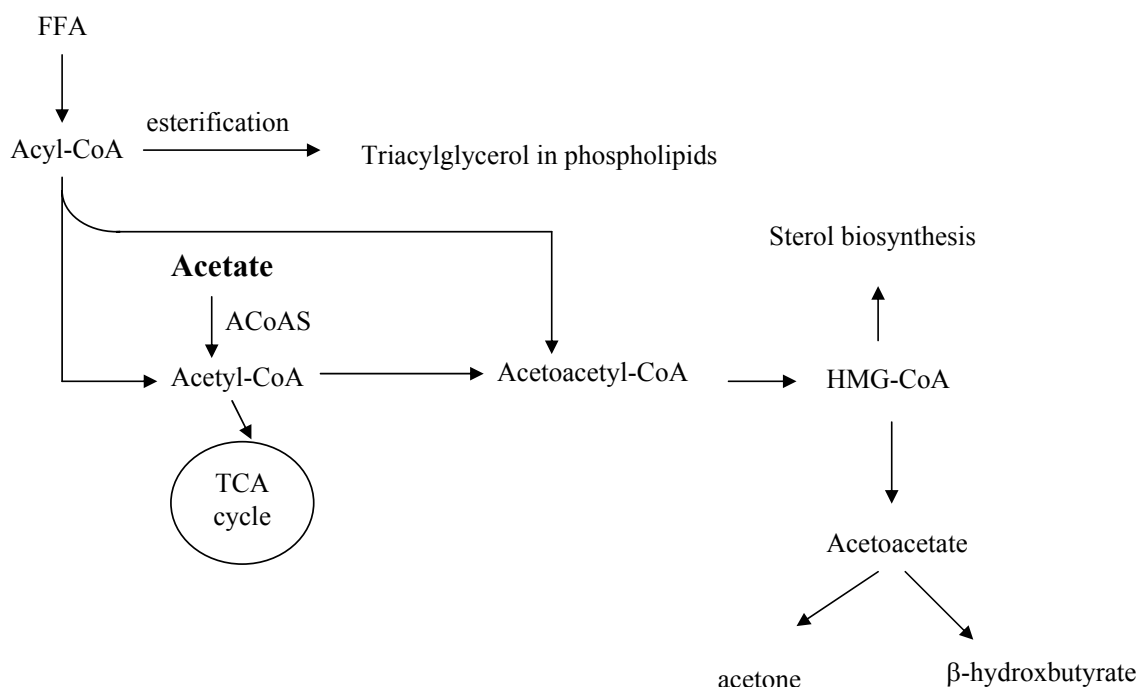


Figure 1.6: Ethanol-Induced Lipogenesis

synthetase is a phylogenetically ancient enzyme that is well conserved in eubacteria, archaeobacteria, and eukaryotes (Karan et al., 2001). It is found in mitochondria, and thus it stands to reason that for cells that possess mitochondria (i.e. all cells except red blood cells), the major impediment to using acetate as a substrate may be the ability to transport it across the plasma membrane (Waniewski and Martin, 1998). ^{13}C and ^{14}C studies have shown that rat skeletal (Bertocci and Lujan, 1999), and cardiac muscle (Tran-Dinh et al., 1998) utilize acetate, as does hog vascular smooth muscle (Allen and Hardin, 1998). Similar studies have shown that rabbit kidney tubule (Chauvin et al., 1997), and rat adipocytes can metabolize acetate (Borges-Silva et al., 2005). (Although rabbits apparently have relatively high blood acetate concentrations, as compared to humans or rats (Chauvin et al., 1997).)

1.7 EtOH and brain

Though most people are familiar with the effects of various doses of ethanol on behavior, the neurochemical basis for these effects remains incompletely understood, in large part because ethanol interacts with a number of neurotransmitter systems. Rather than

explore all of these, the following section will review the effect of ethanol on glutamate and GABA systems, since these are the ones we will probe with the ^{13}C experiments described in Chapter 4.

1.7.1 Ethanol Dependence and Withdrawal

Chronic ethanol consumption results in dependence that is characterized by tolerance and a hyperexcitable withdrawal syndrome that includes anxiety, tremors, and occasionally seizures. This hyperexcitability is attributed to the brain's inability to quickly reverse the neuroadaptations that confer tolerance to ethanol (De Witte et al., 2003): increased sensitivity of glutamate-NMDA receptors (Rudolph et al., 1997; Chandler et al., 1993) and decreased sensitivity of GABA_A receptors (Devaud et al., 1997). When ethanol is present, these adaptations allow surprisingly normal brain function, even at ethanol concentrations that would induce coma in ethanol-naïve individuals. However, cessation of ethanol consumption results in a positive feedback cycle of hyperexcitability and increased glutamate release (Tsai and Coyle, 1998; Dahchour et al., 1998). Withdrawal from ethanol represents a neurotoxic event (Tsai and Coyle, 1998), and repeated episodes of withdrawal have a cumulative detrimental effect (Ballenger and Post, 1978). While the basis for withdrawal-related neurotoxicity is only partially understood, increased extracellular glutamate plays an important role (De Witte et al., 2003; Tsai et al., 1995). Glutamate, the principal excitatory neurotransmitter in the brain, is neurotoxic if released in large quantities, or when not promptly removed from the extracellular space by astrocytes (Danbolt, 2001). Just as altered receptor sensitivity allows pharmacologic tolerance to ethanol (yet represents pathology because it contributes to hyperexcitability during withdrawal), enhanced acetate metabolism in astrocytes may represent metabolic tolerance that becomes pathologic when acetate is removed, decreasing the capacity for astrocytic uptake of glutamate. Traditionally, the focus in alcohol research has been on neuronal pathology following ethanol exposure, with astrocytes neglected completely or regarded as passive bystanders. Recent evidence, however, suggests that the functional significance of astrocytes may have been overlooked.

1.7.2 Altered astrocyte function: A Potential Biochemical Basis for Dependence and Craving

Spanagel et al. showed that increased voluntary alcohol consumption in a strain of mice possessing a particular mutation is due to decreased expression of the glutamate transporter EAAT1 (excitatory amino acid transporter 1; also known as GLAST) on astrocytes, leading to increased extracellular glutamate in the ventral striatum (Spanagel et al., 2005). This finding supports the concept that craving and relapse may result from an attempt to decrease anxiety and other symptoms of hyperexcitability by self-medication with ethanol (De Witte, 2004). Moreover, it demonstrates that astrocytic pathology can itself produce a hyperglutamatergic state with direct relevance to ethanol consumption. The predominant mechanism for cellular uptake of glutamate in the brain is transport into astrocytes (Anderson and Swanson, 2000). Astrocytic glutamate transporters rely upon sodium and potassium concentration gradients; these gradients require energy. During ischemia, reversal of the glutamate transporter on astrocytes accounts for approximately half of glutamate released into the extracellular space (Phillis et al., 2000), but transporter reversal precedes complete collapse of ionic gradients, suggesting that less severe energy compromise may still produce physiologically significant decreases in glutamate uptake (Jabaudon et al., 2000). It is therefore logical to assume that if adaptation of astrocytes to utilize acetate produces lasting deficits in glutamate uptake, the resulting increased extracellular glutamate might contribute to anxiety, craving, and other processes that complicate recovery from ethanol addiction.

If cessation of chronic alcohol ingestion (and therefore acetate production) contributes to withdrawal due to metabolic failure in astrocytes and reduced glutamate uptake, then administration of acetate during withdrawal should reduce withdrawal severity. In the only publication we could find on this topic, Derr et al. (Derr et al., 1981) found that intragastric (i.g.) injections of sodium acetate significantly reduce the incidence of whole body tremors in rats following Majchrowicz's 4 day ethanol exposure paradigm (Majchrowicz, 1975). Though published in a somewhat obscure journal and not replicated during the past 24 years, this result is consistent with the hypothesis that acetate administration during withdrawal supplies the brain with a critical substrate for astrocytic metabolism and thereby averts tremors during withdrawal. Although it supports our hypothesis of a metabolic contribution to ethanol/acetate dependence and withdrawal, this result does not provide definitive proof: evidence is lacking that

(i) metabolic adaptation results from chronic exposure to ethanol and acetate, and (ii) cessation of ethanol intake (and therefore acetate production) causes metabolic pathology that precedes and contributes to hyperexcitability. The experiments described in this dissertation will address both of these issues. Whereas complete metabolic failure of astrocytes can produce toxic overabundance of extracellular glutamate, other metabolic pathology in astrocytes can decrease glutamatergic neurotransmission, and this phenomenon may also be significant in alcoholism. Neurons rely on astrocytes for metabolic support, including supply of precursors for synthesis of glutamate. Inhibition of the astrocytic TCA cycle or glutamine synthetase impairs release of transmitter glutamate (Hertz and Zielke, 2004), leading to cognitive deficits. Inhibition of the astrocytic TCA cycle by fluoroacetate in day-old chicks inhibits glutamate-dependent aversive learning, but injection of glutamate overcomes this effect (Hertz et al., 1996). If astrocytes fail to support neuronal synthesis of glutamate required for aversive learning, this could contribute to perseverative behavior observed after withdrawal (Obernier et al., 2002b) that interferes with recovery. In addition, recent evidence implicates astrocytes as active participants in synaptic events, capable of releasing glutamate in a Ca^{2+} -dependent fashion (Newman, 2003). Thus, astrocytes may be involved with more subtle forms of cognitive function, and disruption of these could also be a significant obstacle to recovery from ethanol addiction.

1.7.3 Ethanol & Cerebral Metabolism: Availability of Acetate During Intoxication

Ethanol is oxidized to acetate in the liver, and more than 90% of this acetate is released into the blood (Jucker et al., 1998). In the absence of ethanol, a small amount of acetate is produced by bacterial flora, leading to a blood acetate concentration of 0.2-0.3mM (Waniewski and Martin, 1998). In humans given a single dose of ethanol (0.5g/kg i.v.), blood acetate rises 3-fold to approximately 1mM (Orrego et al., 1988). In rats, similar increases were observed after a single intraperitoneal dose of ethanol (Carmichael et al., 1991) (also, see Fig. 3.2). Elimination of intoxicating doses of ethanol occurs at a constant rate (zero-order kinetics (Norberg et al., 2003)), which implies a constant rate of acetate production. Following a single dose of ethanol, blood acetate remains at a constant level until ethanol metabolism is nearly complete (and no longer zero order) (Orrego et al., 1988). Thus, it is reasonable to suppose that an individual on a binge may have peaks and valleys in blood ethanol concentration, but that blood acetate

will remain at a relatively constant, elevated level until intake ceases and virtually all ethanol is eliminated. During chronic ethanol exposure, metabolic tolerance to ethanol in the liver ensues, increasing the rate of ethanol oxidation in both humans and animals (Lieber and DeCarli, 1970). Since ethanol is oxidized to acetate at a faster rate, alcoholics reach a higher blood acetate plateau (mean 1.48mM, max 1.90mM) during intoxication than do occasional drinkers and controls (Korri et al., 1985), demonstrating that there is a more abundant supply of acetate in the blood during prolonged ethanol consumption.

1.7.4 Ethanol & Cerebral Metabolism: Cerebral Utilization of Acetate

Early studies using [^{14}C] acetate demonstrated that carbons from acetate were preferentially incorporated into cerebral glutamine rather than glutamate, while the reverse occurred when [^{14}C] glucose was provided as the tracer molecule (O’Neal and Koeppe, 1966). These observations gave rise to the hypothesis that cerebral metabolism consists of two compartments: one that preferentially metabolizes acetate and contains a small glutamate pool that is rapidly converted to glutamine, and a second compartment that utilizes glucose and contains a large glutamate pool (Van den Berg et al., 1969). Since astrocytes express glutamine synthase (Norenberg and Martinez-Hernandez, 1979), it was supposed that they represent the small glutamate pool, and that cerebral acetate metabolism takes place mainly within astrocytes. This view is now widely accepted ((Zwingmann and Leibfritz, 2003) and references therein), and it has been shown that the selectivity of acetate in labeling the astrocytic compartment is due to avid uptake by a specific acetate carrier on astrocytes (Waniewski and Martin, 1998). Not only is exogenous acetate a substrate for brain metabolism, but Roach et al. also showed that [^{14}C] ethanol given intraperitoneally labeled brain Gln, Glu, and GABA (Roach and Resse, 1972). This result is presumably due to cerebral metabolism of [^{14}C] acetate, though the ^{13}C NMR studies in this proposal will provide more definitive data. Further, activity of ACoAS (the enzyme that converts acetate to acetyl-CoA) increases 36% in homogenates of rat cortex following chronic ethanol treatment (Kiselevski et al., 2003). Taken together, these observations support the hypothesis that during chronic ethanol intoxication, astrocytes adapt their metabolism to utilize the unusually abundant supply of blood acetate.

1.8 Outline of Dissertation

1.8.1 Metabolomic Studies

We began with an NMR-based metabolomic study of the effect of ethanol on liver, blood, and brain biomolecules. Along the way we investigated several unknown peaks in the NMR spectra, and Chapter 2 details our assignment of one of the unknown signals to ethyl glucuronide. In Chapter 3 we present all of the findings from the metabolomic analysis, including (i) ethanol inhibits gluconeogenesis, (ii) high doses of ethanol produce ethyl glucuronide in the liver within 3 hours, (iii) the anti-oxidant BHT inhibits the formation of ethyl glucuronide.

1.8.2 ^{13}C NMR Analysis of Brain Metabolism

In order to address the hypotheses presented above regarding cerebral metabolism of ethanol-derived acetate, we used ^{13}C tracers and ^{13}C NMR spectroscopy of tissue extracts. To our knowledge, this is the first study of brain metabolism of ethanol-derived acetate using ^{13}C methods; the results are presented in Chapter 4. The ^{13}C fractional enrichment data provide the strongest support to date for the concept that ethanol-derived acetate is metabolized in brain. Contrary to our expectations, chronic ethanol exposure did not increase the net cerebral utilization of acetate, probably because transport of acetate into astrocytes did not increase substantially. However, chronic ethanol caused significant alterations in labeling of the neurotransmitter GABA, which may reflect neuroadaptation in dependent animals.

Chapter 2

Proton NMR Spectroscopic Determination of Ethanol-Induced Formation of Ethyl Glucuronide in Liver

The following chapter is the first report describing detection of ethyl glucuronide in liver by proton NMR spectroscopy. It has been submitted to Analytical Biochemistry.

2.1 Abstract

Ethyl glucuronide (ethyl- β -D-6-glucosiduronic acid, EtG), a unique metabolite of ethanol, has received much recent attention as a sensitive and specific biological marker of ethanol consumption. Formed in the liver via conjugation of ethanol with activated glucuronate, EtG remains detectable in serum, plasma, and hair for days after ethanol abuse. Thus far, GC-MS and ELISA assays have been developed to detect trace quantities of EtG for forensic purposes, but reports of the NMR properties of EtG have been scarce. Herein we present the first report of EtG determination using proton NMR spectroscopy. We collected 700MHz proton spectra of liver extracts from rats treated with a 4-day binge ethanol protocol (average ethanol dose: 8.6 g/kg/day). An unexpected signal (triplet, 1.24 ppm) appeared in ethanol-treated liver extracts but not in control samples; based on chemical shift and multiplicity, we suspected EtG. We observed quantitative hydrolysis of the unknown species to ethanol while incubating our samples with β -glucuronidase, confirming that the methyl protons of EtG were

responsible for the triplet at 1.24ppm. This study demonstrates that proton NMR spectroscopy is capable of detecting EtG, and that future NMR-based metabolomic studies may encounter this metabolite of ethanol.

2.2 Introduction

Ethyl glucuronide (ethyl- β -D-6-glucosiduronic acid, EtG) is a minor direct metabolite of ethanol that has received much recent attention as a sensitive and specific biological marker of ethanol consumption. Due to interest in developing methods capable of detecting minute quantities of this compound for forensic applications (Wurst et al., 1999; Droenner et al., 2002; Skipper et al., 2004), efforts have focused on gas chromatography-mass spectrometry (GC-MS) (Schmitt et al., 1995; Weinmann et al., 2004; Wurst et al., 2004), and even enzyme linked immunosorbant assay (ELISA) techniques (Zimmer et al., 2002), but the nuclear magnetic resonance (NMR) properties of EtG have not been reported to our knowledge. In the emerging field of metabolomics, NMR spectroscopy is a prominent tool for the analysis of compounds found in biofluids and tissue extracts (Reo, 2002; Griffin, 2003; Viant et al., 2003) because it is capable of detecting many classes of molecules in the same sample without pre-selection of analytes (Imbenotte et al., 2003). Moreover, the sensitivity of NMR has increased dramatically in recent years due to technical advances such as cold probes that increase the signal to noise ratio, small volume sample tubes that allow the detection of smaller amounts of material, and improved digital electronics that increase the effective dynamic range of the technique. These advances extend the detection limit for NMR and thus increase the number of compounds which may be identified during experiments and screening tests. As the number of detected compounds grows, it will be of great use to have access to publications that give NMR spectral properties for molecules that have not yet received great attention. Therefore, we present what is to our knowledge the first published report describing the detection of ethyl glucuronide by proton NMR spectroscopy. We hope that the presentation of this information will facilitate the correct interpretation of NMR data from future clinical and animal metabolomic studies in which ethanol intake is a possibility.

2.3 Materials and Methods

2.3.1 Animals

Adult male Sprague Dawley rats (275-325g) were treated with a modified 4 day binge ethanol protocol as previously described (Obernier et al., 2002a). A 15% (w/v) ethanol Reitz High Fat diet was used with an appropriate isocaloric control. Rats were given an initial dose (5g/kg, 25%w/v, in a vehicle of nutritionally complete diet) with subsequent doses determined using a six-point behavior scale (Majchrowicz, 1975). Control animals received a diet equal to the average of all ethanol treated animals. All animals had free access to water throughout experiment. This protocol produces physical dependence to ethanol (Majchrowicz, 1975) and induces neuropathology modeling that found in human alcoholics (Obernier et al., 2002a). Blood ethanol concentration (BEC) was measured using electrochemical detection of an enzymatic reaction with an Analox Instruments model GM-7 analyzer (Analox Instruments, MA). Ethanol groups had mean blood levels around 300 mg/dl (range 250-375 mg/dl). Within one hour after the last treatment, all animals were sacrificed, and liver samples were collected and stored at -80 C until further analysis. All protocols in this study were approved by the Institutional Animal Care and Use Committee and were in accordance with National Institute of Health regulation for the care and use of animals in research.

2.3.2 Tissue Extraction and Sample Preparation

Liver tissues were removed from the -80 C freezer and placed in liquid nitrogen. Tissues were then pulverized with a stainless steel mortar and pestle, and extracted with perchloric acid (Fan et al., 1986). The extracts were lyophilized, dissolved in D₂O containing TSP and formate (as frequency and concentration references, respectively), and adjusted to pH 7.0 (pD 6.6) with DCl or NaOD prior to NMR analysis.

2.3.3 Enzymatic hydrolysis

To confirm the presence of a glucuronide, we performed an enzymatic hydrolysis by adding 2500IU β -glucuronidase (E.C. 3.2.1.31) (Scarfe et al., 2002) from *Helix pomatia* crude extract (MP Biomedicals, Inc., Irvine, California). We acquired "pre-incubation" proton spectra after adjusting the pH of the liver extracts to 5.0 (pD 4.6) for optimal activity of the *H. pomatia* enzyme using 7M DCl. After acquiring a pre-incubation spec-

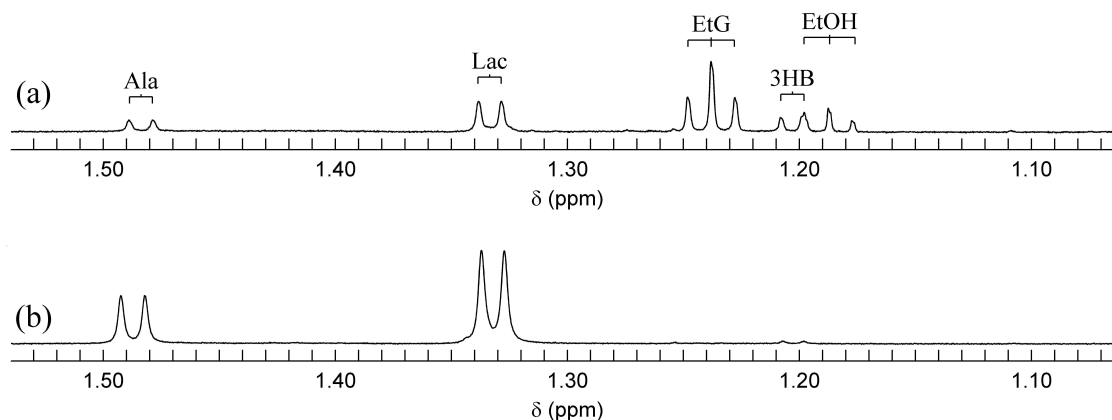


Figure 2.1: Typical 700MHz ^1H spectrum of liver extract from an animal treated with ethanol (a) shows a triplet at 1.24ppm which was later confirmed to be due to ethyl glucuronide. This signal is not due to ethanol, which resonates at 1.19ppm (see Fig. 2.2c). The triplet was absent from spectra of liver extracts from animals that were not given ethanol (b). Abbreviations: alanine, Ala; ethanol, EtOH; ethyl glucuronide, EtG; β -hydroxybutyrate, 3HB; lactate, Lac.

trum, enzyme was added to the liver extract samples, and the samples were incubated overnight in a 37°C water bath. As a positive control, Methyl Glucuronide (Sigma, St. Louis, Missouri) was incubated with β -glucuronidase under the same conditions.

2.3.4 NMR spectroscopy

Initial studies were conducted on a Varian Inova 700MHz spectrometer. Proton spectra were acquired in fully relaxed mode (duty cycle = 45s), at 25°C, with 1s presaturation of water protons immediately prior to a 90° excitation pulse. Other parameters were: 16 transients, spectral width 8600Hz, 64k data points. Hydrolysis of EtG by β -glucuronidase was monitored on a Varian Inova 400MHz spectrometer. Spectra collected before and after overnight incubation were acquired at 25°C with 45s duty cycle, 1.5s presaturation of water protons, 90° excitation pulse, 8 transients, 4000Hz spectral width, and 16k data points. Sequential spectra acquired during incubation with β -glucuronidase were acquired at 37°C, with identical parameters except that 32 transients were acquired for each spectrum.

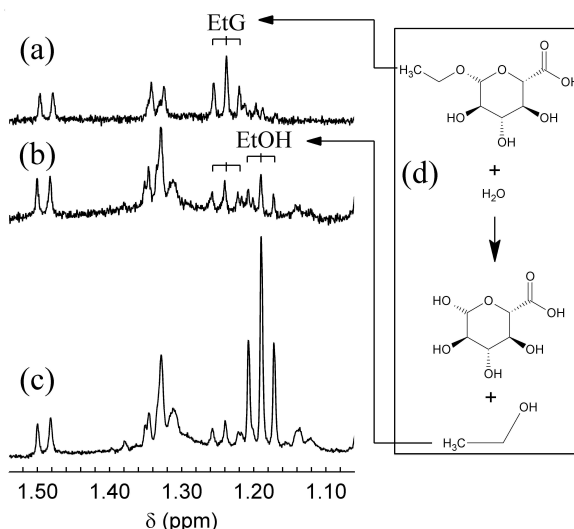


Figure 2.2: Identification of ethyl glucuronide in proton NMR spectra of liver extracts. 400MHz ^1H spectra acquired before (a) and after (b) overnight incubation with β -glucuronidase show decreased intensity of the EtG triplet, and formation of ethanol. Spectrum (c) from the same sample after addition of pure ethanol, which resonates at 1.19ppm, confirms that the triplet at 1.24ppm is not ethanol, and that ethanol is the product of the reaction. Panel (d) shows the hydrolysis of EtG to glucuronate + ethanol catalyzed by β -glucuronidase.

2.3.5 EtG Standard

A sample of EtG (Aurora Analytics, Baltimore, MD) was obtained in order to validate spectral assignments.

2.4 Results and Discussion

Analysis of 700MHz proton spectra of liver extracts revealed an unexpected triplet at $1.2380 \pm 0.006 \text{ ppm}$ ($J = 7.11 \pm 0.05 \text{ Hz}$) (data reported as mean \pm standard deviation of 11 samples). This triplet was present in all spectra of liver extracts from animals that received ethanol ($n=11$, see Fig. 2.1a for a representative spectrum), and absent from control samples ($n=11$, see Fig. 2.1b). The multiplicity of this signal suggested the presence of an ethyl group, but the chemical shift was inconsistent with ethanol, which was confirmed by adding a small amount of ethanol to the sample, reacquiring data at 400MHz, and observing a distinct triplet at 1.19ppm (Fig. 2.2). Based on the presence

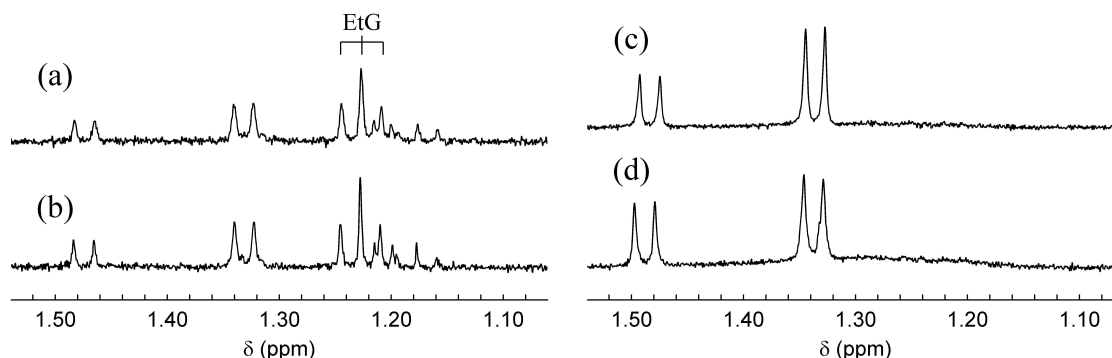


Figure 2.3: Spectra acquired before (a) and after (b) overnight incubation of an EtG-containing liver extract without addition of β -glucuronidase show no evidence of either decreased EtG intensity or formation of ethanol, demonstrating that the reaction in Fig. 2.2a,b is due to enzymatic activity rather than non-specific degradation. Spectra of an extract from control liver that contained no EtG acquired before (c) and after (d) overnight incubation with β -glucuronidase show no formation of ethanol due to incubation, demonstrating a specific requirement for the species that gives rise to the triplet at 1.24ppm as a substrate for the production of ethanol.

of an ethyl group associated with exposure to large doses of ethanol, we suspected that the unassigned triplet was due to ethyl glucuronide ($C_8H_{14}O_7$, see Fig. 2.2d for structure). Comparison of spectra from a liver sample acquired before (Fig. 2.2a) and after (Fig. 2.2b) overnight incubation with β -glucuronidase reveals hydrolysis of EtG to ethanol + glucuronate in a liver extract from an ethanol-treated animal. Incubation with β -glucuronidase resulted in decreased intensity of the triplet at 1.24ppm (EtG), with a corresponding increase in the intensity of the triplet at 1.19ppm (ethanol, Fig. 2.2b). The identity of the triplet at 1.19ppm was confirmed by observing an increased intensity in this triplet in a spectrum acquired after adding ethanol directly to the samples (Fig. 2.2c).

We performed several controls to validate our procedures. In order to rule out the possibility that incubation at 37°C and pH 5 caused non-specific formation of ethanol, we incubated one extract from ethanol-treated liver without addition of β -glucuronidase, and as expected no ethanol formation or EtG hydrolysis were observed (Fig. 2.3a,b). This finding shows that the reaction observed in Fig. 2.2a,b was catalyzed by β -glucuronidase. In addition we incubated one control (non-ethanol-treated)

liver extract which contained no detectable EtG (Fig. 2.3c) in the presence of β -glucuronidase to demonstrate that addition of enzyme and overnight incubation do not cause ethanol to appear in the spectra (Fig. 2.3c,d). This finding demonstrates that (i) the reaction in Fig. 2.2a,b required the source of the unassigned triplet at 1.24ppm as a substrate, and (ii) there was no contamination of the β -glucuronidase with ethanol. Finally, we recorded sequential 400MHz proton spectra at 37°C (Fig. 2.4a) to demonstrate the stoichiometry during the enzymatic hydrolysis of EtG to ethanol. By integrating the baseline-corrected signals from ethanol and EtG, and normalizing by the integral for formate (which had been added as an exogenous concentration reference (Kriat et al., 1992)), we were able to demonstrate that the sum of [ethanol] + [EtG] was approximately constant over the 49 hours during which the data were recorded (Fig. 2.4b). This finding is consistent with the hydrolysis of EtG to form ethanol, and provides important support for our assignment of the triplet at 1.24ppm to EtG. In addition, during the hydrolysis of EtG, we were able to observe an increase of glucuronic acid by monitoring the α -H1 resonance at 5.22ppm. Glucuronic acid exists as α - and β - anomers in solution, but at 37°C the residual water signal overlaps with the β -H1 signal at 4.62ppm, and thus the signal from the β anomer cannot be quantified reliably. During the 49-hour incubation, the increase in signal from the α -H1 proton was several times greater than the increase in the ethanol signal, when adjusted for the number of protons contributing to each resonance. Whereas we observed a quantitative increase in signals from α - and β - anomers of free glucuronate during hydrolysis of methyl glucuronide (a positive control, data not shown), it is likely that the large increase in signal from free glucuronate in liver extracts reflects hydrolysis of glucuronides other than EtG that were present in liver. Nevertheless, increased signal due to free glucuronic acid is expected during hydrolysis of EtG and provides additional confirmation that our unknown signal is caused by EtG.

As an additional step to confirm our assignment, we searched our 700MHz spectra for signals due to the β -anomeric proton of EtG. We discovered a doublet at 4.49ppm, the intensity of which appeared to be correlated to that of the putative EtG triplet at 1.24ppm (Fig. 2.5). Based on the results of peak fitting of these signals in five 700MHz spectra, the ratio of the triplet to doublet signal is 3.03 ± 0.66 , consistent with the assignment of the doublet to the anomeric proton of EtG. We attribute the variance to (i) quantification of very small signals on an imperfect baseline and (ii) inconsistencies in the effect of the presaturation sequence on signals near the water resonance across different spectra. As an additional confirmation, we analyzed the same doublet in the

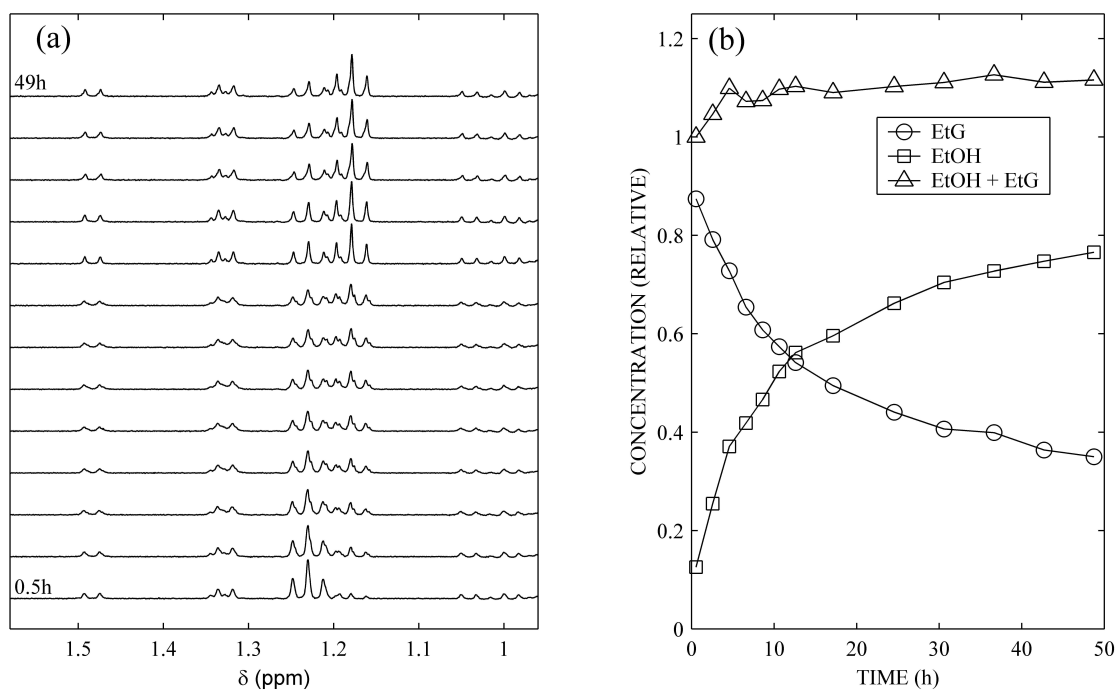


Figure 2.4: Sequential 400MHz proton NMR spectra of a single sample incubated with β -glucuronidase at 37°C. Over time the intensity of EtG (triplet, 1.24ppm) decreases while the intensity of ethanol (triplet 1.19ppm) increases, consistent with hydrolysis of EtG. The right panel (b) shows the relative concentrations of ethanol and EtG over time. The sum of ethanol + EtG (triangles) is approximately constant over time, as would be expected during hydrolysis of EtG to ethanol.

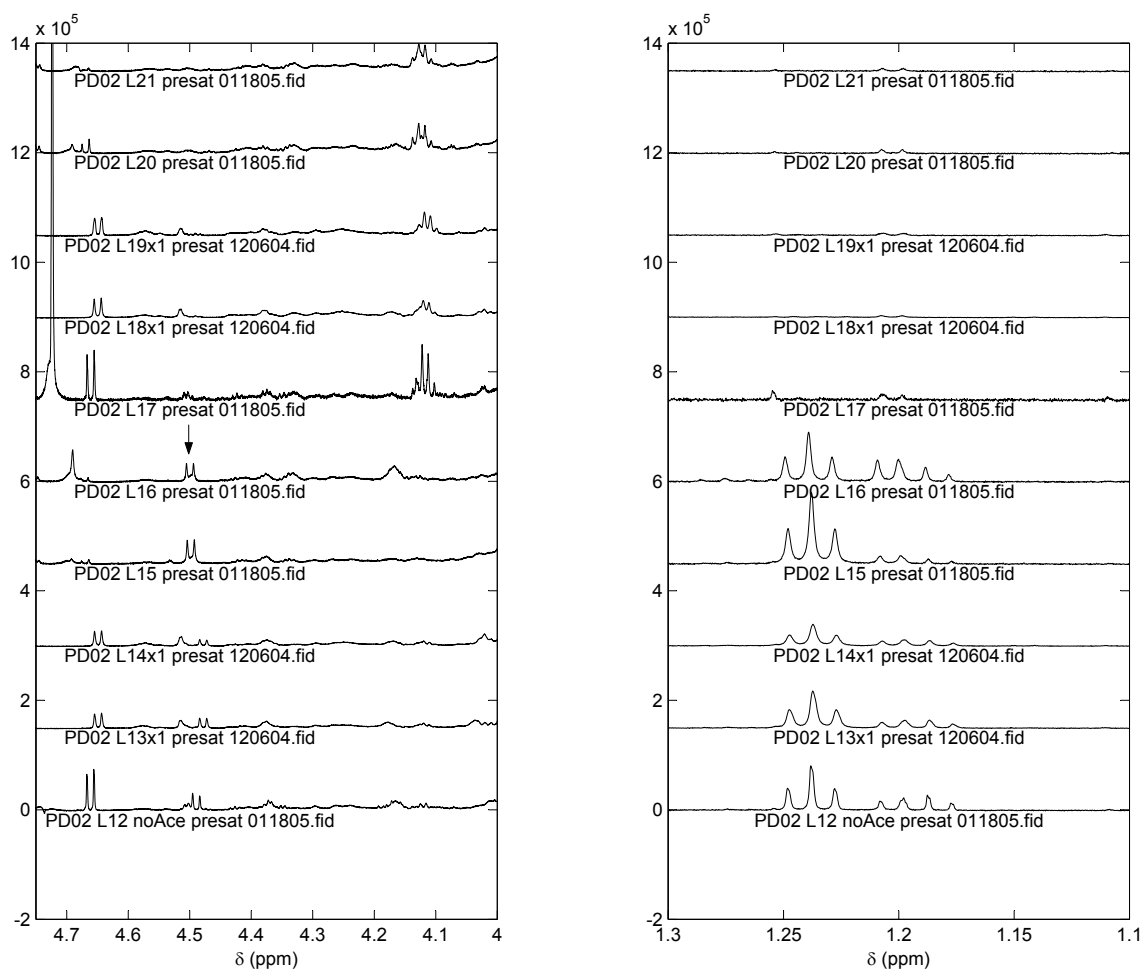


Figure 2.5: Identification of signal from the EtG anomeric proton. Right and left panels show expanded regions from the same 700MHz spectra of liver extracts. Visually, the intensity of the doublet at δ 4.48-4.50ppm (arrow) appears to be correlated to that of the putative EtG triplet at 1.24ppm. The ratio of areas between the triplet and the doublet is 3.03 ± 0.66 , further supporting the assignment.

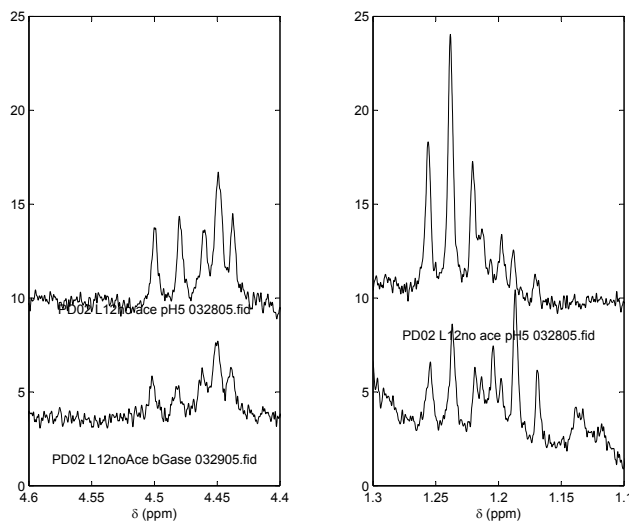


Figure 2.6: Effect of Enzymatic Hydrolysis on Putative EtG Signals. The right and left panels show expanded regions of 400MHz proton spectra of liver extracts before (top) and after (bottom) overnight incubation with β -glucuronidase. Signals from the triplet at 1.24ppm and the doublet at 4.49ppm both decrease on incubation with β -glucuronidase, supporting the assignment of these signals to the methyl and anomeric protons of EtG.

400MHz spectra acquired before and after enzymatic hydrolysis. We found that the doublet, like the putative EtG triplet, decreased after overnight incubation with β -glucuronidase, supporting the assignment of these signals to the anomeric proton and methyl protons of EtG, respectively. Finally, a 400MHz proton spectrum of pure EtG (Fig. 2.7) helped to secure our assignments. The list of resonances is presented in Table 2.1, and these are completely consistent with our interpretation of the enzymatic hydrolysis results.

Previous NMR-based metabolomic studies have identified a triplet at 1.24 ppm.

^1H shift (δ)	Multiplicity	Assignment
1.24	t ($J^{7,8} = 7.1$ Hz)	$^8\text{CH}_3$
3.30	m	^3CH
3.52	m	$^2\text{CH}, ^4\text{CH}$
3.71	m	$^7\text{CH}_2$
3.99	m	^5CH
4.48	d ($J^{1,2} = 8.0$ Hz)	^1CH

Table 2.1: List of EtG resonances observed in a 400MHz proton spectrum in D_2O at pH 7.

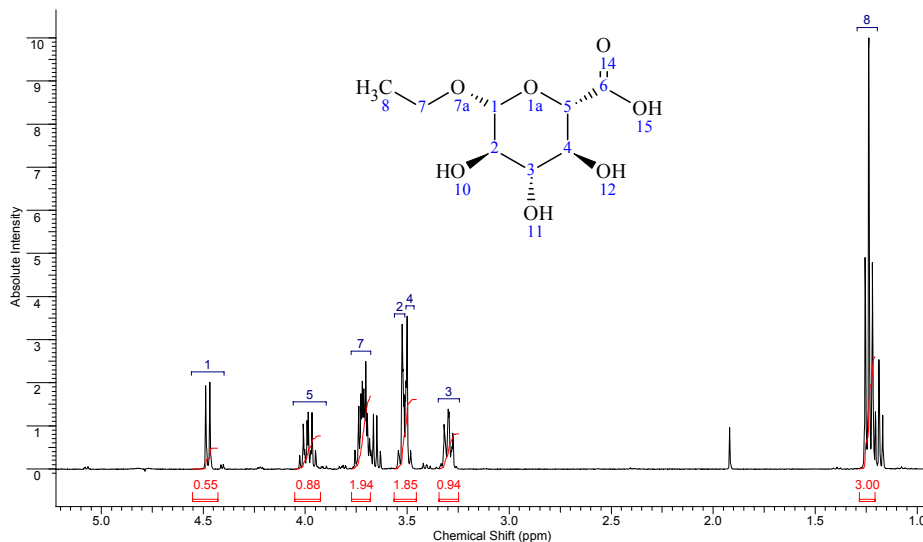


Figure 2.7: Spectrum of EtG with assignments.

Teague et al. report the detection of ethyl glucoside in the urine of human volunteers who had recently consumed rice wine and sake (Teague et al., 2004). Ethyl glucoside, unlike EtG, is not a metabolite in humans (Teague et al., 2004). Rather, it is the fourth most abundant constituent of sake (Hayakawa et al., 2000), formed during the production of this beverage (Mishima et al., 2005). Ethyl glucoside is structurally similar to EtG, with the exception that the carbonyl is reduced to a methylene group, and the two new protons give rise to a doublet of doublets at 3.86ppm that is not present in EtG. The methyl group on ethyl glucoside would give a triplet at nearly the same chemical shift as the one on EtG (1.24ppm). However, (i) we do not find a doublet of doublets at 3.86ppm in our 700MHz spectra of liver extracts (data not shown), (ii) we found evidence of hydrolysis by β -glucuronidase, (iii) we found the signal from an anomeric proton at 4.49ppm, whereas the anomeric proton of ethyl glycoside resonates at 4.93ppm, and (iv) ethyl glucoside is not known to be a metabolite of ethanol. Thus, we conclude that EtG rather than ethyl glucoside is the source of the triplet observed in our liver samples.

Correct attribution of NMR spectral peaks to the molecules in a sample that give rise to these signals is crucial to the proper interpretation of experimental results. Nevertheless, the process of signal assignment is usually the most time-consuming and error-prone aspect of data analysis. For example, a previous 400MHz ¹H NMR study of liver extracts from ethanol-treated rats (36% ethanol liquid diet for 1.5 months)

attributed a triplet at 1.21ppm (referenced relative to the acetate singlet at 1.92ppm at pH 7.5) to residual ethanol that had not evaporated during lyophilization (Ling and Brauer, 1991), yet visual examination of the published spectra reveals the presence of weak signals (possibly a triplet) upfield of the triplet that the authors concluded was due to ethanol. While it is possible that the assignment was correct, this pattern of a weak triplet (ethanol) immediately upfield from a stronger one (EtG) (evident from our 700MHz data, Fig.1a) suggests that the triplet previously observed is consistent with EtG. Therefore, taken together, the data we present suggest that EtG is detectable by proton NMR spectroscopy in liver of ethanol-exposed animals, that EtG may in fact have been detected (though unrecognized) in previous studies, and that signals from this biomarker for ethanol administration will likely be encountered in future NMR studies of liver. Other studies have found EtG in plasma, urine, hair and other tissues (Wurst et al., 2003) suggesting EtG produced in liver is distributed throughout much of the body, where it may persist for some time. Should technical advances in NMR spectroscopy (discussed above) improve the sensitivity and/or dynamic range such that detection of 10-600 μ M EtG (2.2-132 mg/L) in urine and plasma (Wurst et al., 2003) becomes straightforward, direct analysis by NMR may become an inexpensive, simple, fast, and unbiased alternative to the use of derivatization followed by GC/MS to detect and quantify EtG or other xenobiotics. This study highlights the benefits of NMR spectroscopy with minimal pre-selection of analytes as an unbiased method for the discovery of novel metabolites. Though other analytical methods certainly possess superior sensitivity, they require prior knowledge of analytes, and therefore EtG (an unexpected compound) would likely have gone undetected. NMR spectroscopy not only alerted us to the presence of an unexpected compound, but also provided structural information that aided us in its identification.

2.5 Acknowledgments

The authors wish to gratefully acknowledge Dr. Thomas M. O'Connell for useful technical discussions, and Melissa Mann for expert assistance with manuscript submission. This research was supported by the National Institute of Alcohol Abuse and Alcoholism.

Chapter 3

Integrated Multi-organ Analysis of the Effect of Ethanol on Liver, Brain and Serum Metabolites

3.1 Introduction

Ethanol is a unique and widely used drug that is typically consumed in large amounts for pharmacologic effect. The primary route of elimination is hepatic oxidation to acetate. A single dose of ethanol perturbs hepatic regulation of glucose and causes release of large amounts of acetate into the blood. Acetate is a two-carbon fatty acid that can be oxidized via the TCA cycle in many tissues. Of particular interest to us, acetate is metabolized in astrocytes within the brain (Zwingmann and Leibfritz, 2003), and may play a role in intoxication (Israel et al., 1994) and dependence to ethanol (Derr et al., 1981).

Ethanol oxidation proceeds via cytosolic NAD-dependent alcohol dehydrogenase (ADH) and via the NADPH-dependent microsomal ethanol oxidizing system (MEOS), yielding acetaldehyde (Eckardt et al., 1998). Acetaldehyde is oxidized to acetate by mitochondrial aldehyde dehydrogenase (ALDH), and most of the resulting acetate is released from the liver into the blood (Jucker et al., 1998). The challenge for the liver during this process is to maintain an adequate supply of reduced cofactors for these enzymes (Eckardt et al., 1998), while performing its usual regulatory and synthetic functions.

Numerous reports have demonstrated the utility of an NMR-based metabolomic approach coupled with pattern recognition (PR) for the analysis of complex biochemical

responses to exogenous toxins in experimental animals (Nicholson et al., 1999; Solanky et al., 2003), and for the classification of human patients on the basis of their biochemical state (Brindle et al., 2002). Prior to the advent of metabolomics, 400MHz proton NMR spectroscopy of rat liver extracts revealed that chronic ethanol increased acetate and beta-hydroxybutyrate, and decreased alanine (Ling and Brauer, 1991). In comparison, however, our study benefits from (i) analysis of multiple tissues (liver, serum and brain), (ii) the availability of a 700MHz spectrometer that affords substantial gains in resolution and sensitivity, (iii) the availability of recent literature describing assignments of various metabolites in NMR spectra, and (iv) the advent of metabolomic methods for comprehensive spectral analysis. We have chosen to apply a multi-compartment metabolomic analysis to gain additional insight into the metabolic processes affecting multiple organs during intensive ethanol intake. In contrast to the approach adopted in many metabolomic studies, we have attempted to quantify as many individual metabolites as possible in addition to submitting spectral data to unsupervised analysis for validation of the quantitative NMR analysis. By correlating data on multiple organs, we increase our ability to develop a comprehensive understanding of the system-wide metabolic perturbation caused by ethanol, and to identify testable hypotheses for future confirmatory studies.

3.2 Methods and Materials

3.2.1 Animal Handling Procedures and Sample Collection

All protocols in this study were approved by the Institutional Animal Care and Use Committee and were in accordance with National Institute of Health regulation for the care and use of animals in research. Adult male Sprague-Dawley rats (275-325g) were treated with a modified 4-day-binge-ethanol protocol as previously described (Obernier et al., 2002a). A 15% (w/v) ethanol Reitz High Fat diet was used with an appropriate isocaloric control. Rats were given an initial dose (5g/kg, 25%w/v, in a vehicle of nutritionally complete diet) with subsequent doses determined using a six-point behavior scale (Majchrowicz, 1975). Control animals received a diet equal to the average of all ethanol- treated animals. Prior to the start of experiments, half of the animals were treated with the anti-oxidant butylated hydroxytoluene (BHT) (120mg/kg/day in corn oil, i.g.) for 4 days. All animals had free access to water throughout the experiment. This protocol produces physical dependence to ethanol (Majchrowicz, 1975)

and induces neuropathology modeling that found in human alcoholics (Obernier et al., 2002a). Blood ethanol concentration (BEC) was measured using electrochemical detection of an enzymatic reaction with an Analox Instruments model GM-7 analyzer (Analox Instruments, MA). Ethanol groups had mean BECs around 300 mg/dl (range 250-375 mg/dl). Within one hour after the last treatment, all animals were sacrificed, and liver samples were collected and stored at -80°C until further analysis.

In a separate experiment, rats were randomly selected to receive ethanol (5g/kg, 20% w/v in water, i.g.), water (i.g.), or sucrose calorically matched to the ethanol (i.g.). Three hours after dosing, rats were anesthetized with pentobarbital. Following the onset of surgical anesthesia, an abdominal incision exposed the liver and inferior vena cava (IVC). A blood sample (2-4ml) was collected from the IVC and allowed to clot on ice. Next, each animal was decapitated and the skull immediately immersed in liquid nitrogen with agitation in the liquid to hasten the freezing process, while a small piece of liver (1-2g) was quickly removed, wrapped in aluminum foil, and frozen in liquid nitrogen. The time from surgical anesthesia to decapitation was approximately 90 seconds; the time between the start of blood withdrawal and decapitation was less than 45 seconds; the time from decapitation to placing the liver sample in liquid nitrogen was less than 30 seconds. Clotted blood was centrifuged, and serum was removed and stored along with liver and skull samples at -80°C until further analysis.

After the experiment, we became aware that the vehicle for the pentobarbital contained 50% water, 40% propylene glycol, and 10% ethanol (see below). Nevertheless, because this dose (<0.2g/kg) was (i) substantially smaller than the 5g/kg dose given to the ethanol-treated group, (ii) present only for 5 minutes before sacrifice, and (iii) would, if anything, tend to minimize differences between groups, creating a more stringent challenge for the metabolomic approach, we deemed it appropriate to proceed with the analysis.

3.2.2 ¹H NMR Spectroscopic Analysis

Frozen tissues were removed from the -80°C freezer and placed in liquid nitrogen. Tissues were then pulverized with a stainless steel mortar and pestle and extracted with perchloric acid (Fan et al., 1986). Lyophilized extracts were dissolved in a stock solution containing 12.9mM sodium formate and 1.4mM 3-(trimethylsilyl)propionic-2,2,3,3-d4 acid (TSP), adjusted to pH 7.0 (pD 6.6) with DCl or NaOD prior to NMR analysis. Proton spectra were acquired on a Varian Inova 700MHz spectrometer in fully relaxed

mode (duty cycle = 45s), at 25 C, with 1-2s presaturation of water protons immediately prior to a 90 excitation pulse. Other parameters were: 16 transients, spectral width 8600Hz, 64k data points.

Serum samples were prepared by thawing from -80°C in a microcentrifuge at 13000 rpm for 4 minutes, after which 500 μ L of serum was mixed with 250 μ L of stock solution (see above). When less than 500 μ L of serum was available, additional stock solution was added to make 750 μ L total, and the volumes were recorded. 700 μ L of the resulting mixture was transferred to a 5mm NMR tube for analysis. 700MHz proton spectra were acquired using the parameters given above.

In many cases, spectral assignment of well-resolved signals was accomplished with reference to appropriate literature (Waters et al., 2005; Nicholson et al., 1995; Fan, 1996; Govindaraju et al., 2000). In some cases, pure compounds were added to the original samples and additional spectra were collected on a Varian Inova 400MHz spectrometer. Parameters were identical to those used to collect the original spectra, except that the spectral width was 4800Hz.

Time domain data were zero-filled to 128k points, Fourier transformed, phase corrected, and baseline corrected for DC offset. Tissue extracts were referenced to TSP (δ 0ppm), and serum spectra were referenced to formate (δ 8.46). Where possible, peak assignments were made, and well-resolved resonance were integrated, allowing absolute quantification of metabolites in serum (in units of mM) and tissue (in units of mmol/kg wet weight).

3.2.3 Data Reduction and Principle Components Analysis

Spectral data were reduced from 128k to 245 points by integrating the region from δ 0.2-10ppm in segments 0.04ppm wide. The bins containing water (δ 4.68-5.12), propylene glycol (δ 1.12-1.16), and formate (δ 8.40-8.52) were excluded from analysis. In serum samples, ethanol was not removed by lyophilization; thus, in these samples, bins containing ethanol (δ 1.16-1.24 and δ 3.60-3.72) were excluded as well. The remaining bins were submitted to unsupervised analysis. Data were mean centered (Craig et al., 2006) and the principal components (PCs) computed using custom software written in the Matlab (The MathWorks, Inc., Natick, MA) programming environment(PC Nicholas). The PCs are a new set of orthogonal basis vectors: linear combinations of the original spectral data such that the first PC falls along the direction of greatest variance in the original data, the second is orthogonal to the first, and is oriented along the

direction of greatest remaining variance, and so forth (Nicholson et al., 1999). Thus, plotting the original data projected onto PC1 vs PC2 often provides an informative two-dimensional representation of the underlying (200 dimensional) data, with different treatment groups segregating themselves in the new PC coordinates (Lindon et al., 2004). Moreover, analysis of the PC vectors affords the opportunity to determine which spectral regions contributed to the separation of spectra different among treatment groups, thereby providing insight into the biochemical differences and possible mechanisms for toxicity (Nicholson et al., 1999).

3.2.4 Statistical Analysis

In all charts, data are plotted as mean \pm standard deviation, and the number of animals in each group is indicated. When comparing means between different treatment groups, a t-test (two tailed, unequal variance) was used to assess statistical significance. A p-value of less than 0.05 was deemed significant. We have opted to present p-values without correction for multiple comparisons for the following reasons. The first objection concerns the data itself: many of the metabolites quantified in this report are linked via their participation in known biochemical networks, and therefore concentrations of many are not statistically independent; the commonly-used Bonferroni correction is therefore inappropriately conservative (Bland and Altman, 1995). The second objection concerns study design: by their nature (i.e. large number of measured parameters, small number of samples), metabolomic studies are designed to generate hypotheses rather than to test preexisting ones. For this type of study, an optimal multiplicity correction method has not been universally accepted (Sankoh et al., 1997), and the approach of presenting the uncorrected p-values has been advocated instead (Bender and Lange, 1999).

3.2.5 Biochemical Interpretation

To the extent possible, biochemical perturbations due to ethanol exposure were interpreted within the framework of the known chemical reactions of intermediary metabolism. In addition to standard texts, the KEGG database (Kanehisa et al., 2006) was a useful resource for ascertaining metabolic relationships between various molecules.

3.3 Results

3.3.1 ^1H Spectroscopic Analysis of Serum

^1H NMR spectra of serum revealed changes in many metabolites after a single dose of ethanol or sucrose, compared to water (Fig 3.2, 3.1). In comparison to water, sucrose treatment caused an 89% decrease in acetoacetate ($p=0.00092$), a 1.8-fold increase in glucose ($p=0.00020$), and non-significant trends toward increased lactate and acetate. Ethanol, in comparison to water, caused a 57% decrease in lactate ($p=0.0073$), a 62% decrease in alanine ($p=0.00066$), a 2-fold increase in acetate ($p=0.0062$), a 3-fold increase in acetoacetate ($p=0.000074$), and had no effect on glucose. In comparison to animals that received sucrose, ethanol caused lactate to decrease 76% ($p=0.040$), alanine to decrease 62% ($p=0.0015$), glucose to decrease 39% ($p=0.0021$), and acetoacetate to increase 28-fold ($p=0.000079$). In the ethanol-treated animals, serum ethanol concentration 3 hours after dosing was $77\pm 6\text{mM}$. Ethanol ($6\pm 2\text{mM}$) and propylene glycol were discovered in a 1:4 ratio in the serum of sucrose- and water-treated animals since these were components of the vehicle for the pentobarbital anesthetic (see methods). Due to spectral overlap with the very large signal from ethanol, beta-hydroxybutyrate could not be quantified.

3.3.2 ^1H Spectroscopic Analysis of Liver

Ethanol-induced perturbations in several hepatic metabolites were evident in ^1H NMR spectra of extracts (Fig. 3.3, 3.4). In comparison to water controls, single-dose-ethanol animals showed a 72% decrease in alanine ($p=0.038$), a 1.7-fold increase in acetate ($p=0.011$), and non-significant trends towards decreased lactate and increased beta-hydroxybutyrate. Compared to sucrose controls, in single-dose-ethanol animals we found alanine decreased 90% ($p=0.0016$), lactate decreased 80% ($p=0.0040$), and glucose decreased 60% ($p=0.0016$), while beta-hydroxybutyrate increased 5.1-fold ($p=0.011$). Hepatic acetate was comparable between ethanol and sucrose groups, and succinate was not affected by ethanol or sucrose treatment.

Turning our analysis to the binge ethanol groups, we found that binge ethanol decreased hepatic alanine (92%, $p=0.00018$), lactate (89% ($p=0.000083$), and succinate (60%, $p=0.000063$), whereas it increased acetate 9-fold ($p=0.00028$), and beta-hydroxybutyrate 15-fold ($p=0.023$). Overall, the binge control and binge control+BHT groups were similar; the BHT pre-treated group showed modest decreases in lactate

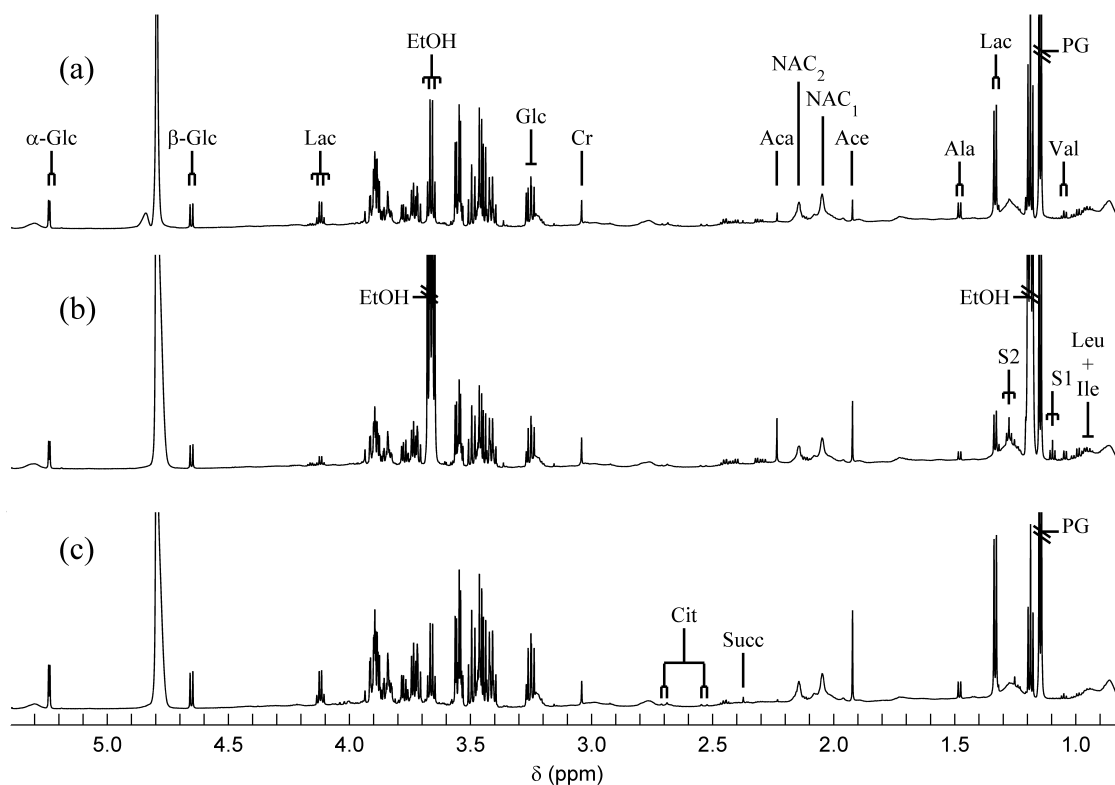


Figure 3.1: 700MHz proton spectra of serum collected from a control animal (a), 3 hours after a single dose of ethanol (b), and 3 hours after dosing with sucrose (c). Large signals from ethanol are evident in the ethanol-treated animals, so large in fact that the satellite peaks due to natural abundance (1.1%) ^{13}C are visible. We found that ethanol decreases lactate and alanine signals, while increasing acetoacetate and acetate, compared to dosing with water. As discussed in methods, the sucrose and water control groups were also inadvertently administered a small dose of ethanol ($<0.2\text{g/kg}$, i.p.) in the vehicle for the pentobarbital anesthetic, and signals from ethanol are seen in (a) and (c). Key: as in 3.3, with the addition of Aca, acetoacetate; Cit, citrate; Nac1/Nac2, composite acetyl signals from α_1 -acid glycoprotein (Waters et al., 2005); S1/S2, ^{13}C satellites of ethanol.

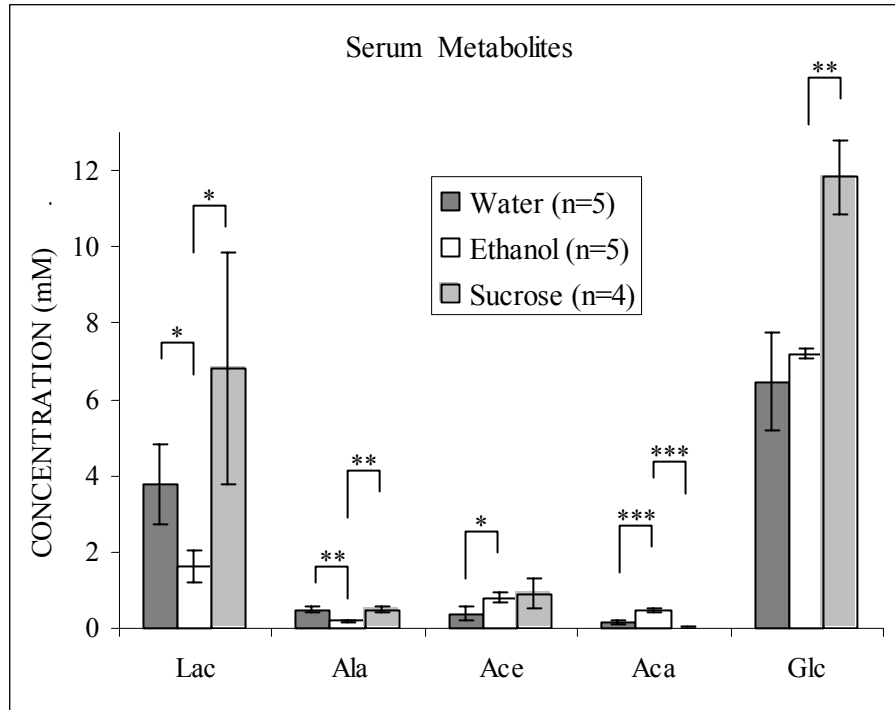


Figure 3.2: Effect on selected serum metabolites 3 hours after i.g. administration of ethanol (5k/kg), water, or sucrose. Lactate and alanine decreased at least 2-fold in ethanol-treated animals in comparison to animals treated with water or sucrose. Acetate increased 2.1-fold in ethanol-treated animals versus water-treated animals, but not in comparison to sucrose-treated animals. It is likely that inadvertent administration of ethanol (in the vehicle of the pentobarbital solution, see methods) to all animals just before sacrifice gave falsely high acetate levels in sucrose and water groups. Serum glucose was 1.6-fold lower in ethanol-treated animals than in sucrose controls.

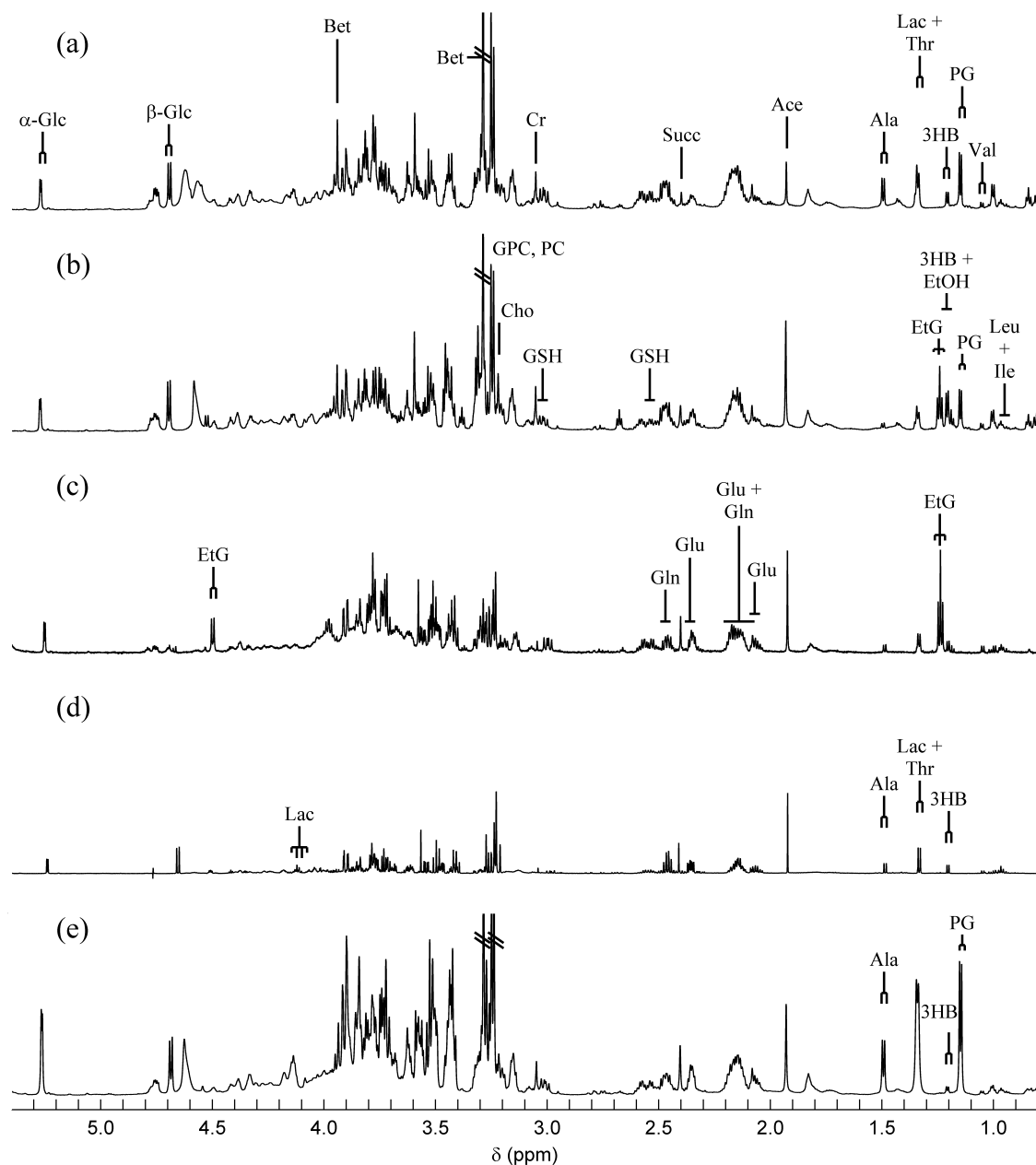


Figure 3.3: 700MHz proton spectrum of liver extracts from (a) control, (b) 3 hours after a single dose (5g/kg) of ethanol, (c) 4 day binge ethanol treatment, (d) 4 day binge ethanol + BHT pre-treatment, (e) 3 hours after sucrose. Both acute and binge ethanol treatment decrease hepatic Lac and Ala, and increase Ace and 3HB. EtG is present 3 hours after a single dose of ethanol, and is greater in the binge-ethanol treated group, whereas in the binge ethanol + BHT group, EtG is scarcely visible. Key: 3HB, beta-hydroxybutyrate; Ace, acetate; α -Glc, α -glucose; Ala, alanine; Bet, betaine; β -Glc, β -glucose; Cho, choline; Cr, creatine; EtG, ethyl glucuronide; Gln, glutamine; GPC, glycerophosphorylcholine; Glu, glutamate; GSH, glutathione; Ile, isoleucine; Lac, Lactate; Leu, leucine; PC, phosphocholine; PG, propylene glycol; Succ, succinate; TMAO, trimethylamine-N-oxide, Thr, threonine; Val, valine.

(31%, $p=0.043$) and alanine (41%, $p=0.019$). For the endogenous metabolites shown in Figure 3.4, binge-ethanol and binge-ethanol + BHT groups showed no significant differences, indicating a lack of effect of BHT pre-treatment on ethanol's perturbation of these metabolites.

Comparing the binge and single-dose groups (Fig. 3.4), the most striking difference is that succinate levels were lower in the single-dose animals than the binge animals (e.g. comparing binge control to single-dose water shows a 94% decrease, $p=0.000069$). Additionally, acetate levels were increased in water- and serum-treated animals relative to binge controls, and the water-treated animals had lower hepatic alanine (77%, $p=0.000065$) and lactate (75%, $p=0.000093$). Thus, both acute and binge ethanol decrease lactate and alanine, and increase acetate and beta-hydroxybutyrate. Taking sucrose treatment and binge control diets to be indicative of the fed state, it appears that overnight fasting and dosing with water also decreases lactate and alanine, but not as much as ethanol. Compared to the fed state, ethanol decreases hepatic glucose levels.

Careful analysis of the spectra revealed an unexpected triplet at 1.24ppm in ethanol-treated animals but not in diet controls. We ruled out the possibility that this signal originated from residual ethanol that had not evaporated during lyophilization (Ling and Brauer, 1991), assigned the signal to ethyl glucuronide (EtG) as described in §2, and quantified it (Fig. 3.5). EtG is undetectable in livers from animals that received no ethanol, but within 3 hours of a large dose of ethanol, hepatic levels rise to the 2mmol/kg range, and remain elevated during the 4-day binge. Interestingly, pretreatment with BHT caused a 90% decrease ($p=0.008$) in EtG during 4 days of binge ethanol treatment. Thus ethyl glucuronide is a unique metabolite found only with ethanol administration that is reduced by BHT.

A strong singlet at 3.28ppm in liver spectra (Fig 3.3) was investigated. We analyzed spectra after addition of betaine and TMAO, two metabolites commonly assigned to signals in this region (Coen et al., 2003). The consistent finding was that the large singlet in our original spectra was due to betaine, and that the signal from TMAO, if present, was generally an order of magnitude smaller (Fig. 3.6). Having identified the signal as originating from betaine, we quantified it and compared results across treatment groups. Betaine did not appear to be altered by a single dose of ethanol, but both binge-ethanol and binge-ethanol + BHT showed a trend of decreased betaine with binge-ethanol + BHT being significantly less than binge-control + BHT ($p=0.0033$), but not binge control. (Fig. 3.7). Thus, BHT seems to elevate liver betaine, a single

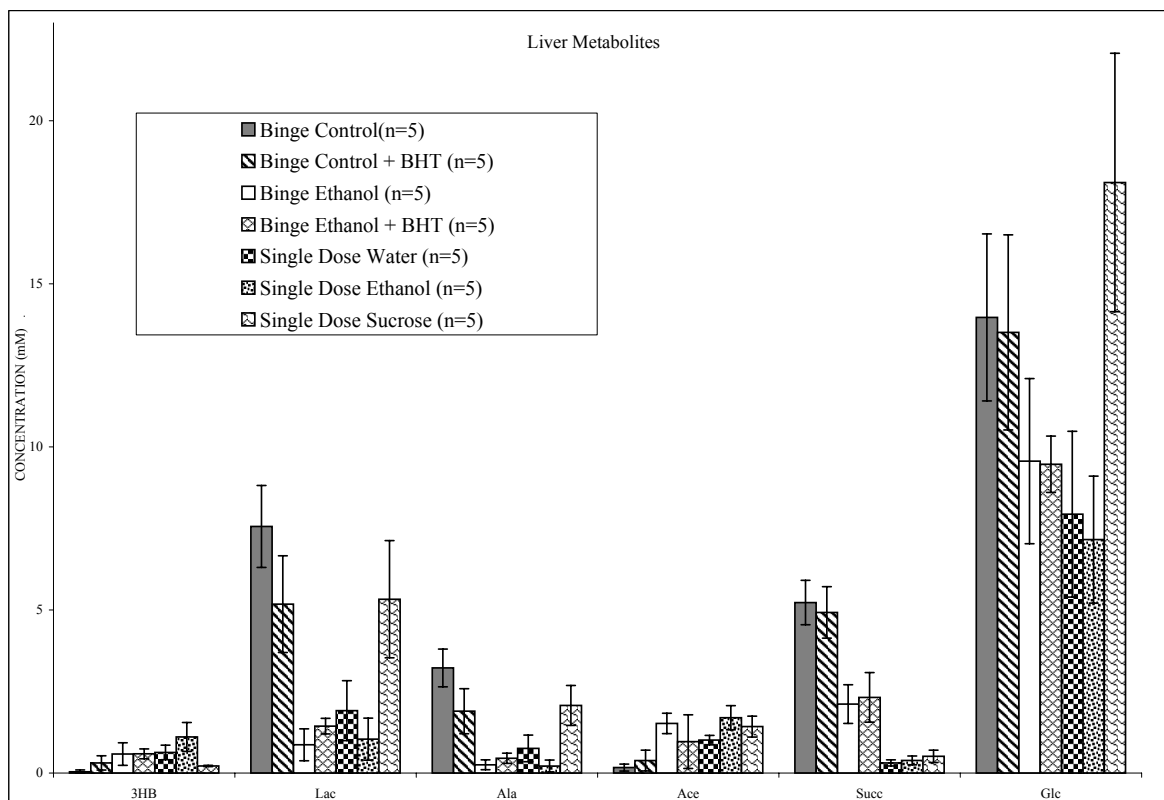


Figure 3.4: Effect of ethanol on selected metabolites in liver quantified by proton NMR spectroscopy of tissue extracts. In comparison to diet controls, hepatic lactate decreased in all animals that received ethanol (9-fold for binge-ethanol, 5-fold for binge-ethanol+BHT, and 5-fold for single dose ethanol), as did alanine (13-fold for binge-ethanol, 7-fold for binge-ethanol+BHT, and 10-fold for single-dose ethanol) and glucose (32% decrease for binge-ethanol, 32% for binge-ethanol+BHT, 60% for single dose). Succinate decreased approximately 60% in binge ethanol treated animals (with or without BHT) versus binge controls. However, succinate was greater in all binge groups than single-dose animals, perhaps due to differences between the liquid diet and standard rat chow. Beta-hydroxybutyrate increased in all animals treated with ethanol (15-fold in binge groups, and 5-fold in the single dose group). Acetate increased 9-fold in binge ethanol animals versus binge controls; in the binge-ethanol+BHT group, the trend was apparent, but it was not statistically significant due to large variance in this group's acetate levels. Acetate levels in the single-dose ethanol group were comparable to the binge-ethanol group, however the sucrose-treated animals showed elevated acetate levels also due to the inadvertent administration of ethanol just before sacrifice in the anesthetic vehicle (see methods).

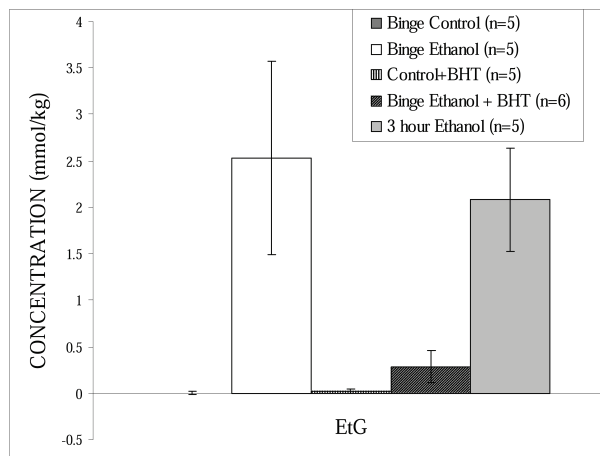


Figure 3.5: Quantification of ethyl glucuronide (EtG) in liver extracts via 700MHz ^1H NMR spectroscopy. EtG reaches $\sim 2\text{mmol/kg}$ in liver within 3 hours after a single dose of ethanol, and remains elevated during binge ethanol treatment. Pre-treatment with BHT caused a 9-fold reduction in EtG ($p < 0.01$ versus binge-ethanol group), possibly because BHT competed against ethanol for access to activated glucuronide (see discussion).

dose of ethanol has no effect, and binge ethanol showed a trend toward a decrease in betaine.

We attempted to collect a ^1H NMR spectrum of pure BHT in order to assign any signals from this molecule in our liver extracts. However, we found that BHT was so hydrophobic that at neutral pH and room temperature we could not dissolve enough in D_2O to detect any signal. Thus our liver spectra from the BHT animals likely do not contain any signals from BHT.

3.3.3 ^1H Spectroscopic Analysis of Brain

Few changes were evident in the signals from brain metabolites (Fig. 3.8). Though signals were well-resolved, and many metabolites were quantified, no clear trends in metabolite concentrations were detectable 3 hours after a single dose of ethanol.

3.3.4 PC Analysis of Liver NMR spectra

As a first pass, we performed PCA on data from all 7 groups of liver extracts (Fig. 3.9). Separation along PC1 (which explained 46.9% of the variance in this data set) primarily differentiated single-dose from binge groups, irrespective of ethanol treatment

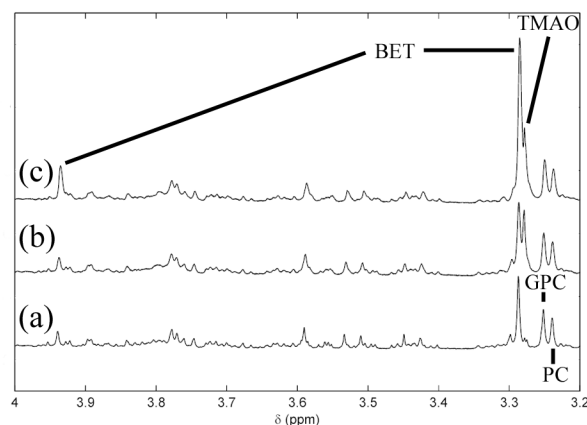


Figure 3.6: Assignment of betaine and TMAO in 400MHz ^1H NMR spectra of liver extracts. Spectra were acquired before addition of exogenous material (a), after sequential addition of TMAO (b) and then betaine (c) in order to assign the large singlet at 3.29ppm in the original spectrum (a, see also Fig 1). Clearly the original signal in (a) is not consistent with TMAO, but is consistent with betaine. Additional confirmation of the assignment is provided by the methylene protons of betaine which produce the singlet at 3.94ppm. TMAO, if present in the original extract before addition of pure compounds (a), is at least an order of magnitude less abundant than betaine.

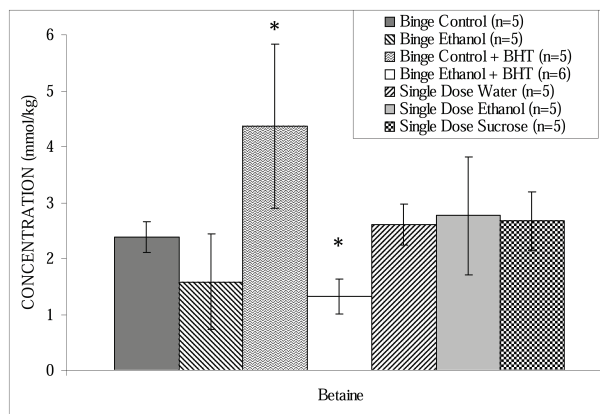


Figure 3.7: Effect of BHT and ethanol on betaine concentration in liver. A single dose of ethanol appears to have no effect on betaine concentration. BHT pre-treatment elevates betaine 2.8-fold versus binge control without BHT ($p = 0.020$), whereas binge ethanol+BHT decreases betaine 3.3-fold ($p=0.0033$) versus control+BHT. There was a trend towards decreased betaine in the binge-ethanol group that received no BHT, but it was not statistically significant.

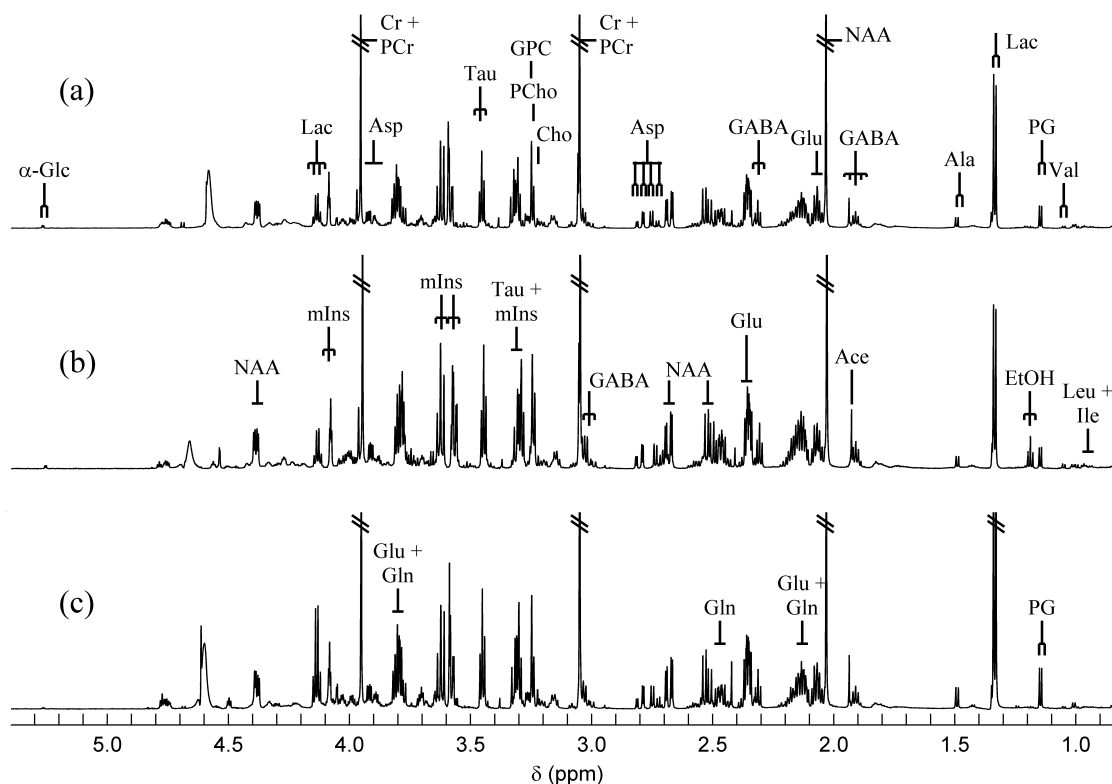


Figure 3.8: 700MHz proton spectra of brain extracts (a) control, (b) 3 hours after a single dose of ethanol (5g/kg), (c) 3 hours after a dosing with sucrose. Lactate and alanine appear to be increased in the sucrose-treated brain, but overall, the spectra are quite similar for the three groups. Abbreviations: as in Fig. 3.1, with the following additions: Asp, aspartate; GABA, gamma-aminobutyric acid; mIns, myo-inositol; NAA, N-acetyl aspartate; PCr, phosphocreatine; Tau, Taurine.

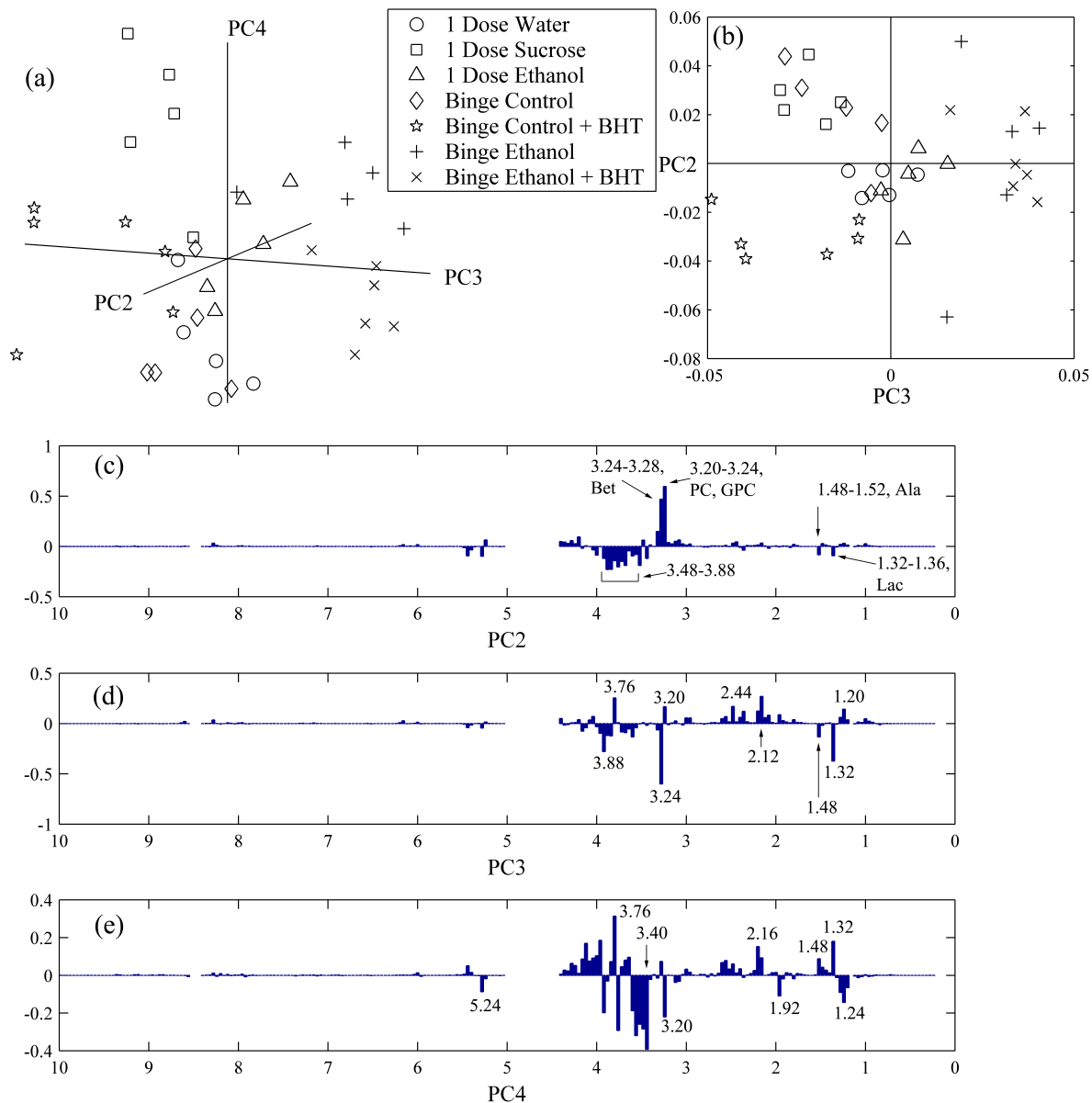


Figure 3.9: PC analysis of 700MHz proton NMR spectra of all livers (binge and single-dose analyzed simultaneously). The three-dimensional scores plot (a) shows good separation of binge-ethanol-treated animals (with and without BHT pretreatment) from the other animals along PC3, and to a lesser extent along PC2. A two-dimensional plot of the data projected onto PC2 vs PC3 (b) demonstrates clear separation of binge-treated animals along PC3, with single dose ethanol animals showing a trend toward separation. The loadings plots are given (c-f); annotations, when given as single numbers, refer to lower bound of a 0.04ppm wide spectral region (see methods). Key: as in Fig. 3.3.

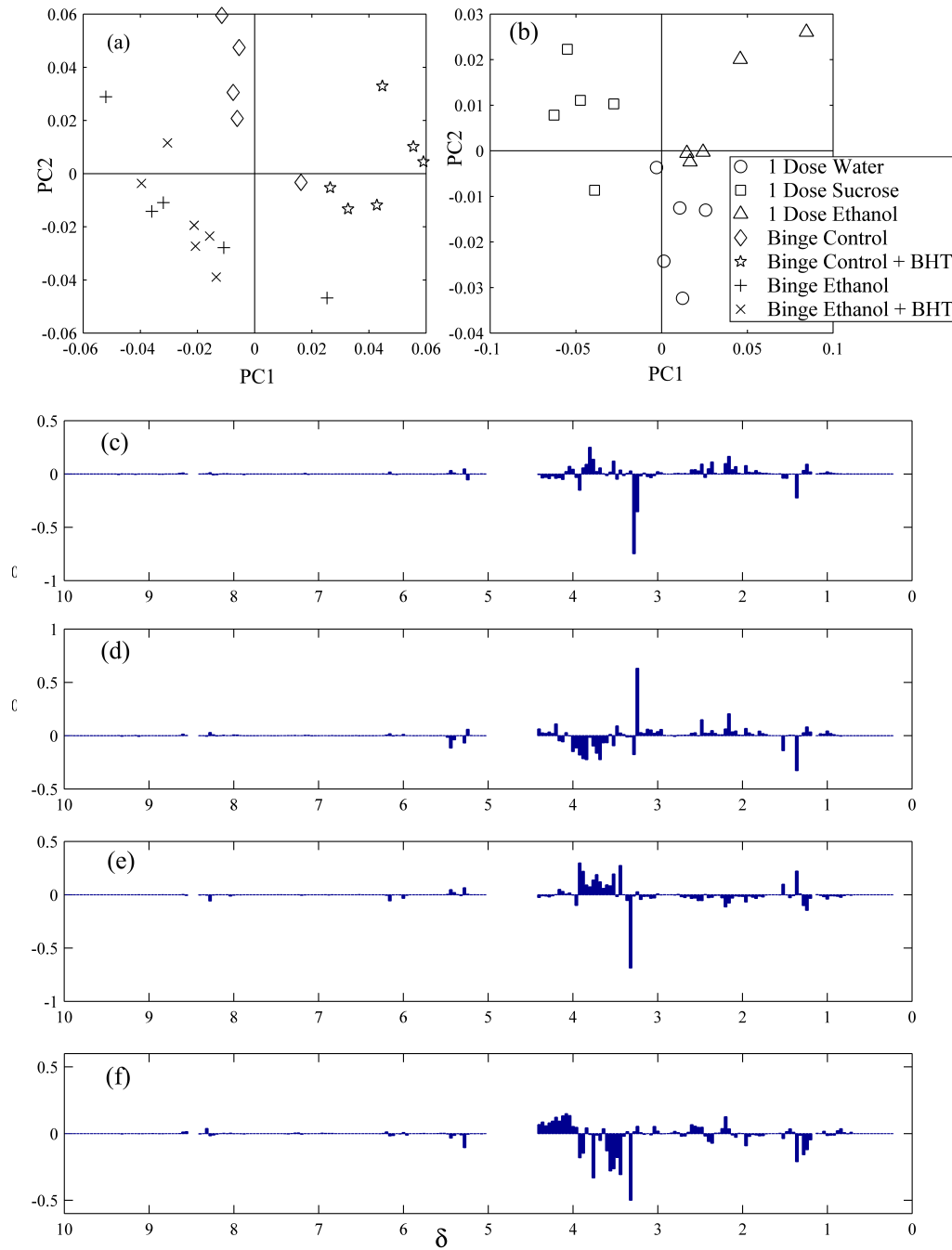


Figure 3.10: PC analysis of liver samples for binge-ethanol and binge-control groups (a), separately from single-dose groups (b). By separating the analysis in this way, the variance due to ethanol treatment is separated from differences in diet and other factors that obscured the effect of ethanol treatment in Fig. 3.9. Loading plots indicating the spectral regions that contribute to separation of various treatment groups: (c) binge PC1, (d) binge PC2, (e) single dose PC1, (f) single dose PC2.

(data not shown). However, binge-ethanol groups (with and without BHT) separated from others along PC2 (16.7% of variance) and PC3 (15.6% of variance), with the single dose ethanol group showing some separation along PC3. Loadings plots for PC2 and PC3 (Fig 3.9c,d) indicate that choline-containing compounds (δ 3.20-3.24), betaine (δ 3.24-3.28, δ 3.92-3.96), lactate (δ 1.32-1.36, δ 4.08-4.16), alanine (δ 3.20-3.24), and EtG (δ 1.20-1.24) were among the largest contributors to separation of the binge-ethanol-treated animals.

For an additional level of analysis, we performed PCA on the binge and single-dose groups separately (Fig. 3.10). By separating the analysis in this way, the variance due to ethanol treatment is separated from differences in diet and other factors that obscured the effect of ethanol treatment in Fig. 3.9. For binge animals (Fig. 3.10a), there was relative separation of the control diet versus control + BHT groups, whereas the binge-ethanol and binge-ethanol + BHT groups co-mingle in PC space. Loadings plots (Fig. 3.10c,d) indicate that choline-containing compounds and betaine made the largest contribution to PC1, with lactate, glutamate (δ 2.12-2.20), and EtG also contributing. These signals also contributed to PC2, with the spectral regions containing unresolved glucose and amino acids (δ 3.3-4.0) also making a contribution.

Single-dose groups show large separation in the scores plot (Fig. 3.10b), with PC1 differentiating ethanol and sucrose, and PC2 separating water from the other groups. The loading plots reveal that once again betaine, lactate, alanine, EtG and sugars were significant contributors to the PCs. In comparison to the binge animals, EtG made a relatively larger contribution to both PC1 and PC2 in the single dose group.

3.3.5 PC Analysis of Serum NMR Spectra

Single-dose animals that received ethanol separated dramatically from water and sucrose groups along PC1 (Fig. 3.11a). Water and sucrose groups show separation along the PC2 axis. Because of the decision not to use relaxation editing (Tang et al., 2004) to suppress signals from proteolipids, the spectra contain many broad components, especially in the 0.5-3.0ppm region, and these are reflected in the loadings plots (Fig. 3.11c,d). Loadings plots revealed that PC1 contained signals from lactate, glucose (δ 3.20-3.28, δ 3.44-3.48, δ 3.52-3.56, δ 3.88-3.92, δ 5.20-5.28), and Nac1 (δ 2.04-2.08) and Nac2 (δ 2.12-2.16); with respect to water and sucrose controls, ethanol-treated animals showed decreases in all of these compounds (negative PC1 values). PC2 separates groups based on an inverse relationship between lactate and Nac1,2, with an additional

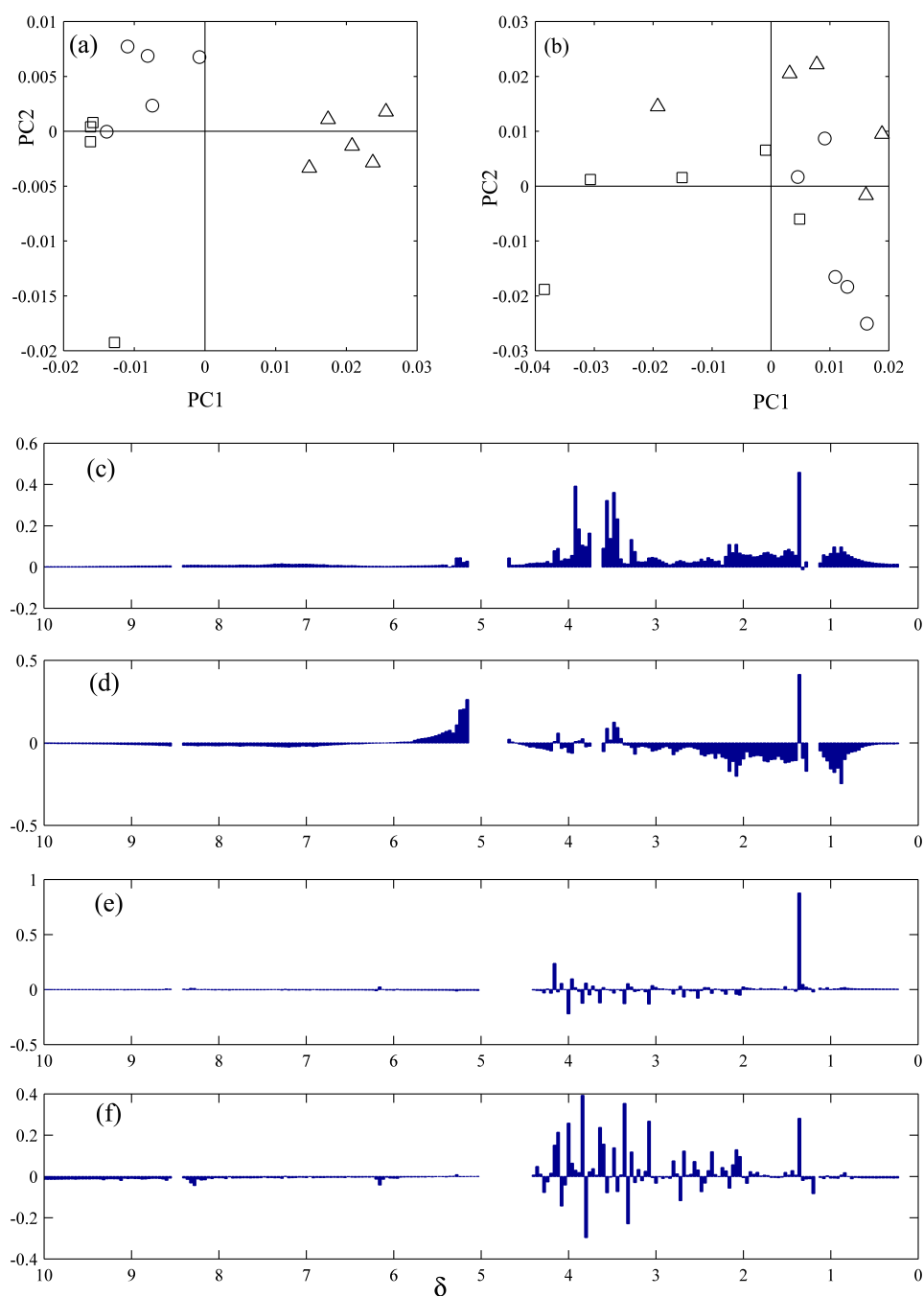


Figure 3.11: PC analysis of single dose serum (a) and brain (b). Serum shows clear separation of alcohol-treated animals (triangles) from water- (circles) and sucrose-treated animals (squares) along PC1, with some separation of water and sucrose treated animals along PC2. Brain shows some separation of groups along PC1, but PC2 appears to be less informative. Loadings plots for serum PC1 (c) and PC2 (d), and brain PC1 (e) and PC2 (f) indicate which spectral regions contribute to the classification of various groups.

contribution from the signal at δ 0.84-0.88. On this basis, sucrose-treated animals appear to have a large Lac/Nac1,2 ratio (positive PC2 values) whereas water-treated animals have a low Lac/Nac1,2 ratio (negative PC2 values).

3.3.6 PC Analysis of Brain NMR Spectra

PC analysis of brain spectra revealed incomplete separation of the ethanol, water, and sucrose groups in the scores plot (Fig. 3.11b), though some trends are evident. The mean PC2 value for the ethanol group is lower than either of the other two groups. The water-treated group is tightly clustered in PC1, but shows large spread in PC2. The loadings plots (Fig. 3.11e,f) reveal that lactate was the largest contributor to PC1 (which explained 45.9% of the variance), followed by creatine+phosphocreatine (δ 3.96-4.00). PC2 showed two dispersive ("one up, one down") pairs indicative of signals (glutamate + glutamine at δ 3.80, and taurine+myoinositol at δ 3.32) whose frequency drifted at least one bin width (0.04ppm, 28Hz) across the data set. Combining these pairs of buckets into a single bin (width 0.08ppm) and repeating PC analysis did not yield appreciable improvement in the separation of the groups in the scores plot (data not shown).

3.4 Discussion

3.4.1 Energy Metabolites in Liver and Serum

Our findings shed light on the effects of ethanol on gluconeogenesis and how lactate and alanine participate in these effects. Our finding that both acute and binge ethanol decreased lactate and alanine in rat liver and in serum are consistent with previous studies (Ling and Brauer, 1991). There exists, however, some debate about the effect of ethanol on glucose regulation. Cohen et al. found in perfused mouse livers that acute ethanol stimulates hepatic utilization of [3- 13 C] alanine for gluconeogenesis (Cohen et al., 1979), and they explained this result on the basis that ethanol oxidation increases the NADH/NAD ratio. An earlier study also found in perfused livers that ethanol stimulated gluconeogenesis from alanine and increased consumption of lactate (Williamson et al., 1969). However, Krebs himself reported that ethanol inhibits gluconeogenesis (Krebs et al., 1969). More recently, Mokada et al. reported that incorporation of 14 C from lactate into glucose in perfused rat liver was inhibited

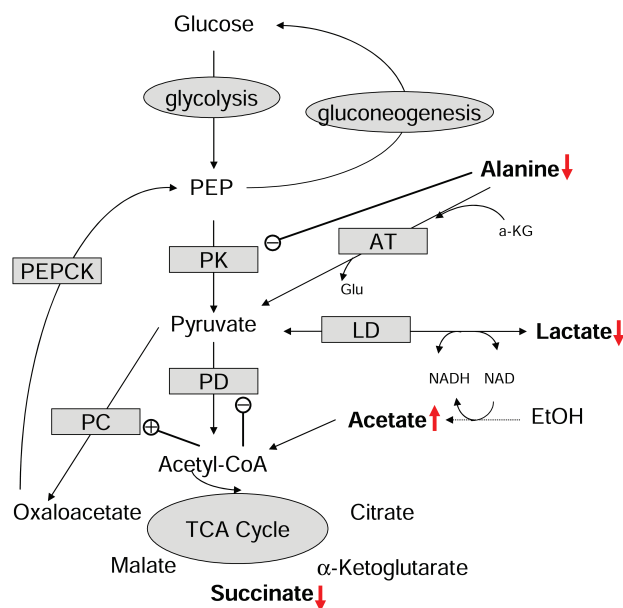


Figure 3.12: Metabolic perturbations in liver during ethanol metabolism. Bold arrows indicate observed changes in hepatic metabolite concentrations in response to binge-ethanol exposure. Ethanol oxidation to acetaldehyde via cytosolic ADH increases cytosolic NADH, and mitochondrial oxidation of acetaldehyde to acetate via ALDH increases intramitochondrial NADH. The elevated acetate and NADH/NAD levels stimulate gluconeogenesis, initially by increasing flux through pyruvate carboxylase (PC; EC 6.4.1.1). Subsequently, lactate and alanine are converted to pyruvate via alanine transaminase (AT; EC 2.6.1.2) and lactate dehydrogenase (LD; EC 1.1.1.27). Reduced alanine levels remove inhibition of pyruvate kinase (PK EC 2.7.1.40), converting phosphoenolpyruvate (PEP) formed in response to the high NADH/NAD ratio to pyruvate, and thus creating a futile cycle.

up to 80% by ethanol (Mokuda et al., 2004), and they point out that hepatic regulation of glucose is different in the fed versus the fasted state. Our data are consistent with consumption of lactate and alanine, but we find no evidence of increased glucose production (Fig. 3.4, Fig. 3.2) following acute or binge ethanol administration; if anything, the data suggest the opposite: decreased glucose after binge ethanol administration (Fig. 3.4), and no increase in hepatic glucose following a single dose of ethanol. Figure 3.12 shows a possible mechanism wherein elevated NADH initially stimulates gluconeogenesis: flux through pyruvate carboxylase (PC) and phosphoenolpyruvate carboxykinase (PEPCK) increase, and gluconeogenic precursors (lactate and alanine) replenish the pyruvate that is consumed. Later, however, decreased alanine levels remove inhibition of pyruvate kinase (PK) (Llorente et al., 1970), leading to a futile cycle from pyruvate to oxaloacetate to phosphoenolpyruvate (PEP), and then back to pyruvate. One may explain the apparently contradictory results of the studies mentioned above by the observation that decreased intracellular alanine during ethanol oxidation is critically important in the regulation of gluconeogenesis. Whereas alanine is rapidly depleted during ethanol oxidation *in vivo* (Fig. 3.4), Cohen et al. supplied alanine in the perfusate, so that intracellular alanine was maintained even during ethanol oxidation. Without a decrease in intracellular alanine, PK remained inhibited, and PEP was used for gluconeogenesis, avoiding the futile cycle. Presumably, when lactate rather than alanine was supplied in the perfusate (Mokuda et al., 2004), alanine was depleted (as it is *in vivo*), and gluconeogenesis was short-circuited by increased PK activity. Though our explanation appears to have resolved the discordant findings, additional studies with labeled tracers are required to prove the operation of a futile cycle during ethanol metabolism. An approach similar to the one used by Petersen et al. (Petersen et al., 1994) might be appropriate, although the preceding discussion highlights the importance of selecting tracer molecules that do not directly modulate the activities of the enzymes under study. Therefore, labeled lactate, perhaps in conjunction with other molecules, may be a better choice than alanine for this purpose. Regardless, our studies suggest that *in vivo* ethanol does not stimulate gluconeogenesis in liver.

We found that ethanol decreased lactate, whereas an entirely different perspective on hepatic lactate metabolism during ethanol exposure was presented by Lieber et al. who report that the elevated NADH/NAD ratio during ethanol oxidation caused conversion of pyruvate to lactate in hepatocytes in order to regenerate reduced NAD cofactors in the cytosol (Lieber et al., 1962) where AHD is active (Eckardt et al., 1998). According to this view, the lactate would be released into the blood where

hyperlactecemia would inhibit excretion of uric acid in the kidney, thus explaining the association between alcohol consumption and gout (Lieber et al., 1962; Lieber, 1965). Despite the conceptual appeal of this explanation (which has been cited in reviews published as recently as 2005 (Yamamoto et al., 2005)), it is at variance with our finding of decreased lactate in both liver and blood after both acute and chronic ethanol exposure. We note that the original finding of increased blood lactate after ethanol infusion (Lieber et al., 1962) was based on a colorimetric assay that relied upon the conversion of lactate to acetaldehyde by heating in concentrated sulfuric acid (Barker and Summerson, 1941). Given that blood ethanol levels were in the 200-300 mg% range (44-65mM) in Lieber et al's study (Lieber et al., 1962), only a small fraction of this ethanol converted to acetaldehyde during the procedure would cause falsely elevated estimates of serum lactate levels. We believe this flaw in the original assay is the most likely explanation for the discordant findings, and that ethanol in fact causes lactate to decrease in both liver and serum.

Another endogenous energy metabolite that may be involved in the pathway shown in Fig. 3.2 is succinate. The difference in hepatic succinate levels between the binge group and the single-dose group may perhaps reflect differences in the liquid diet that the binge animals received, versus rat chow that other animals were fed. Within the binge group, the decrease in hepatic succinate due to ethanol may reflect operation of the mechanism proposed in Figure 3.2. Specifically, if flux of oxaloacetate through phosphoenolpyruvate carboxykinase (PEPCK) versus citrate synthase (CS) was increased, as might be expected by the elevated NADH/NAD ratio during ethanol oxidation (see above), the net result would be increased conversion of succinate to oxaloacetate, and decreased formation of succinate. Though speculative, this explanation is consistent with the available data and known mechanisms of biochemical regulation for the pathways involved. Further experiments are required to clarify ethanol's effect on the PEPCK/CS ratio for oxaloacetate and the impact on succinate.

Effect of Inadvertent Ethanol Dosing in Control Animals

The trend toward increased acetate in liver and serum (Fig. 3.3,3.4, 3.1,3.2) are consistent with the oxidation of ethanol to acetate in the liver, and the release of the 90% or more of the ethanol-derived acetate into the blood (Jucker et al., 1998). Unfortunately, the single-dose animals, for which serum and liver were collected simultaneously, inadvertently received ethanol as a component of the vehicle for the pentobarbital anesthetic, and therefore displayed blood acetate levels greater than the 0.2-0.3mM expected

in the absence of ethanol (Carmichael et al., 1991). Nevertheless, the trends toward increased acetate in serum of ethanol-treated animals are still evident (Fig. 3.2), and in the liver, if the binge-control values (Fig. 3.4) are taken as representative of the baseline state, the effect of a single dose is clearly to increase acetate several-fold. Increased serum acetate could affect metabolism in a number of tissues and suggests that although liver metabolizes much of the ethanol, acetate produced from ethanol could alter metabolism throughout the organism.

Ketone Body Formation

The effect of ethanol on ketone body formation can be seen in the increase in beta-hydroxybutyrate in the liver (Fig. 3.4) and acetoacetate in the serum (Fig. 3.2). It is likely that these molecules represent a means for the liver to dispose of the surfeit of ethanol-derived acetate via the following mechanism. In a reaction catalyzed by acetyl-CoA C-acetyltransferase (EC 2.3.1.9), two molecules of acetyl-CoA condense to form acetoacetyl-CoA that is converted to acetoacetate via 3-ketoacid CoA-transferase (EC 2.8.3.5) (Kanehisa et al., 2006). Subsequently, acetoacetate can be converted to beta-hydroxybutyrate by beta-hydroxybutyrate dehydrogenase (EC 1.1.1.30), regenerating one molecule of NAD from NADH and thus facilitating oxidation of ethanol. The fact that acetoacetate was not detectable in liver spectra suggests that this molecule is transported into the blood. Since both a single dose of ethanol and the 4-day-binge treatment caused a similar increase in beta-hydroxybutyrate, induction of enzymes does not appear to play a role in ethanol-induced ketone body formation.

3.4.2 Energy Metabolites in Brain

Brain tissue is extremely sensitive to ischemia and hypoxia, and despite our efforts to freeze brain samples rapidly, spectra reveal high lactate levels and low glucose levels (Fig 3.8) indicative of anaerobic metabolism during the interval between decapitation and complete freezing of brain tissue. Though this anaerobic interval undoubtedly perturbed levels of energy metabolites such as glucose, ATP, and phosphocreatine, it has been shown not to alter brain amino acid levels (Siesjo, 1978), and the spectra reveal numerous well-resolved signals from various brain metabolites that are within the ranges measured in previous studies (Govindaraju et al., 2000). Thus we felt confident that with the exception of glucose, lactate, and other energy metabolites, the values we measured were reasonable estimates of the *in vivo* concentrations for brain metabolites,

and that therefore metabolomic analysis of these samples was appropriate.

3.4.3 Betaine Metabolism and Transmethylation

Previous studies have found that betaine, an important precursor of s-adenosylmethionine (SAM), is decreased by chronic ethanol administration in rats due to increased activity of betaine-homocysteine S-methyltransferase (EC 2.1.1.5) (Barak et al., 1996). Moreover, dietary supplementation with betaine during chronic ethanol feeding prevents the formation of fatty liver (Barak et al., 1993). It is possible that in control animals, BHT treatment increases betaine levels by providing an alternative donor for methyl groups, but it appears that during binge ethanol exposure, BHT does not prevent a decrease in hepatic betaine (Fig. 3.7). To our knowledge, this is the first finding of decreased hepatic betaine after only 4 days of ethanol intake. Presumably this decrease signifies increased utilization of betaine for the production of SAM, which may be related to the methylation of DNA associated with ethanol exposure (Bleich et al., 2006).

3.4.4 Brain Metabolites

As discussed above, the tissue collection procedure introduced ischemic changes in the brain energy metabolites but should not have altered brain amino acids (Siesjo, 1978). Given the large number of well-resolved peaks from a large number of molecules in the brain spectra, it would seem an ideal data set for metabolomic analysis. The relative lack of effect of ethanol on endogenous brain metabolites is somewhat surprising, but one must keep in mind that ethanol's well-documented effects on the release of various amino acids in brain will not be detected in whole-brain extracts. The only effects that we can observe in this study are those that change the whole-brain concentration of a given molecule: net synthesis, catabolism, or transport. Previous studies using *in vivo* proton NMR spectroscopy (MRS) after a single dose of ethanol failed to detect changes in endogenous brain metabolites in rhesus monkeys (Kaufman et al., 1994), and humans (Mendelson et al., 1990). Following 16 weeks of ethanol treatment in rats, phosphocholine increased 1.2-fold, and after 60 weeks, glycerophosphocholine decreased 1.5-fold (Lee et al., 2003), suggesting that the effect of chronic ethanol exposure varies over time. Other investigators found a 1.25-fold decrease in the mIns/(Cr+PCr) ratio after 8 weeks of ethanol treatment in rats (Braunova et al., 2000). Perhaps a more pertinent measure than the effect of ethanol on concentrations of brain metabolites is the effect of ethanol on various fluxes of metabolites in brain. Brain metabolism is

known to be compartmentalized in astrocytes and neurons, with separate TCA cycles operating in each compartment (Benjamin and Quastel, 1972). Acetate is a substrate for the astrocytic compartment (Waniewski and Martin, 1998), and during chronic ethanol exposure it may disrupt the normal metabolic coupling between neurons and astrocytes required for neurotransmission (Sibson et al., 1998). Studies are currently underway to address this point.

3.4.5 Ethyl Glucuronide

Previous studies have found that high concentrations of ethanol cause formation of EtG in the liver. Reports have focused on determination of ethyl glucuronide using sensitive techniques such as ELISA and GC-MS to achieve low detection thresholds. However, quantification via NMR has not been demonstrated to date. The fact that hepatic EtG reached near-maximal levels (2mmol/kg) within 3 hours of ethanol consumption (Fig. 3.5) while the time constant for elimination is on the order of days (Wurst et al., 2004), suggests a significant barrier to the release of EtG from the liver into the blood. Our studies suggest that EtG is elevated by the first dose of ethanol and remains elevated for days during ethanol treatment.

Interestingly, BHT reduced the formation of EtG. The simplest explanation for the decreased formation of EtG in binge-ethanol animals pretreated with BHT is that the BHT (35% of which is eliminated via glucuronidation (Lanigan and Yamarik, 2002)) was a better substrate for activated glucuronide than was ethanol. Our reasoning is as follows: if a large (80mM BEC) dose of ethanol is required to produce EtG, but even at that concentration, only 0.1% is metabolized via glucuronidation, whereas 35% of a much smaller dose of BHT is glucuronidated, then BHT is at least 350 times more likely to react with activated glucuronide than is ethanol. On the other hand, the daily dose of BHT (120mg/kg) is, on a molar basis, 1/320 the size of the daily ethanol dose. Therefore, in terms of the probability of reacting to form a glucuronide, a 120mg/kg dose of BHT and an 8.6g/kg dose of ethanol might reasonably be expected to compete on an equal basis for activated glucuronide. On the other hand, our data do not allow us to exclude the possibilities that (i) BHT enhanced release of EtG from liver without altering formation, or (ii) that BHT decreased EtG formation via a more complex mechanism than the one described above. Further studies will be required to clarify this point. In any case, to our knowledge, this is the first report of a compound that could be consumed as part of a normal diet that can decrease the formation of

EtG. If our interpretation is correct, one would anticipate an even greater inhibition of EtG formation in humans who excrete almost twice as much (63%) of a dose of BHT as glucuronide conjugates, compared to rats (Lanigan and Yamarik, 2002). This effect has important implications for the use of EtG as a biomarker for ethanol use since the formation of EtG can be reduced by recent consumption of BHT, and, presumably, many other compounds that are eliminated via glucuronidation would exert a similar effect. While this phenomenon would not produce false-positive results, it may diminish the value of negative EtG test results in ruling out recent ethanol use (Wurst et al., 2000; Skipper et al., 2004; Droenner et al., 2002). Additional studies, particularly in humans, will be required to clarify this issue.

3.4.6 PC Analysis

PC analysis provided an unbiased assessment of the spectral changes induced by ethanol in each of the tissues studied. Given the small sample size relative to the number of spectral regions analyzed, the clustering of the 7 treatment groups in Figure 3.9 indicates that significant and consistent perturbations of the endogenous metabolites were present in each treatment condition. Moreover, when the samples from the 4-day binge treatment were analyzed separately, the ethanol-treated samples could be classified with 100% accuracy using a linear separation in the scores plot (Fig. 3.10a). The same is true of the serum samples (Fig. 3.11a). While clustering of the brain data was less impressive, it appears that certain metabolites with large amplitude in PC2 may be altered by ethanol. The limited sample size in this study precludes any definite conclusion on this point. A larger study, perhaps including binge-ethanol-treated brain samples would have a greater chance of identifying metabolites that are altered in brain. In addition, though previous studies indicate that rapid freezing after decapitation does not substantially alter brain amino acids (Siesjo, 1978), it might be the case that certain biochemical differences due to ethanol are lost during the sacrifice and tissue collection procedure. Microwave irradiation, funnel-freeze, or freeze-blow techniques to collect brain tissue might reveal differences that cannot be detected with the techniques and equipment used in this study.

3.4.7 Conclusion

Using NMR-based metabolomics we have identified key metabolic effects of both acute and 4-day binge ethanol exposure. By determining that ethanol decreased lactate and

alanine in both the liver and blood, we were able to focus on key differences between isolated perfusion studies and the conditions that prevail *in vivo*. This metabolomic analysis led to the insight that the depletion of hepatic alanine *in vivo* could produce a futile cycle that would not be discovered during the perfusion of isolated livers, and thus led us to propose a model that resolves apparently discordant findings regarding the effect of ethanol on gluconeogenesis.

In addition, the use of NMR spectroscopy removed potential confounding issues associated with chemical assays used to measure serum lactate in an older study. We were therefore able to show that a single dose of ethanol actually decreases serum lactate contrary to previous reports.

Finally, although PC analysis provides a useful tool for identification of metabolites perturbed by exogenous toxins, we note that detailed spectral analysis is required to understand the biochemical information at the mechanistic level. Of critical importance is correct assignment of spectral signals to the metabolites that produce them. Towards this end we have clarified the identity of betaine in liver extracts in this report, and identified ethyl glucuronide in a separate report (chapter 2). The identification of these metabolites in our spectra enabled us to extract information latent in our metabolomic data, and thus to report for the first time that 4-day binge ethanol administration decreases hepatic betaine, and that BHT reduces hepatic EtG levels during binge ethanol administration.

Chapter 4

Cerebral Metabolism of Ethanol-Derived Acetate: A Metabolic Basis for Dependence?

4.1 Introduction

Ethanol is consumed in alcoholic beverages in large quantities that contribute nutritional calories and cause a major alteration in metabolism. Ethanol is perhaps the only drug that produces millimolar blood levels of its direct metabolite, acetate, which can be a source of energy. Ethanol oxidation in the liver accounts for more than 90% of ethanol elimination (Norberg et al., 2003), producing the two-carbon fatty acid, acetate, much of which is not metabolized in liver. Nearly all of the acetate produced during hepatic ethanol oxidation is released into the blood (Jucker et al., 1998). Acetate can enter the TCA cycle to be metabolized. However, it needs to be converted to acetyl-CoA by Acetyl-CoA Synthetase (ACoAS, EC 6.2.1.1) which may regulate the level of acetate metabolism by cells. Thus, the metabolic effects of ethanol involve primarily ethanol metabolism in liver and subsequent metabolism of acetate in multiple other tissues.

Acetate metabolism might be important in tissues with high metabolic activity and blood flow such as the brain. In fact, it has been hypothesized that brain acetate metabolism may increase during chronic ethanol consumption, perhaps contributing to neuroadaptation and dependence to ethanol (Roach and Resse, 1972; Derr et al., 1981; Israel et al., 1994; Volkow et al., 2006). The rationale for this hypothesis is based on the following findings. Acetate is produced at low levels by intestinal flora (Waniewski and

Martin, 1998), leading to a basal blood acetate concentration of approximately 0.1-0.3 mM in humans (Sarkola et al., 2002), and rats (Carmichael et al., 1991). During hepatic oxidation of ethanol, more than 90% of the resulting acetate is released into the blood (Jucker et al., 1998), causing the blood acetate concentration to rise 3- to 7-fold to the 1-2mM range (Carmichael et al., 1991; Sarkola et al., 2002). The zero-order kinetics of ethanol elimination imply a constant rate of acetate production for nearly the entire duration of ethanol metabolism. Thus, blood acetate is maintained at a significantly elevated levels throughout the period of ethanol intoxication (Orrego et al., 1988). In alcoholics and heavy drinkers, the rate of ethanol metabolism is more rapid, resulting in acetate plateau levels approximately 2-fold higher in alcohol-tolerant individuals than in controls (Korri et al., 1985), suggesting greater availability of acetate as a substrate for brain metabolism. Therefore, ethanol metabolism results in an abundant supply of acetate in the blood that could alter brain metabolism.

Early studies using [^{14}C] acetate demonstrated that carbons from acetate show rapid metabolism in brain and preferential incorporation into cerebral glutamine rather than glutamate, while the reverse occurred when [^{14}C] glucose was provided as the tracer molecule (O'Neal and Koeppe, 1966). These observations gave rise to the hypothesis that cerebral metabolism consists of two compartments: one that preferentially metabolizes acetate and contains a "small" glutamate pool which is rapidly converted to glutamine, and a second compartment that utilizes glucose and contains a "large" glutamate pool (Van den Berg et al., 1969). Since astrocytes express glutamine synthetase (Norenberg and Martinez-Hernandez, 1979), it was supposed that they represent the "small" glutamate pool, and that cerebral acetate metabolism takes place mainly within astrocytes (See Fig. 4.1). This view is now widely accepted (Zwingmann and Leibfritz, 2003), and an acetate transporter that is absent on neurons appears to account for the selectivity of acetate in labelling the astrocytic compartment (Waniewski and Martin, 1998). Whereas many studies used exogenous acetate as a tracer, Roach et al. showed that [^{14}C] ethanol given intraperitoneally to hamsters labeled brain glutamine, glutamate, and GABA (Roach and Resse, 1972), supporting the idea that acetate derived from ethanol oxidation is a substrate for the brain. These findings suggest that ethanol derived plasma acetate is metabolized by brain astrocytes providing an energy source that differs from that provided by glucose.

Recently, Volkow et al. used PET studies in human volunteers to show that modest doses of ethanol reduce the rate of brain glucose utilization by 10-23% (Volkow et al., 2006). These decrements in glucose utilization are out of proportion to the sedative

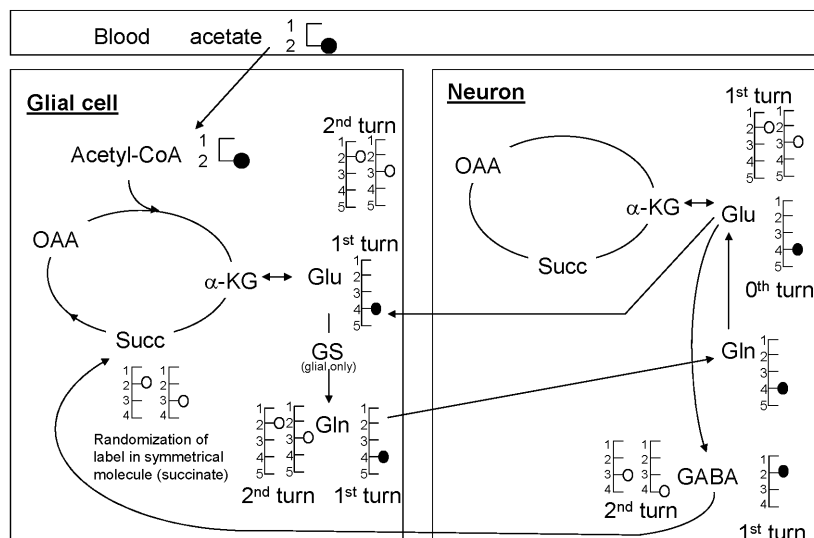


Figure 4.1: Model for cerebral metabolism of $[2-^{13}\text{C}]$ acetate showing incorporation of ^{13}C into the astrocytic TCA cycle and the resulting effect on the glutamine-glutamate cycle. Acetate is transported into astrocytes, converted into Acetyl-CoA by ACoAS, and enters the TCA cycle. After the first quarter turn, labeled carbon skeletons can leave the TCA cycle as glutamate, which is rapidly converted to glutamine in astrocytes. Both glutamine and glutamate will be labeled at the 4-carbon (closed circles) from this first turn labeling. Astrocytic glutamine is transported to neurons as a precursor for neurotransmitter glutamate. Glutamate released from neurons is taken up by astrocytes, thus completing the glutamine-glutamate cycle. Carbons which traverse a complete turn of the TCA cycle are scrambled due to the molecular symmetry of succinate, and thus glutamate and glutamine C3 and C2 are labeled equally on the second turn (open circles). GABA derived from glutamate labeled in C2 and C3 will be labeled in C3 and C4. Abbreviations: α -Ketoglutarate, α -KG; Oxaloacetate, OAA, Succinate, Succ, Glutamate, Glu, Glutamine, Gln, γ -aminobutyric acid, GABA; Glutamine Synthetase, GS.

effect of ethanol, suggesting that ethanol does not decrease brain metabolic demand at these doses. Therefore, this finding could indicate a shift in substrate utilization from glucose to acetate during ethanol consumption, even at low doses of ethanol. The same group found that larger doses of ethanol (1g/kg) caused similar reductions in brain metabolism of glucose, with greater reductions in alcoholics than control subjects (Volkow et al., 1990), suggesting that alcohol exposure may result in increased brain utilization of acetate. Likewise, decreased glucose metabolism in brain during ethanol exposure occurs in rats (Learn et al., 2003) and hamsters (Roach and Reese, 1971), demonstrating that rodents are suitable model organisms for the study of this phenomenon. Taken together, these data support the hypothesis that brain may adapt to chronic ethanol intake by increasing brain metabolism of acetate. One putative mechanism could involve greater capacity to transport acetate into astrocytes and greater activity of ACoAS, an enzyme required to bring acetate into the TCA cycle to form glutamine-glutamate. Kiselevski et al. found a 36% increase in cortical ACoAS activity in homogenates of rat cortex following 7 days of ethanol treatment (Kiselevski et al., 2003), consistent with an adaptive increase in acetate metabolism by brain during chronic ethanol exposure.

Neurons and glia are metabolically linked. Neurons rely on astrocytes for metabolic support, including supply of precursors for synthesis of glutamate. Inhibition of the astrocytic TCA cycle by fluoroacetate in day-old chicks inhibits glutamate-dependent aversive learning, but injection of glutamate overcomes this effect (Hertz et al., 1996). If astrocytes fail to support neuronal synthesis of glutamate required for aversive learning, this could contribute to perseverative behavior observed after withdrawal (Obernier et al., 2002b) that interferes with recovery. In addition, recent evidence implicates astrocytes as active participants in synaptic events, capable of releasing glutamate in a Ca^{2+} -dependent fashion (Newman, 2003). Derr et al. (Derr et al., 1981) found that intragastric (i.g.) injections of sodium acetate significantly reduce the incidence of whole body tremors in ethanol withdrawing physically dependent rats (Majchrowicz, 1975). This result is consistent with acetate becoming a component of the development of ethanol dependence, perhaps by alterations in brain use of acetate. To investigate ethanol-acetate metabolism in brain after acute and chronic ethanol treatment we designed experiments using ^{13}C -labeled tracers. Our objectives were to determine conclusively whether ethanol-derived acetate is a substrate for brain metabolism, and also to determine whether chronic ethanol exposure would induce an increase in cerebral acetate metabolism. To our knowledge, ours are the first studies of brain metabolism

after administration of ^{13}C ethanol. The ^{13}C NMR studies we report offer an important advantage over previous ^{14}C studies (Mushahwar and Koeppe, 1972; Roach and Resse, 1972) because ^{13}C NMR spectra inherently contain positional information about the particular carbon atoms within a given metabolite that are labeled by the tracer. This additional level of detail enables the differentiation of carbon isotopomers, and thereby reveals the metabolic history of the labeled carbon skeletons. Thus, ^{13}C isotopomer analysis strengthens any conclusions about which labeled substrates derived from ethanol, if any, are metabolized in the brain. Finally, we collected serum samples from all animals at the time of sacrifice to determine which labeled substrates were available in blood as substrates for brain metabolism.

4.2 Methods

4.2.1 Chemicals

[2- ^{13}C] acetate, [2- ^{13}C] ethanol, and 3-(trimethylsilyl)propionic-2,2,3,3-d $_4$ acid (TSP) (all 99% enriched) were obtained from Isotec (Miamisburg, OH). All other chemicals were of the highest purity available.

4.2.2 Animal Procedures

All procedures for handling and sacrifice of animals were approved by the UNC-Chapel Hill Internal Animal Care and Use Committee (IACUC) and were in accordance with National Institute of Health regulation for the care and use of animals in research. Adult male Sprague-Dawley rats (Charles River Labs, Inc.) were allowed to acclimate for 2-4 days prior to the start of all experiments. One group of animals was fasted overnight and given a single dose of either [2- ^{13}C] ethanol (1g/kg, i.g.), [2- ^{13}C] acetate (0.5g/kg i.p.), or natural abundance ethanol (1g/kg, i.g.). Animals were sacrificed at 30 minutes (acetate) or 15, 30, 60, and 240 minutes (ethanol) after being dosed (see Fig. 4.2, "Acute group"). Time points were selected on the basis of previous studies using ^{13}C acetate in rats (Hassel et al., 1995). The dose of [2- ^{13}C] acetate was selected on the basis of the same studies, and the dose of [2- ^{13}C] ethanol was selected on the basis that 1g/kg of ethanol produces near maximal serum acetate levels (Carmichael et al., 1991). Five minutes prior to sacrifice, animals were anesthetized with pentobarbital sodium (0.65ml of a 50mg/ml solution in water, i.p.). Following the onset of surgical anesthesia, an abdominal incision exposed the liver and inferior vena cava (IVC). A

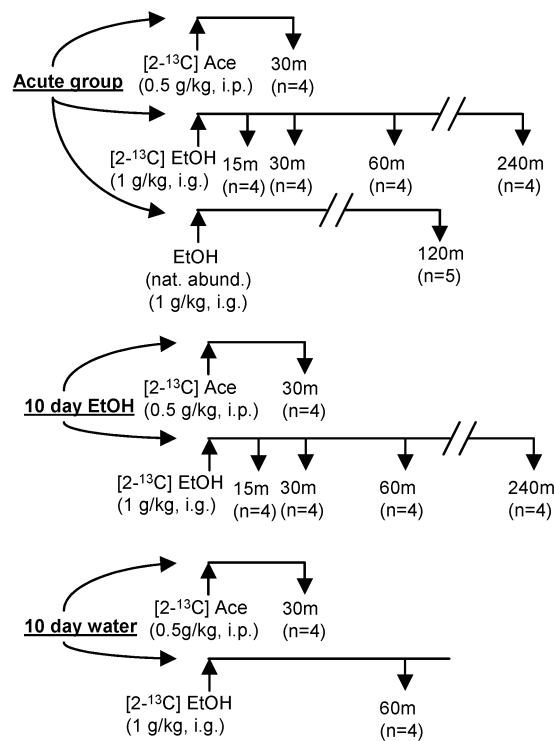


Figure 4.2: Experimental Design. Three treatment groups were studied: (i) acutely dosed, ethanol-naïve animals, (ii) animals dosed for 10 days with natural abundance ethanol (5g/kg/day, i.g. of 20% ethanol w/v in water), and (iii) control animals dosed for 10 days with water (i.g.). Animals from each group were selected randomly for dosing (up arrows) with ¹³C-enriched ethanol, or acetate, or natural abundance ethanol. Animals were sacrificed (down arrows) and tissues were collected (as described in the text) at the time points indicated.

blood sample (2-4ml) was collected from the IVC and allowed to clot on ice. Next, each animal was decapitated and the skull immediately immersed in liquid nitrogen with agitation in the liquid to hasten the freezing process, while a small piece of liver (1-2g) was quickly removed, wrapped in aluminum foil, and frozen in liquid nitrogen. The time from surgical anesthesia to decapitation was approximately 90 seconds; the time between the start of blood withdrawal and decapitation was less than 45 seconds; the time from decapitation to placing the liver sample in liquid nitrogen was less than 30 seconds. Clotted blood was centrifuged, and serum was removed and stored, along with liver and skull samples, at -80°C until further analysis.

A second group of animals received either ethanol (5g/kg, 20% w/v, i.g.) or water (i.g.) daily for 10 days. During this time animals had free access to food and water, and were monitored for signs of distress. Following the 10-day treatment with either ethanol or water, animals were fasted overnight, and on the 11th day they were dosed with either [2-¹³C] ethanol (1g/kg, i.g.) or [2-¹³C] acetate (0.5g/kg i.p.) and sacrificed as described above (see Fig. 1). Two animals were excluded from analysis, one due to incomplete ethanol dosing and one due to loss of tissue homogenate during processing.

4.2.3 Tissue extraction

Brains were removed from skulls under liquid nitrogen using a rotary cutting tool (Dremel) and a hammer and chisel. Frozen brains were pulverized under liquid nitrogen in a stainless steel mortar and pestle and extracted twice with ice cold 8% perchloric acid (Gutmann and Wahlefeld, 1974). The pooled extracts were neutralized with 5M K₂CO₃, insoluble potassium perchlorate salts were removed by centrifugation at 0°C, and the extracts were lyophilized to a dry white powder (Fan et al., 1986).

4.2.4 NMR and HPLC sample preparation

Lyophilized extracts were dissolved in 2ml/g tissue of D₂O (99.9%, Cambridge Isotope Laboratories, Andover, MA) containing 0.1M phosphate buffer at pH 7.0 (pD 6.6), 0.1% 1-4 dioxane (Fisher Chemicals, Fair Lawn, NJ) as a ¹³C chemical shift and concentration reference (Kanamatsu and Tsukada, 1999), 14.4mM sodium formate (Alfa Aesar, Ward Hill, MA) as a proton concentration reference (Kriat et al., 1992), and TSP as a proton chemical shift reference. Sample pH (uncorrected) was adjusted to 6.90-7.10 using DCl and NaOD, and the sample was centrifuged to sediment insoluble perchlorate salts. 700 L was withdrawn for NMR analysis, 100 L was diluted 7.5-fold with HPLC-grade water

for HPLC analysis, and this was frozen alongside the remainder of the NMR sample at -80°C .

Serum samples were prepared by thawing from -80°C in a microcentrifuge at 13000 rpm for 4 minutes, after which $500\mu\text{L}$ of serum was mixed with $250\mu\text{L}$ of a stock solution containing 14.4mM sodium formate and 1.6mM TSP in 99.9% D_2O . $700\mu\text{L}$ of the resulting mixture was transferred to a 5mm NMR tube for analysis.

4.2.5 NMR spectroscopy

Prior to ^{13}C NMR spectroscopy of brain extracts, proton spectra were acquired on a Varian Inova 400MHz spectrometer equipped with a 5mm broad band probe, using the following parameters: duty cycle 45s, flip angle 90° , 2 s weak irradiation of residual water protons, 32k points, 4200 Hz spectral width. Next, proton-decoupled 100.54 MHz ^{13}C NMR spectra of brain extracts were acquired on the same instrument, with the inner coil of the probe tuned to ^{13}C . The spectra were accumulated in 4096 transients, using a 45° flip angle, 25kHz spectral width, 64k data points, and a duty cycle of 8 seconds. Some samples were acquired with WALTZ proton decoupling during acquisition while others were acquired with continuous GARP decoupling. Appropriate saturation factors were computed for each acquisition method. Proton spectra of serum samples were acquired on a 700MHz Varian Inova spectrometer with a cold probe using the following parameters: duty cycle 45 s, 8 repetitions, 2 s weak irradiation of residual water protons, 32k points, 12 kHz spectral width.

All spectra were acquired with oversampling to increase the effective dynamic range.

4.2.6 NMR spectral processing

All NMR data processing was accomplished using software written in-house for this purpose in the Matlab environment (The MathWorks, Inc., Natick, MA), and validated by processing selected spectra in alternative commercial (ACD) and non-commercial packages. The first 3 points of each FID were calculated using linear back prediction (basis = points 4-516, 32 coefficients) in order to remove pulse breakthrough. FIDs were zeropadded by a factor of 2, and ^{13}C FIDs were apodized with an exponential function corresponding to 5Hz lorentzian broadening prior to fourier transformation. Spectra were phase corrected, and integrals of the real spectrum were used for quantification of proton spectra. Peak heights were judged to be more reliable quantitative measures in the ^{13}C NMR data (Garcia-Espinosa et al., 2003).

4.2.7 HPLC analysis

HPLC analysis was accomplished using precolumn derivitization with 6-aminoquinolyl-N hydroxysuccinimidyl carbamate (AQC) (Cohen and Michaud, 1993), separation on a C18 reverse phase column ($5\mu\text{m}$, 4.6×250 mm Agilent Zorbax SB-C18) with gradient elution (solvent A: acetonitrile, solvent B: ammonium acetate, pH 4.9), and fluorescence detection ($\lambda_{ex} = 245\text{nm}$, $\lambda_{em} = 395\text{nm}$). Small injection volumes ($10\mu\text{L}$) were important to maintain good separation of the early-eluting peaks (Liu et al., 1998).

4.2.8 Calculation of Fractional Enrichment from ^{13}C NMR data

Saturation factors for each carbon resonance due to T1 relaxation and NOE effects were computed as described previously (Cohen, 1983; Brainard et al., 1989). Briefly, after acquiring data on control samples from animals that received natural abundance ethanol, additional pure (natural abundance) compounds were added to the NMR sample to raise the concentration to the 10-30mM range, $20\mu\text{L}$ was withdrawn and diluted for HPLC analysis, and 1H-decoupled- ^{13}C spectra were re-acquired. Saturation factors were computed based on the ratio

$$SF_{xn} = \frac{[x_n]_{\text{apparent}}}{[x]_{\text{actual}}}, \quad (4.1)$$

where SF_{xn} is the saturation factor for the resonance of carbon n in molecule x , $[x_n]_{\text{apparent}}$ is the apparent concentration of x_n based on the ratio of its NMR intensity to that of the dioxane concentration reference, and $[x]_{\text{actual}}$ is the actual concentration of x measured by HPLC. For animals that received ^{13}C tracers, absolute concentration of ^{13}C in each carbon of each molecule was estimated by the ratio of the peak intensity for each resonance to that of the natural abundance of the 4 dioxane carbons, divided by the saturation factor calculated above. Fractional enrichment (FE) above natural abundance for each carbon atom in each molecule was calculated as described in (Badar-Goffer et al., 1990):

$$FE_{xn} = \frac{([x_n] - 0.01108 * [x])}{[x]}, \quad (4.2)$$

where FE_{xn} is the fractional enrichment of carbon n in molecule x , $[x]$ is the concentration of molecule x measured by HPLC, and 0.01108 reflects the the $\sim 1.1\%$ natural

abundance of ^{13}C .

4.2.9 Calculation of Fractional Enrichment from ^1H NMR data

In regions of the proton spectra where a metabolite signal and its ^{13}C satellite peaks were well-resolved (e.g. the signals from methyl protons of acetate and lactate, and the α -anomeric proton of glucose), ^{13}C fractional enrichment was estimated (Cerdan et al., 1990). By comparing proton spectra of each sample with and without ^{13}C -decoupling during acquisition, we verified that suspected ^{13}C satellite peaks in the proton spectrum were in fact due to ^{13}C - ^1H coupling due to enrichment of ^{13}C . The lower bound for fractional enrichment measurement using this method was determined by computing the signal-to-noise ratio (SNR) (based on the peak-to-peak noise) for the protons attached to the carbon in question, and assuming that a signal-to-noise ratio (SNR) greater than 3 was required for unequivocal detection of ^{13}C satellites. The minimum fractional enrichment that would give $\text{SNR} > 3$ for ^{13}C satellite peaks is

$$FE_{min} = \frac{(3 + 3)}{(SNR + 3 + 3)} = \frac{6}{SNR + 6}. \quad (4.3)$$

4.2.10 Model of Cerebral Metabolism and analysis

To interpret the labeling of cerebral amino acids from ethanol-derived acetate, we used the accepted two-compartment model of cerebral metabolism in which neuronal and glial TCA cycles operate independently (Fig. 2) (Haberg et al., 1998). The metabolism of $[2-^{13}\text{C}]$ acetate by astrocytes results in first-turn labeling of glutamate C4, which is rapidly converted to glutamine by the action of glutamine synthase. The operation of the glutamate-glutamine cycle moves glutamine to neurons where it is converted to glutamate, released during neurotransmission, and taken up into astrocytes where it is converted back to glutamine. In GABAergic neurons, GABA can be synthesized either from glutamate carbon skeletons derived directly from astrocytic glutamine, or from the pool of neuronal glutamate that has traversed the neuronal TCA cycle (Hassel et al., 1995). We used the approach described by Hassel et al. to estimate the fractional loss of labeled intermediates from the TCA cycle on each turn via the C3/C4 ratio in glutamate and glutamine, and the corresponding C3/C2 ratio in GABA (Hassel et al., 1995).

4.2.11 Statistical analysis

The statistical significance of differences between means of measured parameters in different treatment groups was assessed using a t-test (2-tailed, unequal variance). When multiple comparisons were made, Bonferroni correction was applied. When comparing the FE of carbons predicted by our model to have identical enrichment, data for each animal were analyzed using a paired t-test (2-tailed).

4.3 Results & Discussion

4.3.1 Animals and tissue extraction

Acute treatment resulted in maximal blood levels of $\sim 20\text{mM}$ (Table 1) at 30 min after dosing. Animals dosed with ethanol for 10 days prior to dosing with labeled ethanol reached maximal blood levels of $\sim 15\text{mM}$ at 60 minutes after dosing (Table 1). It is likely that increased first-pass metabolism of ethanol contributed to the lower and delayed peak ethanol levels in the 10-day ethanol group.

During the 10-day treatment with ethanol, animals were observed to show mild tremors during handling starting on day 6, but no seizures were observed. During the 10 day treatment, animals in both the ethanol and water groups gained weight. Ethanol is known to have wasted calories and to reduce weight gain. For comparison, group weights were, acute: $277 \pm 9.2\text{g}$ ($n=26$), 10-day-ethanol: $323 \pm 20.8\text{g}$ ($n=22$), and 10-day-water: 343 ± 23.2 ($n=8$). The trend towards lower weight in the ethanol-treated group versus the 10-day-water group did not reach statistical significance. There was, however, a significant difference between the pooled weights of all 10-day animals (ethanol- and water-treated): ($328 \pm 22.9\text{g}$, $n=30$) versus the acute group ($p < 10^{-13}$, two tailed t-test, unequal variance). Differences were also significant ($p < 0.0001$) when comparing either the 10-day-water or 10-day-ethanol group to the acute group. In summary, both groups of 10-day animals gained weight (1.2-fold, on average) compared to the acute group.

4.3.2 Serum: availability of ^{13}C -acetate for brain metabolism

Analysis of 700MHz proton spectra of serum (Fig. 4.3) collected at sacrifice enabled us to determine concentrations and fractional enrichments of various potential substrates for brain metabolism in each group (Table 1). By 15 min after dosing with $[2-^{13}\text{C}]$ ethanol, acutely-treated animals reached serum acetate levels of 0.67mM at 80% frac-

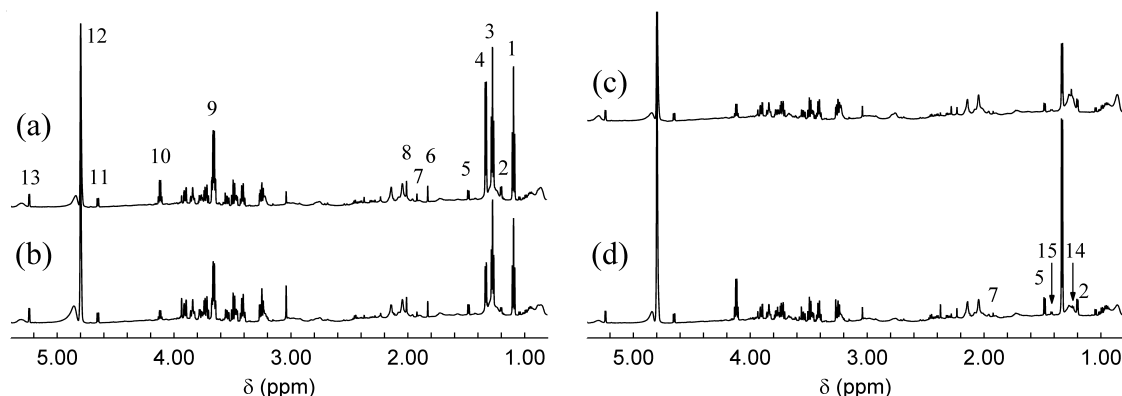


Figure 4.3: 700MHz proton spectra of serum. 15 minutes after dosing with with $[2-^{13}\text{C}]$ ethanol, both acutely dosed (a) and 10-day-ethanol-treated (b) animals show substantial ($>2/3$) fractional enrichment of serum acetate, indicating that $[2-^{13}\text{C}]$ ethanol is rapidly metabolized to $[2-^{13}\text{C}]$ acetate in the liver and quickly released into the blood. The quick rise in $[2-^{13}\text{C}]$ acetate indicates that abundant ethanol-derived acetate was available as a substrate for brain metabolism within minutes of ethanol ingestion. By 240 minutes after dosing with $[2-^{13}\text{C}]$ ethanol, both nave (c) and 10-day-ethanol-treated (d) animals eliminated almost all ethanol. The fractional enrichment of acetate decreased substantially versus 15 minutes post-dose, due to the exhaustion of the supply of $[2-^{13}\text{C}]$ ethanol. However, ^{13}C -satellite peaks are visible for lactate, indicating that ^{13}C label has traversed the hepatic TCA cycle and entered lactate and glucose (see Fig. 4). By comparing spectra collected with and without ^{13}C -decoupling, we were able to verify that suspected ^{13}C satellite peaks were in fact due to ^{13}C coupling (see Fig. 4). The only molecules that had appreciable ^{13}C labeling in the 700MHz proton spectra of serum were ethanol, acetate, lactate, and glucose. By virtue of the high signal to noise of spectra collected using the 700MHz spectrometer with the cold probe, we were able to measure fractional enrichment as low as 1 (see Fig 4). Assignments: 1 t, half ethanol $2-^{13}\text{CH}_3$; 2 d, beta-hydroxybutyrate- CH_3 ; 3 t, half ethanol $2-^{13}\text{CH}_3$; 4 d, lactate $3-\text{CH}_3$; 5 d, alanine $3-\text{CH}_3$; 6 s, half acetate $2-^{13}\text{CH}_3$; 7 s, acetate $2-^{12}\text{CH}_3$; 8 s, half acetate $2-^{13}\text{CH}_3$; 9 q, ethanol $1-\text{CH}_2$; 10 q, lactate $2-\text{CH}$; 11 d, beta-glucose $1-\text{CH}$; 12 residual water protons; 13 d, alpha-glucose $1-\text{CH}$; 14 d, half lactate $3-^{13}\text{CH}_3$; 15 d, half lactate $3-^{13}\text{CH}_3$; Abbreviations: d, doublet; q, quartet; s, singlet; t, triplet;

Table 1: Serum concentrations and enrichments after dosing with [2-13C] ethanol or [2-13C] acetate

Naive									
Treatment	time (min)	n	Ethanol [](mM)	Acetate		Lactate		Glucose	
				[(mM)]	C-2FE(%)	[(mM)]	C-3FE(%)	[(mM)]	C-1FE(%)
2-13C E	15	4	14.61±2.27	0.67±0.17	79.75±1.82	3.67±1.11	2.41±1.08	2.68±0.25	0.16±0.40
2-13C E	30	3*	20.28±2.64	0.51±0.17	80.02±0.57	3.87±1.79	3.35±1.29	3.49±0.27	0.56±0.36
2-13C E	60	4	17.35±2.62	0.75±0.16	82.00±1.10	3.04±0.58	5.34±0.88	2.08±0.43	0.77±1.12
2-13C E	240	4	0.94±0.42	0.20±0.17	32.61±43.47	3.81±1.79	6.33±2.67	1.89±0.56	4.65±0.91 d
2-13C A	30	4	0.59±0.10	4.26±1.13	82.02±1.74	2.35±1.02	3.67±0.75	3.38±0.78	1.83±0.71 d
10-day ethanol									
Treatment	time		Ethanol [](mM)	Acetate		Lactate		Glucose	
				[(mM)]	C-2FE(%)	[(mM)]	C-3FE(%)	[(mM)]	C-1FE(%)
2-13C E	15	4	9.69±1.52 c	0.97±0.06 a	84.17±2.42	2.72±0.62	3.14±0.63	3.60±0.39	0.44±0.61
2-13C E	30	4	12.94±2.88 c	0.72±0.22	84.26±2.14	3.09±1.15	3.04±0.94	3.04±0.34	0.75±0.28 d
2-13C E	60	4	15.36±5.09	0.69±0.06	82.90±7.40	6.14±3.05 e	2.87±1.09	2.97±0.59	1.14±0.33 d
2-13C E	240	4	3.07±2.86	0.11±0.03	21.22±12.48	8.06±3.47 e	3.09±2.13	2.10±0.47	3.54±0.90 d
2-13C A	30	4	0.51±0.14	1.09±0.72 b	78.31±5.83	4.70±4.79	3.39±1.49	3.31±0.38	1.67±0.92 d
10-day water									
Treatment	time		Ethanol [](mM)	Acetate		Lactate		Glucose	
				[(mM)]	C-2FE(%)	[(mM)]	C-3FE(%)	[(mM)]	C-1FE(%)
2-13C E	60	4	16.62±1.86	0.57±0.10	83.87±1.61	2.56±0.54	4.21±1.14	3.02±0.20	1.09±0.70 d
2-13C A	30	4	0.40±0.11	1.05±0.30	83.65±2.79	2.31±0.57	3.64±0.95	3.41±0.48	1.72±0.92 d

*: one animal was excluded because it had low serum ethanol (6.7mM), suggesting it may have regurgitated part of its dose.

a: p<0.05 via 2-tailed t-test (unequal variance) versus Naive group at same time

b: p<0.005 via 2-tailed t-test (unequal variance) versus Naive group at same time

c: p<0.02 via 2-tailed t-test (unequal variance) versus Naive group at same time

d: p<0.05 single sample t-test versus mean=0

e: not significant (p>0.05 via 2-tailed t-test (unequal variance) versus Naive group at same time)

Table 4.1: Serum Concentrations and Enrichments After Dosing with [2-13C] Ethanol or Acetate.

tional enrichment (Fig. 4.3a, Table 3). Ethanol concentration peaked at 30 minutes after dosing at $\sim 20\text{mM}$. The acetate concentration continued to rise to 0.75mM at 60 min, and acetate fractional enrichment remained approximately 80% during this time. The elevated serum acetate concentration during ethanol metabolism together with the high fractional enrichment, confirm the availability of ethanol-derived acetate (Jucker et al., 1998) as substrate for brain metabolism within minutes of ethanol ingestion.

For the chronic ethanol group dosed with $[2-^{13}\text{C}]$ ethanol, serum acetate reached 0.95mM 15 minutes after dosing, significantly higher than in the acutely-treated group. As with the acutely-treated group, serum acetate remained elevated with FE $\sim 80\%$ for the first hour. In this group, ethanol peaked 60 minutes after dosing at $\sim 15\text{mM}$; the delayed peak and lower blood ethanol in the chronic group (Table 1) are most likely the result of increased first-pass ethanol metabolism (Eckardt et al., 1998). We anticipated that our 10-day ethanol treatment would produce even greater increases in acetate production, analogous to the finding of ~ 2 -fold greater acetate levels in human alcoholics during intoxication (Korri et al., 1985). However, it is possible that either this treatment was insufficient to produce such dramatic increases, or that a larger dose of ethanol would be required to demonstrate the changes.

Acutely-treated animals injected intraperitoneally with $[2-^{13}\text{C}]$ acetate achieved significantly higher blood acetate levels (mean 4.26mM , range 3.41 to 5.92mM , $n=4$) than animals treated with $[2-^{13}\text{C}]$ ethanol (see Table 1). Curiously, animals injected with $[2-^{13}\text{C}]$ acetate after 10 days of either water or ethanol treatment showed significantly lower serum acetate concentrations (mean 1.07mM , range 0.53 to 2.13 , $n=8$) than acutely-treated animals (Table 1). The lower serum acetate in the 10-day animals is somewhat puzzling, but since the control (water-treated) group exhibited the same trend as the ethanol treated group, we speculate that altered pharmacokinetics in the 10-day groups (which weighed on average 24% more than the acutely-treated group) may have been responsible. Increased abdominal fat and relatively larger volume of distribution may have contributed to lower serum acetate levels in the larger animals.

4.3.3 Serum: assessment of ^{13}C -labeling in molecules other than acetate

Though 90% of the acetate produced during hepatic metabolism of $[2-^{13}\text{C}]$ ethanol is released into the serum (Jucker et al., 1998), the remaining 10% may enter the TCA cycle and label other molecules with ^{13}C . On the first turn of the TCA cycle, glutamate

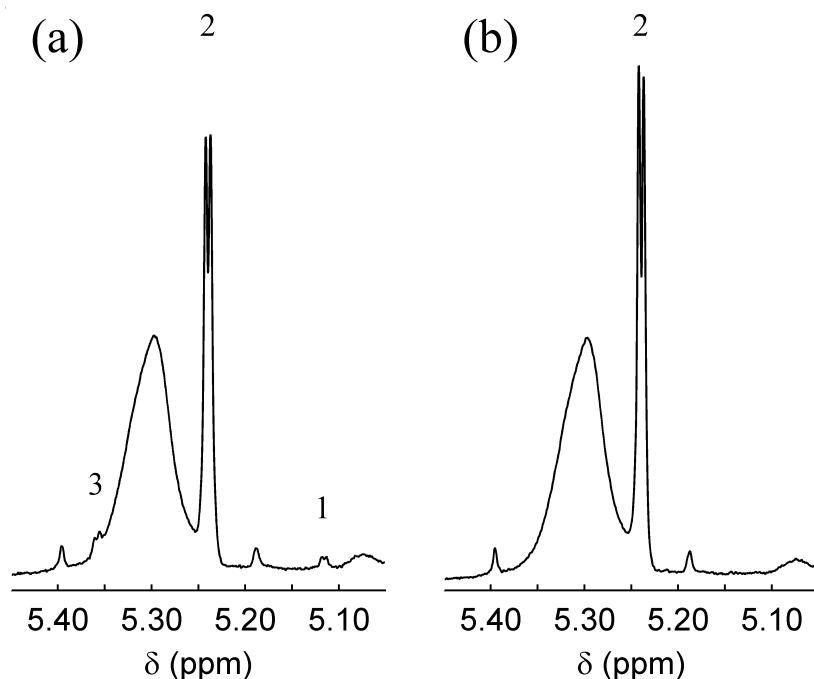


Figure 4.4: Confirming the identification of glucose ^{13}C satellite peaks in 700MHz proton spectra. Panel (a) represents an expanded view of the spectrum shown in Fig. 3c (serum 240 minutes after dosing with $[2-^{13}\text{C}]$ ethanol in a nave animal), collected without ^{13}C -decoupling. In this spectrum, glucose and carbon satellites of glucose are evident. In the ^{13}C -decoupled 700MHz proton spectrum of the same sample (b), the ^{13}C -satellites are no longer present. While the enrichment of the 1-carbon in glucose was greater than natural abundance, even at 4 hours the FE was less than 5%, affirming the expectation that $[2-^{13}\text{C}]$ acetate was the primary labeled substrate available for brain metabolism in these experiments. Assignments: 1 d, half $[2-^{13}\text{C}]$ alpha-glucose 1-CH; 2 d, alpha-glucose 1-CH; 3 d, half $[2-^{13}\text{C}]$ alpha-glucose 1-CH;

(and also glutamine) labeled in the C4 position could result (Fig. 2). Subsequently, oxaloacetate labeled in the C2 or C3 position could continue through the second turn of the TCA cycle to produce glutamate and glutamine labeled at the C2 or C3 position. Alternatively, the labeled oxaloacetate could enter the gluconeogenic pathway, producing pyruvate labeled in the C2 or C3 position, which in turn could produce glucose labeled with equal probability in C1, C2, C5 or C6, or lactate labeled in C2 or C3. Thus, we measured the availability of these ^{13}C -labeled molecules in serum by observing ^{13}C -satellite peaks in our proton spectra. By comparing proton spectra collected with and without ^{13}C -decoupling, we verified that suspected ^{13}C -satellite peaks were in fact due to ^{13}C -1H coupling (Fig. 4). No evidence of significant enrichment of serum glutamine was detected (though glutamine is a poor substrate for brain metabolism at physiologic concentrations (O’Neal and Koeppe, 1966)). Concentrations and fractional enrichments for serum lactate and glucose are summarized in Table 1, and as expected, FE in these molecules was less than 5% at all time points up to 60 min. In acutely-treated animals, glucose fractional enrichment was not statistically greater than zero until 240 min. In 10-day-ethanol-treated animals, glucose FE was statistically elevated at 30 min, probably reflecting increased gluconeogenesis in these animals, though it remained less than 5% even at 240 min. These findings support our decision to omit from our model (Fig. 2) the influx of ^{13}C label into brain from substrates other than acetate.

In addition to entering metabolites via the TCA cycle, acetate can enter ketone bodies without traversing the TCA cycle. Acetoacetate is formed (via acetoacetyl-CoA) by condensation of two molecules of acetyl-CoA, and thus would be labeled in C2 and/or C4, as would beta-hydroxybutyrate, both of which can serve as substrates for cerebral metabolism. We measured both acetoacetate and beta-hydroxybutyrate in serum, but there was no detectable ^{13}C enrichment of C4 (FE<20%) in either molecule.

4.3.4 Brain Fractional Enrichment: Acetate and other potential substrates

Having established the availability in serum of ^{13}C -labeled substrates for brain metabolism, we examined ^{13}C incorporation into brain (Fig. 5). Despite 80% fractional enrichment of serum acetate in animals treated with $[2\text{-}^{13}\text{C}]$ ethanol, fractional enrichment in brain acetate was substantially lower in these animals; in most cases it was below the detection threshold in our proton spectra. By contrast, acutely-treated animals treated with

[2-¹³C] acetate showed 38% FE of brain acetate, and also a 1.57- to 2.19-fold increase in brain acetate concentration versus acutely-treated animals treated with [2-¹³C] ethanol. This was the same group of animals that achieved a serum acetate concentration of more than 4mM, suggesting that serum acetate concentration is an important determinant for acetate entry into brain, as would be expected based on the K_m of 9.4mM for the acetate transporter determined by Waniewski and Martin (Waniewski and Martin, 1998). We speculate that in animals with serum acetate in the 1mM range, labeled acetate that entered the brain may have entered the astrocytic TCA cycle without mixing with the free acetate pool, whereas higher serum acetate in the acutely-treated [2-¹³C] acetate-treated group caused labeled acetate to enter the brain faster than the astrocytic TCA cycle consumed it. For all other animals, the finding of low fractional enrichment of brain acetate in the face of 80% FE of serum acetate, and clear evidence of acetate metabolism by brain (see below) suggests that the pool of free acetate in the brain is not in exchange with the pool of acetate that enters the astrocytic TCA cycle. It is possible that a pool of free acetate exists within neurons. In addition, the low fractional enrichment of brain acetate suggests that the metabolism of acetate by the brain during ethanol metabolism is limited by transport of acetate into the brain rather than by entry of acetate into acetyl-CoA and the astrocytic TCA cycle.

Fractional enrichment in brain lactate was less than 5% for all groups of animals except the acutely-treated animals 240 min after dosing with [2-¹³C] ethanol, and in these animals it was only 6.85%. Brain lactate concentration was significantly elevated in 10-day ethanol animals versus acutely-treated animals at 60 and 240 min after dosing with [2-¹³C] ethanol. These groups of animals showed a trend toward increased serum lactate (Table 1), and though not statistically significant due to the large standard deviation, it is likely that increased uptake of lactate from blood into brain (O’Neal and Koeppe, 1966) accounted for some of the increase in brain lactate.

4.3.5 Fractional Enrichment of Brain Amino Acids

To determine the metabolic path of ethanol-acetate metabolism we examined proton-decoupled ¹³C spectra of brain following administration of [2-¹³C] ethanol and [2-¹³C] acetate (Fig. 6). As predicted by our model (Fig. 2), the most intense labeling occurs in glutamate and glutamine C4, with significant labeling in C2 and C3 of these molecules as well (see Table 3). Consistent with our proton spectra (Fig. 5), acetate C2 was substantially enriched in brain only following i.p. injections of [2-¹³C] acetate

Table 2: Concentration and FE of lactate and acetate in brain

Naïve						
Treatment	time		Lactate		Acetate	
	(min)	n	[] (mM)	FE (%)	[] (mM)	FE (%)
[2-13C] E	15	3	5.48 ± 1.16	0.99 ± 1.47	0.63 ± 0.04	1.92 ± 3.20
[2-13C] E	30	3	4.58 ± 2.49	1.33 ± 2.60	0.88 ± 0.07	3.85 ± 2.97
[2-13C] E	60	4	4.99 ± 1.32	2.41 ± 2.72	0.88 ± 0.38	2.06 ± 0.44
[2-13C] E	240	4	4.91 ± 1.02	6.85 ± 4.00	0.71 ± 0.16	2.25 ± 1.85
[2-13C] A	30	4	5.22 ± 2.81	3.07 ± 1.41	1.38 ± 0.31 b	38.43 ± 9.61 a
10-day ethanol						
Treatment	time		Lactate		Acetate	
	(min)	n	[] (mM)	FE (%)	[] (mM)	FE (%)
[2-13C] E	15	4	4.89 ± 0.66	0.08 ± 1.54	0.43 ± 0.11	10.34 ± 5.58
[2-13C] E	30	4	6.20 ± 1.56	2.32 ± 0.61	0.27 ± 0.05	13.04 ± 6.21
[2-13C] E	60	4	8.95 ± 0.62 c	1.28 ± 0.20	0.37 ± 0.16	4.64 ± 3.44
[2-13C] E	240	4	7.69 ± 0.43 c	3.21 ± 2.61	0.42 ± 0.08	0.87 ± 6.26
[2-13C] A	30	4	6.44 ± 1.85	1.93 ± 2.15	0.46 ± 0.08 e	11.59 ± 12.6
10-day water						
Treatment	time		Lactate		Acetate	
	(min)	n	[] (mM)	FE (%)	[] (mM)	FE (%)
[2-13C] E	60	4	7.94 ± 2.01 d	0.86 ± 0.68	0.38 ± 0.18	8.17 ± 8.51
[2-13C] A	30	4	6.48 ± 2.78	2.18 ± 0.44	0.53 ± 0.18 e	8.31 ± 2.56

Abbreviations: E, ethanol; A, acetate, [], concentration; FE, fractional enrichment.

a: p<0.05 2-tailed t-test, unequal variance versus acetate FE for every other Naïve group, with Bonferoni correction.

b: p<0.005 2-tailed t-test, unequal variance versus [acetate] for all other Naïve animals

c: p<0.01 2-tailed t-test, unequal variance versus [Lactate] in corresponding Naïve groups

d: not significant by 2-tailed t-test, unequal variance versus [Lactate] in corresponding Naïve group

e: p<0.05 2-tailed t-test, unequal variance versus [acetate] in Naïve group, with Bonferoni correction

Table 4.2: Concentration and FE of lactate and acetate in brain.

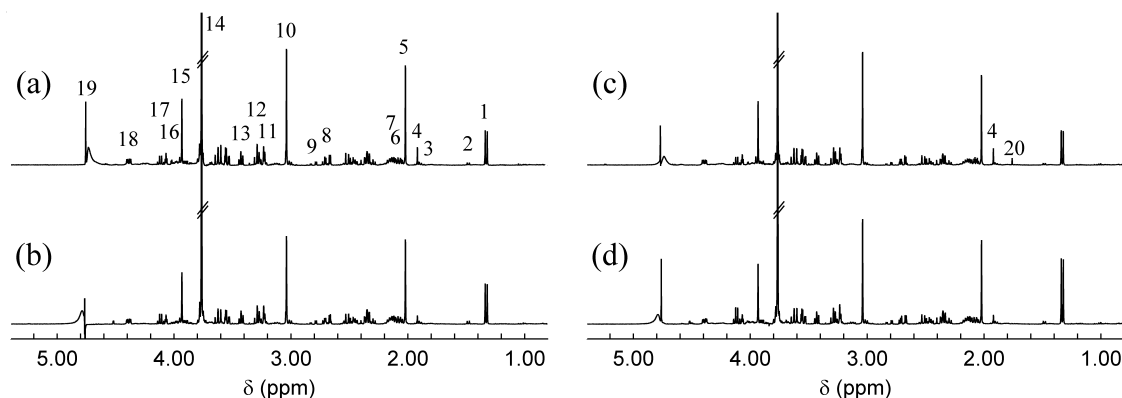


Figure 4.5: 400MHz proton spectra of perchloric acid extracts of brain. 60 minutes after dosing with with $[2-^{13}\text{C}]$ ethanol, both nave (a) and 10-day-ethanol-treated (b) animals show relatively low fractional enrichment of brain acetate, as judged by the size of ^{13}C satellite peaks. On the other hand, positive control brain collected 30 minutes after dosing nave animals with $[2-^{13}\text{C}]$ acetate (c) show appreciable fractional enrichment of brain acetate. In these animals, the serum acetate concentration was $4.3 \pm 1.1\text{mM}$, approximately 6-fold higher than $[2-^{13}\text{C}]$ ethanol-treated animals in (a) and (b), and 4-fold higher than in 10-day ethanol-treated animals given $[2-^{13}\text{C}]$ acetate (d). Given that serum acetate fractional enrichment was approximately 80% in all animals, and that the pattern of fractional enrichment in brain amino acids (Table 3) was consistent with entry of acetate into the astrocytic TCA cycle, it appears that when serum acetate is in the 1mM range, acetate that enters the brain proceeds directly into the TCA cycle without mixing with free acetate in the brain. Thus, the rate-limiting step for incorporation of acetate carbons into brain amino acids during ethanol metabolism appears to be entry of acetate into the brain rather than conversion to acetyl-CoA or entry into the TCA cycle. Fractional enrichment of acetate C2 and lactate C3 were quantified by observing ^{13}C satellite peaks (Table 4.2). The detection threshold was approximately 6% for lactate, and 18-38% for acetate, depending on the concentration of acetate. Assignments: 1 d, lactate 3-CH₃; 2 d, alanine 3-CH₃; 3 qui, GABA 2-CH₂; 4 s, acetate 2-12CH₃; 5 s, NAA N-C(O)-CH₃; 6 m, Glutamine 2-CH₂; 7 m, Glutamate 2-CH₂; 8 dd, NAA 3-CH₂; 9 dd, Aspartate 3-CH₂; 10 s: Creatine + Phosphocreatine N-CH₃; 11 singlets from Choline, Phosphorylcholine, Glycerophosphocholine, N(CH₃)₃; 12 triplets from taurine 2-CH₂ and myo-inositol 5-CH; 13 t, taurine 1-CH₂; 14 s, dioxane; 15 s: Creatine + Phosphocreatine 2-CH₂; 16 t, myo-inositol 2-CH; 17 q, lactate 2-CH; 18 dd, NAA 2-CH; 19 residual water protons; 20 half $[2-^{13}\text{C}]$ acetate 2-¹³CH₃; Abbreviations: d, doublet; dd, doublet of doublets; m, multiplet; q, quartet; qui, quintet; s, singlet; t, triplet; NAA N-acetyl aspartate.

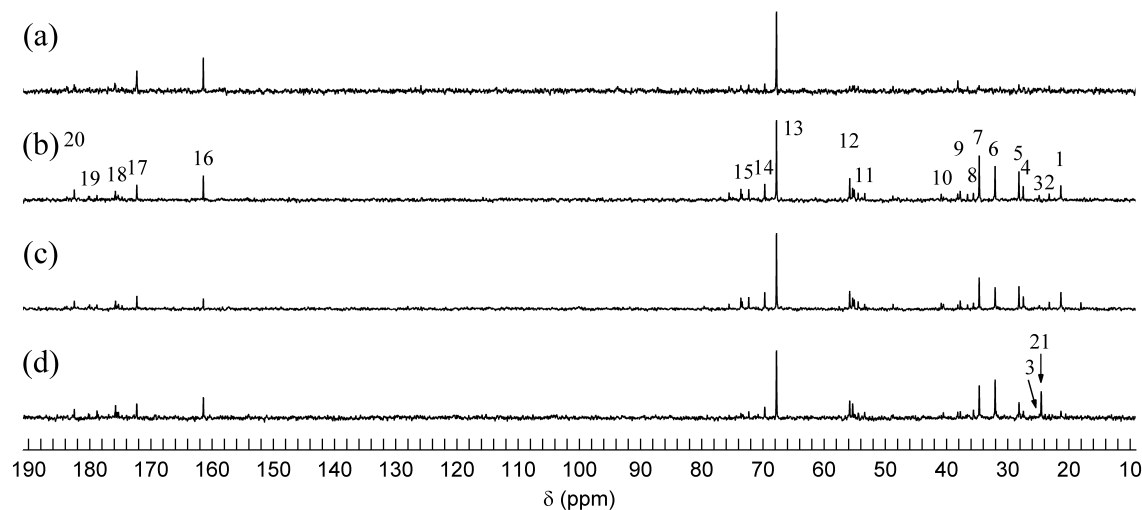


Figure 4.6: 100MHz proton-decoupled ^{13}C spectra of perchloric acid extracts of brain. Negative control spectrum (a) collected 120 minutes after dosing with natural abundance ethanol shows smaller ^{13}C signals than spectra from animals dosed with $[2-^{13}\text{C}]$. Spectra from brain 60 minutes after dosing with $[2-^{13}\text{C}]$ ethanol in nave (b) and 10-day-ethanol-treated (c) animals show similar patterns of enrichment in brain metabolites. Positive control spectrum (d) from brain 30 minutes after dosing $[2-^{13}\text{C}]$ acetate shows relatively selective labeling of glutamine-C4 and glutamate-C4, as well as signal from acetate-C2. Assignments: 1 Lac-C3; 2 NAA-C6; 3 GABA-C3; 4 Gln-C3; 5 Glu-C3; 6 Gln-C4; 7 Glu-C4; 8 GABA-C2; 9 Asp-C3; 10 Asp-C2; 11 Gln-C2; 12 Glu-C2; 13 Dioxane 14 Lac-C2; 15 Ins-C1-C6; 16 U; 17 U; 18 Glu-C1 and Gln-C1; 19 Gln-C5; 20 Glu-C5 and GABA-C1; 21 Ace-C2; Abbreviations: Ace, Acetate; Asp, aspartate; GABA, gamma-aminobutyric acid; Lac, lactate; Glu, glutamate; Gln, glutamine; Ins, inositol; NAA N-acetyl aspartate U, unassigned.

(Fig. 6d). Comparison of spectra from acutely-treated versus 10-day-ethanol-treated animals (Fig 6b vs c) suggests that the pattern and magnitude of labeling from [2- ^{13}C] ethanol was similar in these two groups. This impression is borne out in the detailed analysis of fractional enrichment data for each treatment group (Table 3).

Positive control animals dosed with [2- ^{13}C] acetate show highest FE in glutamine C4, followed by glutamate C4 and GABA C2, and then the carbons labeled during the second turn (Table 3). This pattern of labeling in brain amino acids is predicted by our model (Fig. 2), and was found during other studies in which [2- ^{13}C] acetate was administered (Hassel and Sonnewald, 1995; Hassel et al., 1995; Chateil et al., 2001). The FE of brain amino acids following [2- ^{13}C] ethanol administration is consistent with cerebral metabolism of [2- ^{13}C] acetate derived from hepatic oxidation of ethanol. At 15 min post-dose, the most intense labeling is in C4 of glutamine, followed by glutamate C4, and at later time points, labeling of C2 and C3 of glutamine and glutamate becomes apparent (Table 4). These data represent the first measurement of brain metabolism of ethanol-derived acetate using ^{13}C NMR, and provide additional evidence to support the conclusion that acetate produced from hepatic oxidation of ethanol is a substrate for brain metabolism.

Comparison of the brain FE values for acutely-dosed animals versus those treated with ethanol for 10 days and then dosed with [2- ^{13}C] ethanol reveals no difference between the groups, contrary to our hypothesis. Further comparison with the control groups that received 10 days of water confirms the lack of effect of the 10-day ethanol treatment on [2- ^{13}C] acetate metabolism in brain. The unchanged labeling of brain metabolites following [2- ^{13}C] ethanol administration could be caused by a failure to increase transport of acetate into brain, or a failure to increase ACoAS activity. The low FE of brain acetate in the 10 day group suggests that free acetate from serum (which was 80% enriched in ^{13}C) did not accumulate due to an increase in transport without an increase in ACoAS activity. Rather, the fact that brain amino acid FE was statistically equivalent in acutely-treated and 10-day ethanol-treated animals, together with the low FE of brain acetate, suggests that acetate transport continued to limit incorporation of ^{13}C into brain amino acids as it did in the control group. Hence we conclude that transport of acetate into brain did not increase appreciably in response to 10 days of ethanol treatment. With this finding in mind, we can reconcile our findings with those of Kiselevski et al. who found that ACoAS activity increased 36% after 7 days of ethanol treatment (Kiselevski et al., 2003) by noting that if the animals in our study failed to increase acetate transport, we might not find a difference

Table 3: Fractional Enrichment (%) of carbon-13 in brain amino acids

Naïve															
Tracer	n	Glutamate					Glutamine					GABA			
(Time)		C1	C2	C3	C4	C5	C1	C2	C3	C4	C5	C1	C2	C3	C4
2-13OE (15min)	3	N.D.	N.D.	N.D.	0.98 ±0.56	N.D.	N.D.	0.86 ±0.25	0.18 ±0.39	3.24 ±1.30	N.D.	2.32 ±0.88	1.76 ±0.75	1.91 ±1.03	1.08 ±0.58
2-13OE (30min)	3	0.67 ±0.26	0.77 ±0.68	0.62 ±0.29	2.38 ±0.37	0.88 ±0.48	N.D.	1.48 ±0.49	1.10 ±0.77	5.98 ±0.34	N.D.	2.85 ±1.84	1.52 ±0.91	2.44 ±1.06	2.90 ±0.89
2-13OE (60min)	4	1.14 ±0.25	1.97 ±0.37	2.05 ±0.49	3.23 ±0.55	1.49 ±0.39	1.39 ±0.14	2.12 ±0.25	2.30 ±0.43	8.53 ±2.14	1.60 ±0.77	3.37 ±1.37	4.43 ±0.99	2.51 ±1.30	1.71 ±1.20
2-13OE (240min)	4	6.49 ±0.74	6.62 ±1.23	7.41 ±0.77	5.87 ±1.92	5.31 ±0.75	4.87 ±1.19	5.89 ±0.88	6.43 ±0.44	8.94 ±2.63	5.79 ±2.30	11.88 ±5.73	7.32 ±1.58	8.99 ±1.15	8.65 ±1.53
2-13CA (30min)	4	1.40 ±0.41	2.31 ±0.24	2.10 ±0.35	5.61 ±0.35	1.24 ±0.27	1.00 ±0.15	3.93 ±0.69	2.04 ±0.27	17.18 ±1.59	1.16 ±0.62	2.88 ±0.63	6.41 ±0.97	4.37 ±2.94	3.30 ±0.93
10-day Ethanol															
Tracer	n	Glutamate					Glutamine					GABA			
(Time)		C1	C2	C3	C4	C5	C1	C2	C3	C4	C5	C1	C2	C3	C4
2-13OE (15min)	4	N.D.	0.25 ±0.08	0.14 ±0.12	0.75 ±0.18	N.D.	0.53 ±0.28	1.55 ±0.51	0.56 ±0.16	2.90 ±0.74	0.54 ±0.25	1.06 ±0.58	0.88 ±0.32	N.D.	0.54 ±0.43
2-13OE (30min)	4	0.30 ±0.24	0.79 ±0.13	0.57 ±0.11	1.73 ±0.15	0.62 ±0.18	0.57 ±0.35	1.55 ±0.32	1.22 ±0.32	4.83 ±1.21	1.01 ±0.62	1.84 ±0.74	1.58 ±0.78	N.D.	N.D.
2-13OE (60min)	4	1.13 ±0.25	1.87 ±0.19	1.69 ±0.21	2.94 ±0.22	1.24 ±0.23	1.52 ±0.65	2.65 ±0.34	2.19 ±0.33	6.56 ±0.64	1.67 ±0.66	2.45 ±1.07	2.78 ±0.58	1.81 ±0.57	1.60 ±0.70
2-13OE (240min)	4	4.33 ±0.44	5.22 ±0.35	5.30 ±0.36	3.96 ±0.49	3.50 ±0.35	4.22 ±0.63	5.46 ±0.67	5.28 ±0.42	4.70 ±0.96	5.75 ±0.14	5.20 ±2.26	4.91 ±0.91	5.44 ±0.67	6.25 ±0.99
2-13CA (30min)	4	1.00 ±0.31	2.14 ±0.66	1.70 ±0.47	4.44 ±1.72	1.21 ±0.38	1.34 ±0.47	3.53 ±1.59	2.42 ±0.80	11.56 ±5.70	1.74 ±0.48	1.93 ±2.46	4.84 ±1.66	2.67 ±0.92	2.19 ±1.10
10-day Water															
Tracer	n	Glutamate					Glutamine					GABA			
(Time)		C1	C2	C3	C4	C5	C1	C2	C3	C4	C5	C1	C2	C3	C4
2-13OE (60min)	4	1.23 ±0.35	1.80 ±0.39	1.54 ±0.23	2.83 ±0.46	1.22 ±0.28	1.47 ±0.37	2.56 ±0.58	2.13 ±0.39	6.19 ±1.15	1.91 ±0.51	2.73 ±1.18	3.11 ±0.59	1.38 ±0.30	2.02 ±0.47
2-13CA (30min)	4	0.53 ±0.19	1.56 ±0.29	1.27 ±0.13	3.47 ±0.76	1.07 ±0.23	0.76 ±0.21	2.85 ±0.61	2.00 ±0.15	10.13 ±2.50	1.44 ±0.45	2.25 ±1.48	4.28 ±1.04	1.75 ±0.20	2.34 ±0.57
N.D.: not determined															

a: p<0.05 2-tailed, paired t-test versus FE of C3 in the same molecule

Table 4.3: Brain ^{13}C FE of amino acids after dosing with $[2-^{13}\text{C}]$ ethanol or acetate.

Table 4: carbon-13 labeling ratios in brain amino acids

Pre-Treatment	n	C3/C4 Glutamate		C3/C4 Glutamine	C3/C2 GABA	
Naïve	4*	0.65 ± 0.21	a	0.28 ± 0.10	0.42 ± 0.16	*
10-day Ethanol	4	0.57 ± 0.04	b	0.33 ± 0.05	0.64 ± 0.10	c
10-day Water	4	0.54 ± 0.04	b	0.35 ± 0.05	0.45 ± 0.10	

* one sample was excluded as an outlier (GABA C3/C2 = 1.17)

a: marginal significance: p=0.053 via paired t-test (2-tailed) versus ratio in Glutamine

b: p<0.001 via paired t-test (2-tailed) versus C3/C4 ratio in Glutamine

c: p<0.05 2-tailed, t-test, unequal variance versus GABA C3/C2 ratio
in pooled data from 10-day water and Naïve animals

Table 4.4: ^{13}C labeling ratios in brain amino acids

in ^{13}C incorporation into brain amino acids, even if ACoAS activity did increase. It is worth noting that the serum acetate levels of 10-day-ethanol-treated animals were not elevated over acutely-treated and control animals to the extent we expected. An increase in serum acetate, even in the absence of a decrease in the transporter K_m , would drive entry of additional acetate into the brain, and if activity of ACoAS was increased also, we might see a corresponding increase of ^{13}C incorporation beyond that due to high serum acetate alone. Future studies will be required to address this point.

4.3.6 Unequal labeling of Glutamine C2 and C3

One feature of our brain FE data that deviated from our model's prediction was the unequal labeling of "second-turn" carbons. For example, glutamine C2 and C3 are predicted to have equal FE, as are glutamate C2 and C3, and GABA C3 and C4, but our data show greater labeling of glutamine and glutamate C2 than C3 (Table 3). Ours is not the first observation of this phenomenon. Badar-Goffer et al. noted greater intensity in glutamate C2 versus C3 from guinea pig brain slices incubated with $[1-^{13}\text{C}]$ glucose, and attributed the discrepancy to the formation of doubly-labeled $[3,4-2\text{C}^{13}]$ glutamate which gave a doublet due to carbon-carbon coupling (Badar-Goffer et al., 1990). These authors state that there is no C2-C3 discrepancy if the satellite resonances are taken into account. While no value for the size of the apparent discrepancy is given, from the published spectra it appears that the doubly-labeled species accounts for ~10% of the C3-labeled glutamate. Close inspection of our spectra suggests that while formation of doubly-labeled glutamate may account for the discrepancy in some

groups of animals, it cannot explain the discrepancy in others. For example, to explain the observed glutamine C2-C3 discrepancy in the acutely-treated animals dosed with [2- ^{13}C] acetate on the basis of C3-C4 coupling alone, approximately 50% of C3-labeled glutamine would have to be doubly-labeled in C4 as well. By peak fitting of the spectral data for this group, we estimate that of the C3-labeled glutamine, only 13.5% was doubly labeled, which suggests that another process must be at work. Moreover, using integral regions that captured satellite peaks for all resonances did not alter the trends shown in Table 3. Hassel et al. offered a metabolic explanation for greater labeling in brain glutamate C2 than C3 after [2- ^{13}C] acetate dosing: cleavage of citrate to oxaloacetate by citrate lyase in cytosol (Hassel et al., 1995). This explanation hinged on the assumption that citrate lyase cleaves a different carbon-carbon bond than the one formed by citrate synthase. Thus [2- ^{13}C] acetate was to have labeled citrate, which when cleaved by citrate lyase, produced [3- ^{13}C] oxaloacetate. However, it appears to be the prevailing view that citrate synthase and citrate lyase are both highly stereospecific, and both act on the same bond, so that citrate lyase could not effectively transfer ^{13}C label from acetate to oxaloacetate (Sreere, 1975).

Having discounted previous explanations by investigators who have observed this phenomenon, we were forced to consider others. One report by Stern et al. indicates the stereospecificity of pig heart citrate synthase may be as low as 90% (Stern et al., 1966). If this were true, up to 10% of our label from [2- ^{13}C] acetate could have proceeded directly to the 2C of glutamate and glutamine on the first turn of the TCA cycle. We implemented a computer simulation incorporating this unexpected flux, and, if present, it would account for the C2-C3 discrepancy we observed (data not shown). However, two years after the first report, O'Brien and Stern published a second paper stating that pig heart citrate synthase is absolutely stereospecific (O'Brien and Stern, 1968), and this appears to be the currently accepted view (Sreere, 1975). Finally, we note reports of so-called "channeling" of TCA cycle intermediates (Sumegi et al., 1990) that suggest that randomization of label through the formation of the symmetrical molecules succinate and fumarate may be incomplete because these molecules are shuttled between enzymes rather than diffusing freely. This is an intriguing possibility, and if proven, must be incorporated into models used to analyze labeling from ^{13}C NMR experiments.

4.3.7 Steady-state analysis

Based on the serum data which suggest that during the first hour after [2-¹³C] ethanol administration acetate concentration and fractional enrichment were relatively constant, we decided to analyze the data from our 60 min time points using a steady-state analysis. Hassel et al. showed that in the steady state, the C3/C4 ratio in glutamine and glutamate (and the corresponding C3/C2 ratio in GABA) give an indication of the fraction of carbon skeletons that exit the TCA cycle on each turn (Hassel et al., 1995). Further, they noted that the comparison of this ratio in GABA to that in glutamate and glutamine allows an assessment of the fraction of GABA derived from glutamine carbon skeletons, versus skeletons from the glutamate pool that have traversed the neuronal TCA cycle. We found that ratios for the acutely-treated animals and the 10-day water animals were approximately 0.6 in glutatmate, 0.3 in glutamine, and 0.45 in GABA (Table 4), consistent with the ratios found by Hassel et al. in [2-¹³C] acetate-treated animals. Thus we may conclude that a 1g/kg dose of [2-¹³C] ethanol does not perturb the balance between oxidative and synthetic fates for TCA intermediates. In addition, if we assume that the ratio in GABA reflects synthesis from glutamate skeletons (high C3/C4 ratio) as well as direct synthesis from glutamine skeletons (low C3/C4 ratio), we can express this mathematically as an equation of a single variable:

$$\text{GABAC3/C2} = (x)(\text{GluC3/C4}) + (1 - x)(\text{GlnC3/C4}) \quad (4.4)$$

where x is the fraction of GABA derived from glutamate. Solving for x , we find that for acutely-treated animals $x=0.38$, and for 10-day-water animals $x=0.53$. In the 10-day-ethanol group, the C3/C4 ratios for glutamate and glutamine were similar to the ratios in the acutely-treated animals (Table 4). However, there was a marked increase in the C3/C2 ratio for GABA. If we calculate x for the 10-day-ethanol group, we find that GABA is almost exclusively derived from glutamate skeletons, suggesting that the ethanol treatment reduced synthesis of GABA from glutamine skeletons. Further studies are required to clarify whether this finding represents altered regulation of GABA synthesis in response to ethanol exposure.

4.4 Conclusion

The data presented support the conclusion that acetate derived from hepatic oxidation of ethanol is a substrate for brain metabolism, contributing carbons to glutamate,

glutamine, and other amino acids. Moreover, under these experimental conditions, transport of acetate from blood to brain appears to be the factor limiting use in both acutely treated and ethanol-treated animals. Our data show that 10 days of ethanol treatment at 5g/kg/day in rats is insufficient to increase cerebral metabolism of ethanol-derived acetate. Additional studies are required to determine whether it is possible for prolonged ethanol administration to decrease the K_m of the brain monocarboxylate transporter, allowing greater entry of acetate into brain. We predict that ethanol pretreatments that induce large increases in hepatic ethanol oxidizing capacity should produce greater serum acetate concentrations and increased metabolism of ethanol-derived acetate due to greater entry of acetate into brain, independent of possible effects of ethanol on the K_m of the transporter.

We have demonstrated that ethanol-derived acetate is a substrate for brain metabolism, consistent with the notion that ethanol-induced reductions in cerebral glucose utilization may reflect cerebral metabolism of ethanol-derived acetate. However, our data do not establish to what extent, if any, cerebral metabolism of ethanol-derived acetate causes a reduction in glucose utilization. Future studies will be required to clarify ethanol's effect on the relative contributions of acetate and glucose to brain metabolism.

While acetate supplies only 5% of the energy in the adult brain (Roach and Resse, 1972), it is important to consider acetate's significance as a substrate in the context of normal brain function. The astrocytic TCA cycle contributes 14% to oxidative metabolism in the brain (Lebon et al., 2002), which suggests that acetate supplies one third of the energy for astrocytic compartment in the healthy brain. If the use of acetate during intoxication increased, sudden withdrawal of acetate could jeopardize astrocytic support of neuronal function, with profound consequences. The predominant mechanism for cellular uptake of glutamate in the brain is transport into astrocytes (Anderson and Swanson, 2000), a process that relies upon sodium and potassium concentration gradients. During ischemia these gradients collapse, and the ensuing reversal of the glutamate transporter on astrocytes accounts for approximately half of the glutamate released into the extracellular space (Phillis et al., 2000). However, transporter reversal precedes complete collapse of ionic gradients, suggesting that less severe energy compromise may still produce physiologically significant decreases in glutamate uptake (Jabaudon et al., 2000). Spanagel et al. showed that increased voluntary alcohol consumption in Per2 mutant mice is due to decreased expression of the glutamate transporter EAAT1 (excitatory amino acid transporter 1; also known as GLAST) on astrocytes, leading to increased extracellular glutamate in the ventral striatum (Spanagel

et al., 2005). This finding supports the concept that craving and relapse may result from an attempt to decrease anxiety and other symptoms of glutamate-induced hyperexcitability by self-medication with ethanol (De Witte, 2004). Moreover, it demonstrates that astrocytic pathology can itself produce a hyperglutamatergic state with direct relevance to ethanol consumption.

Chapter 5

Conclusions and Future Directions

By design, metabolomic studies raise more questions than they answer. With the exception of Chapter 2, which we believe contains definitive evidence that we have identified EtG in liver extracts using proton NMR, each result we obtained led us into new territory. As we had not anticipated that we could measure EtG in liver, we certainly had no preconceived hypothesis regarding the impact of BHT on EtG pharmacokinetics. Nonetheless, we developed a hypothesis, and below we propose some experiments to test it. Similarly, we did not set out to address the impact of ethanol on gluconeogenesis, but our findings in liver directed us to consider this issue, and provided enough data for us to propose a hypothesis that explains our results as well as those of previous investigators. As Christopher Newgard said in a 2005 symposium on metabolomics, "We don't have a hypothesis. We have a philosophy which is that we need to obtain more data before we can formulate intelligent hypotheses." The studies in this dissertation demonstrate the utility of selecting a reasonable model organism and using untargeted analysis to generate focused, testable hypotheses.

5.1 Future Studies on Ethanol and Pyruvate Metabolism in Liver

As discussed in §3.4.1, the metabolic effect of ethanol on pyruvate metabolism in liver is quite complex, and different groups have obtained conflicting results in perfused organs, depending upon which gluconeogenic precursor they supplied in the perfusate. The specific hypothesis proposed in Fig. 3.12 involves a futile cycle of pyruvate (pyruvate \rightarrow oxaloacetate \rightarrow phosphoenolpyruvate (PEP) \rightarrow pyruvate). Ignoring for a moment the experimental details, an ideal test of this hypothesis would be to selectively enrich

hepatic lactate and/or alanine with ^{13}C and then administer ethanol. ^{13}C NMR spectroscopy could then determine whether pyruvate, oxaloacetate, and phosphoenolpyruvate are labeled by carbons from lactate when ethanol is present. The problem is that it is difficult to label lactate (or alanine) *in vivo* without also labeling glucose and glycogen, which would make it difficult to distinguish between gluconeogenesis, glycolysis, and glycogenolysis.

Thus, the best approach may be in use a similar protocol to that employed by Petersen et al., for the study of futile cycling in hyperthyroid rats (Petersen et al., 1994). To study the effect of ethanol, we would infuse $[3-^{13}\text{C}]$ lactate rather than alanine to avoid perturbing the regulation of pyruvate kinase (see §3.4.1). Like $[3-^{13}\text{C}]$ alanine, $[3-^{13}\text{C}]$ lactate would produce $[3-^{13}\text{C}]$ pyruvate, which would produce $[3-^{13}\text{C}]$ oxaloacetate via pyruvate carboxylase. However, due to the rapid exchange between oxaloacetate, malate and symmetrical fumarate, there will be some randomization of label between C3 and C2 of oxaloacetate. Thus $[2,3-^{13}\text{C}]$ PEP will be formed via PEPCK. If, as we hypothesize, PK activity is increased when alanine is depleted, $[2,3-^{13}\text{C}]$ pyruvate will result. Thus we may observe futile cycling of pyruvate by measuring enrichment of pyruvate C2 when co-administering $[3-^{13}\text{C}]$ lactate with ethanol. To the extent that labeling in pyruvate equilibrates with alanine, we may also use enrichment of $[2-^{13}\text{C}]$ alanine as a measure of futile cycling. As Petersen et al. point out, malic enzyme (ME) can also transfer label from oxaloacetate to pyruvate, but the flux is typically an order of magnitude less than that via PK.

5.2 Future Studies of Ethanol-Induced Formation of Ethyl Glucuronide

In Chapter 3, we found that administration of the anti-oxidant BHT reduced the formation of ethyl glucuronide in the liver during a 4-day binge exposure. We hypothesized that BHT, though present in small amounts, was a better substrate than ethanol for glucuronidation. In part, this hypothesis is based on the observation that "low" doses of ethanol (10-20mM) do not produce EtG, and even during high doses ($\sim 100\text{mM}$), only a tiny fraction of the ethanol is metabolized via this pathway, suggesting that the reaction is highly unfavorable. One way to test this hypothesis would be to administer a single dose of ethanol to three groups of animals: controls, BHT-pretreated, and fluoroquinolone pretreatment + coadministration. Fluoroquinolone antibiotics are

eliminated via glucuronidation, and (at doses comparable to the BHT doses in Chapter 3) do not appear to induce toxicity when co-administered with ethanol (Olsen et al., 2006). In addition, since these antibiotics are widely prescribed, especially in alcoholic patients who present with pneumonia, it would be significant to understand their impact on the formation of EtG. According to our hypothesis, we would anticipate that fluoroquinolones would decrease formation of EtG by competing for activated glucuronide.

It would also be interesting to determine (using GC-MS, which is now commercially available) the impact of BHT pretreatment on blood and urine EtG over time. It is possible, of course that BHT actually facilitates transport of EtG out of liver, but that low sensitivity of our NMR measurements failed to detect an increase in serum EtG. Either way, it would be interesting to obtain data on the kinetics of EtG elimination and the effect of BHT on this process.

5.3 Future Studies on Cerebral Metabolism of Ethanol-Derived Acetate

There are many exciting avenues to pursue with ^{13}C studies of cerebral metabolism and the effect of ethanol and acetate.

5.4 Cerebral Utilization of Glucose

One specific hypothesis regarding the impact of chronic acetate metabolism in astrocytes is as follows: Chronic ethanol exposure may cause flux through pyruvate dehydrogenase (PDH) to decrease relative to flux through pyruvate carboxylase (PC). As shown in Figure 1.3, astrocytes can use acetate to supply acetyl-CoA for the TCA cycle, diminishing the need for acetyl-CoA to be derived from pyruvate via PDH when acetate is abundant. It is not certain what effect such a change in the PC:PDH ratio would have, but we hypothesize that if acetate were suddenly removed, energy failure in astrocytes could occur, which would impair astrocytic uptake of excitatory glutamate, perhaps leading to anxiety, or even seizures.

In order to probe the PC:PDH ratio in brain, $[2-^{13}\text{C}]$ glucose is an ideal substrate because it labels different carbons in the 5-carbon pool (glutamate (Glu) and glutamine (Gln)), depending on whether it is metabolized via PC or PDH. As shown in Figure

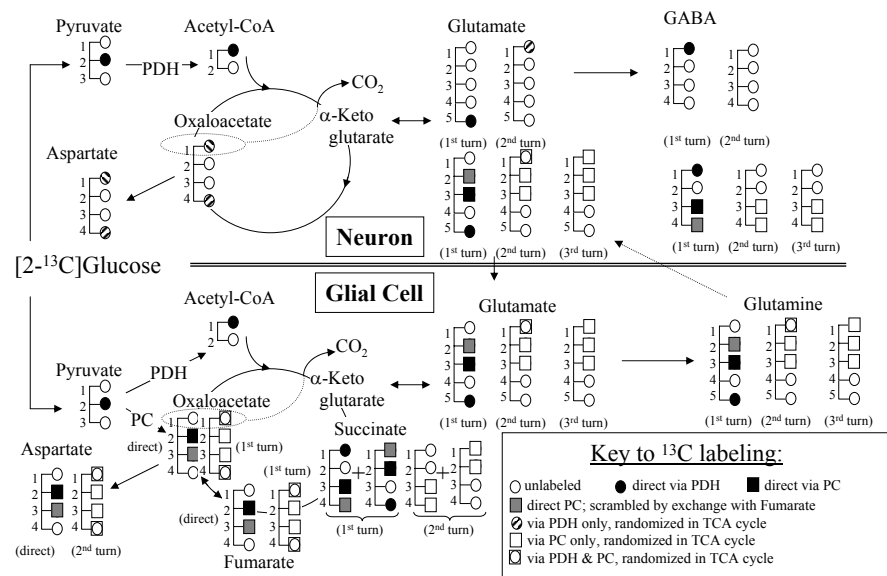


Figure 5.1: $[2-^{13}\text{C}]$ glucose is an ideal tracer for studying changes in the PC:PDH ratio. Flux via PDH directly labels C5 of glutamate and glutamine, whereas flux via PC labels C3 directly, and C2 due to randomization of label at fumarate. TCA cycling does not scramble the C5 and the C3 positions, thus enabling an estimate of the PC:PDH ratio in glutamate, glutamine, GABA, and aspartate.

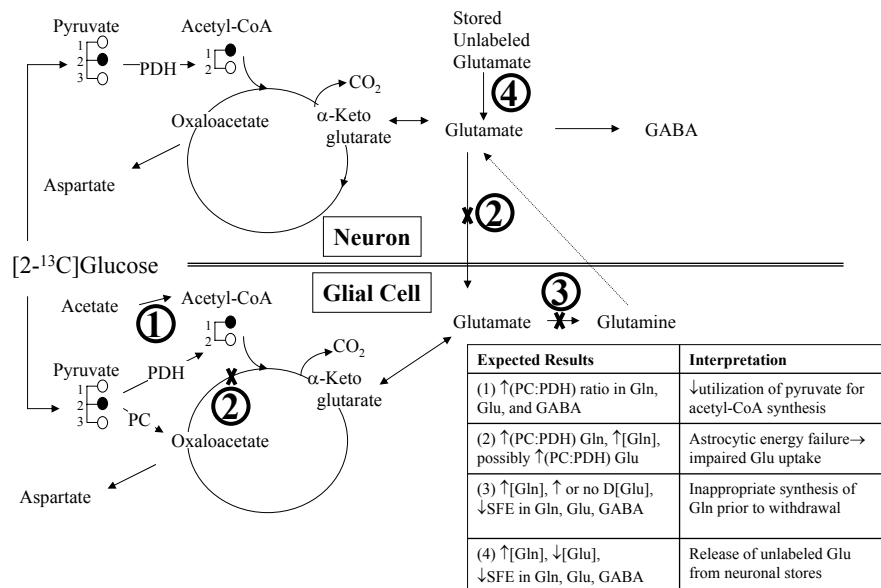


Figure 5.2: Expected results using $2-^{13}\text{C}$ glucose to study the effect of chronic ethanol and acetate exposure on brain metabolism. Abbreviations: ↑, increase; ↓, decrease; Δ, change; Σ, total; →, causes.

5.1, the C5 of glutamate is labeled due to flux via PDH, whereas the C2 and C3 are labeled due to PDH flux.

According to our hypothesis, we expect to find evidence of decreased astrocytic utilization of pyruvate for synthesis of acetyl-CoA following chronic ethanol exposure (scenario 1 in Fig. 5.2) due to increased reliance on acetate which is abundant during ethanol intoxication. In this scenario, we would expect to find an elevation of the PC:PDH ratio in Gln. To the extent that glial Gln serves as a precursor for Glu and GABA, the PC:PDH ratio would be elevated in these molecules as well. Since utilization of pyruvate via PC actually uses 1 molecule of ATP (as opposed to producing 3 ATP if pyruvate entered the TCA cycle via PDH and exited at α -ketoglutarate, or 12 ATP if it entered via PDH and continued through the cycle), inappropriately high PC activity in the absence of alternative sources of acetyl-CoA could impair the ability of astrocytes to maintain the electrochemical gradients required for uptake of glutamate (Anderson and Swanson, 2000) (scenario 2 in Fig. 5.2). This scenario would be suggested by increased PC:PDH ratio in Gln, Glu and GABA with decreased total concentration of Gln; to the extent that the Gln produced by astrocytes continues to serve as a precursor for Glu, an increase in the PC:PDH ratio for Glu may occur as well. During time course measurements, we might expect to observe evidence for scenario 1 (decreased flux of pyruvate through PDH) at early time points, and at later time points this might evolve into scenario 2 (energy failure due to increased PC:PDH flux). Another anticipated finding would be increased Gln resulting from astrocytic overproduction during ethanol intoxication due to an overabundant supply of acetate. If the Gln concentration were great enough to inhibit the activity of Glutamine synthase, the total FE in Gln, Glu, and GABA would be reduced, but the concentrations of Glu and GABA would not be decreased (and might increase) due to the abundance of precursor Gln (scenario 3, Fig. 5.2). A final alternative is the release of unlabeled, preformed Glu from neurons. This scenario would be characterized by decreased Glu concentration, increased Gln (due to astrocytic conversion), and a decrease of total FE in Glu, Gln, and GABA since unlabeled Glu will be entering the metabolic cycle (scenario 4, Fig. 5.2).

5.5 Ethanol-GABA Interactions

It is very tempting to interpret our finding of altered GABA metabolism in 10-day-ethanol-treated rats as a metabolic manifestation of increased GABA release (Roberto et al., 2004). However, Roberto et al.'s findings apply to the central amygdala, and not

necessarily the entire brain. It might be very interesting to combine electrical recordings of tissue slices with metabolic studies to determine if these effects have a common basis. As a first pass, it might be possible to simply replace natural abundance glucose in the perfusate with ^{13}C -labeled glucose, or to supplement the media with natural abundance (or ^{13}C -labeled) acetate. Then electrical work could proceed as usual, and the tissue could be extracted afterwards. It might be difficult to obtain NMR signals if the mass of tissue extracted were less than 100-200mg, but otherwise, given the correct equipment, NMR analysis should be straightforward.

On a related topic, it occurs to us that some of the results attributed to increased neuronal release of GABA could perhaps be the result of decreased uptake of GABA by astrocytes, thus potentiating GABA's effect. Additional studies would be required to clarify this point.

5.6 The Future of Metabolomics

Several important challenges must be met in order for the field of metabolomics to progress from the exploratory phase to a point where significant advances can occur. In my view, the most important are (i) validation of quantitative methods, (ii) standardization of data collection methods, (iii) standardization of protocols for data analysis, including the treatment of outlier data, and (iv) formation of public databases into which results must be entered as a condition of publication in first-tier journals.

Recently, the first steps towards validation of metabolomic methods have been published (Dumas et al., 2006), investigating the reproducibility of metabolomic analysis at sites in Chicago, Japan, and China. The main findings were that ^1H NMR-based metabolomic analysis of urine has a coefficient of variation (CV) of 0 to 10% across metabolite signals, which is substantially better than pyrolysis metastable atom bombardment time-of-flight mass spectrometry (Py-MAB-TOFMS) that showed 20-250% CV in the analysis of bovine urine (Dumas et al., 2002), and comparable to the 8% CV obtained with GC-MS analysis of plant metabolites (Fiehn et al., 2000).

The importance of solid technique in acquiring the data and "good-faith data mining" are fairly obvious. Unfortunately, neither a coherent set of NMR acquisition parameters nor a reasonable procedure for multivariate analysis have been widely adopted thus far. A combination of monte carlo simulations and systematic exploration of instrument parameters on actual metabolomic samples will be required.

The rationale for insisting on the formation of a database is as follows: By their

very nature, metabolomic studies generate "information overload", and the design is inappropriate for journal-only presentation format in which the authors attempt to draw summary conclusions from the data. Statistical significance in this type of analysis is an elusive concept (see §3.2.4), and therefore by forming a database in which metabolite concentrations are stored in meaningful units (e.g. mM for serum or mmol/kg tissue), new hypotheses, perhaps independent of those that motivated the original work, can be explored *in silico*, increasing the value of the original experiments. Also, such a resource would facilitate the differentiation between shoddy technique and genuine biochemical differences. In addition, by presenting a consensus view on the properties (e.g. NMR properties) of various metabolites, the assignment of spectral data can be simplified and effort can be focused on the characterization of signals due to progressively fewer "unknown" sources. Similar logic applies to the need to create databases that provide a biochemical context for various metabolites.

Clinical Metabolomics: the Holy Grail

Thus far, metabolomics has demonstrated great potential, but there are few concrete examples of successful applications. While the elucidation of biochemical pathways in plants, cell cultures, or laboratory animals is academically interesting, the greatest achievement would be to meaningfully improve human health.

A number of areas appear to be on the verge of a major breakthrough. Metabolomic screening for certain types of cancer might prove lifesaving if early detection can be translated into increased survival. If it is possible to diagnose coronary artery blockage by analysis of a blood sample, it might be possible to determine the likelihood that a younger person will develop heart disease and thereby focus preventative measures on those at the greatest risk. Metabolomic analysis for staging of certain cancers seems to be a very sensible and promising approach.

One important limitation in many clinical metabolomic studies is sample size. For example, in their exciting paper on the metabolomic classification of patients undergoing coronary angiography, Brindle et al. included data from only 66 subjects (Brindle et al., 2002). In the supplementary material for their paper, the authors argue that the sample size is "... certainly large enough: the statistical analysis makes it clear that the diagnostic power we have demonstrated is very unlikely to be due to chance." This argument, while probably correct (i.e. their ability to classify the subjects in their study was probably not due to random chance), misses the more significant question of whether within a larger group of subjects additional variance would overwhelm the

model's ability to classify based on differences related to risk of heart disease. In particular, would inclusion of subjects at different sites (where important factors such as diet and intestinal flora are likely to vary) decrease the predictive power of the approach? Without being able to provide a definitive negative answer to this question, the results, while academically interesting, are of little practical value. Larger data sets, preferably focused on clinically significant diseases, will ensure that the potential value of metabolomics is realized in the clinic.

Appendix A

NMR Essentials

I must begin this section with a disclaimer: it is beyond the scope of this dissertation to provide a complete description of NMR spectroscopy. Rather, the intent is to provide relevant background for the methods employed in this dissertation. The interested newcomer is referred to excellent texts by Timothy Claridge or Frank van de Ven.

A.1 History of NMR

Nuclear magnetic resonance has been an extremely fruitful field, the history of which can be traced by recounting the contributions of the many Nobel laureates who contributed to its development:

- 1943 Otto Stern for discovery of the magnetic moment of the proton
- 1944 Isidor I. Rabi for development of the "resonance method for recording the magnetic properties of atomic nuclei"
- 1952 Felix Bloch and Edward M. Purcel "for their discovery of new methods for nuclear magnetic precision measurements and discoveries in connection therewith"
- 1991 Richard R. Ernst for developing high resolution NMR data collection methods, notably fourier transform NMR and multidimensional NMR
- 2002 Kurt Wutrich for developing methods to determine the three dimensional structure of biological molecules using NMR
- 2003 Paul C. Lauterbur and Peter Mansfield for developing Magnetic Resonance Imaging (MRI)

While this is by no means a complete account, it highlights the most important events: the discovery of the nuclear magnetic moment, the development of technology and

Type	ν (Hz)	λ (m)	Transition
UV	10^{16}	3×10^{-8}	Electronic
IR	10^{13}	3×10^{-5}	Vibrational
NMR	10^8	3	Nuclear

Table A.1: Comparison of ultraviolet (UV), infrared (IR) and NMR spectroscopy. NMR spectroscopy uses low energy (long wavelength) EM radiation (radio waves) to probe the low energy nuclear transitions in a sample.

methods for manipulating and recording signals from nuclear magnetic moments, and the applications of these techniques to the study of chemistry and medicine.

A.2 NMR as a spectroscopic method

Nuclear magnetic resonance (NMR) spectroscopy (NMRS) shares many similarities with other forms of spectroscopy, as well as some important differences. Spectroscopy, by definition, is the study of the interaction of electromagnetic (EM) radiation with matter ("the sample"). These interactions drive transitions between energy states in the sample, and the energy difference between the states determines the frequency of the radiation:

$$\Delta E = h\nu \tag{A.1}$$

where h is Planck's constant. For the sake of comparison, the characteristic transitions and corresponding energies for various forms of spectroscopy are given in TableA.2.

NMR uses very low energy (low frequency, long wavelength) radiation to drive nuclear transitions.

Certain differences between NMRS and other forms of spectroscopy are worth noting: (i) whereas the molecular energy levels in laser spectroscopy are always available, the nuclear energy levels that form the basis for NMRS must be induced by placing the sample in an external magnetic field, (ii) whereas other forms of spectroscopy involve an interaction with the electric component of the radiation, NMRS involves an interaction with the magnetic component, (iii) unlike many other forms of spectroscopy, a semi-classical description can provide a satisfactory explanation of basic NMRS experiments.

Nucleus	\vec{I}	g (10^7rad/T/s)	Natural Abundance (%)	NMR frequency (MHz) @ 2.35T
^1H	1/2	26.75	99.985	100
^{13}C	1/2	6.728	1.108	25.14
^{15}N	1/2	-2.713	0.37	10.13

Table A.2: Properties of some isotopes commonly studied by NMR

A.3 Physics of Magnetic Resonance

Though the majority of applications for NMRS are in the fields of chemistry, biochemistry, medicine, and other life sciences, the physical basis for the signals involves good old-fashioned physics: spin, current, magnetic dipoles, vectors, and the like. A solid understanding of these concepts enables an intuitive approach to experimental design and analysis, so a brief overview will be presented here.

A.3.1 Nuclear Spin and Nuclear Magnetism

Only certain nuclei exhibit magnetic resonance behavior. Just as electrons can be stacked into orbitals, and unpaired electrons in metals give rise to paramagnetism, nucleons (neutrons and protons) within the nucleus that are unpaired give rise to nuclear spin and a nuclear magnetic dipole moment. Intuitively, a spinning nucleus which bears a positive charge can be viewed as a tiny circulating current, which produces a magnetic dipole. The faster the spin, the greater the current, and the greater the resulting magnetic field. Thus, the nuclear magnetic dipole moment, $\vec{\mu}$, is proportional to the nuclear spin \vec{I} via a characteristic constant for each nucleus termed the gyromagnetic ratio, γ :

$$\vec{\mu} = \gamma \vec{I} \quad (\text{A.2})$$

The properties for various commonly-studied isotopes are given in Table A.3.1.

A.3.2 Equation of Motion

Figure A.3.2 depicts a spinning nucleus in an external magnetic field \vec{B} . The equation of motion is:

$$\frac{d}{dt}[\vec{\mu}] = -\gamma \vec{B} \times \vec{\mu} \quad (\text{A.3})$$

indicating that the force on $\vec{\mu}$ is always perpendicular to $\vec{\mu}$, so as to cause precession of the magnetic moment about the external field.

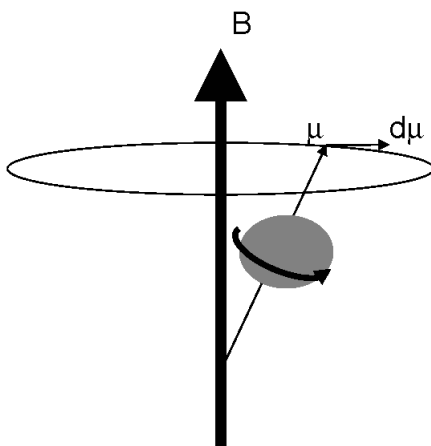


Figure A.1: Free precession of a spin in a magnetic field.

The frequency of precession in a static field of magnitude B_0 is given by the famous Larmor equation:

$$\omega_0 = \gamma B_0 \quad (\text{A.4})$$

An additional consequence of placing a magnetic dipole in an external field is that there are only two orientations in which the field exerts no torque on the dipole: when the dipole is aligned parallel or antiparallel to the field. These are so-called "spin-up" and "spin-down" configurations. Intuitively, the parallel "spin-up" state has a lower energy than the antiparallel state, and the difference between these states, ΔE , is proportional to the strength of the external field (as in the Zeeman effect in atomic orbitals).

A.3.3 Equilibrium Magnetization

At thermal equilibrium there is a very slight excess of spins oriented parallel to the magnetic field, which depends on the strength of the field and the temperature

$$\frac{\text{spin} - \text{up}}{\text{spin} - \text{down}} = e^{\frac{-\Delta E}{kT}} \quad (\text{A.5})$$

k is Boltzman's constant. In a 100MHz magnet (2.35T) at room temperature (300K), the population excess in the low energy (spin-up) state is about 10 spins per million. At first glance, this seems like a hopelessly small number, but one must keep in mind that a $\sim 1\text{mL}$ NMR sample contains more than 10^{22} water protons. If we consider the vector sum of all the $\vec{\mu}$, the bulk magnetization, \vec{M} , things no longer look so bad.

A.3.4 Relaxation

Without discussing for the moment how we manage to tip the magnetization away from the external field, it is important to discuss the return to equilibrium. Transverse relaxation describes the process by which magnetization perpendicular to the external field decays over time. Longitudinal relaxation describes the regrowth of magnetization parallel to the external field. In all situations relevant to the work described in this dissertation, these processes can both be modeled by exponential decay:

$$M_{\perp}(t) = M_{\perp}(0)e^{-t/T_2} \quad (\text{A.6})$$

$$M_z(t) = M_0 + (M_z(0) - M_0)e^{t/T_1} \quad (\text{A.7})$$

where T_1 is the characteristic longitudinal relaxation time, T_2 is the characteristic transverse relaxation time, and M_0 is the equilibrium magnetization. Physically, the process of longitudinal relaxation involves exchange of energy between excited nuclei and "the lattice". Transverse relaxation involves the loss of phase coherence due to randomly timed interactions between neighboring spins (so-called "spin-spin relaxation"). A far more detailed description of relaxation mechanisms and their significance can be found in Vladimir Bakhmutov's "Practical NMR Relaxation for Chemists".

A.4 Modern NMR methods

Early continuous wave (CW) instruments consisted of electromagnets, chart recorders and/or oscilloscopes, and though certain key experiments were conducted using this technology, modern instruments are vastly superior.

A.4.1 The Spectrometer

At the heart of the modern NMR spectrometer is a superconducting electromagnet which must be bathed in liquid helium to maintain its temperature at 4K. In fact, 90% or so of the bulk of a spectrometer is vacuum-sealed chambers to hold cryogens. As long as the superconducting coils remain at 4K, they have zero resistance; current is induced in the magnet once when it is installed, and afterwards it runs indefinitely. The sample is introduced into an radio frequency (RF) coil inside the magnet, which allows precisely controlled bursts of RF energy to excite nuclei in the sample. After the nuclei have been excited by an RF pulse, the same coil can be used to monitor the

emission signal from the sample.

A.4.2 NMR processing

Time domain data is collected by the instrument and saved in digital form on the acquisition computer. Fourier transformation yields a frequency domain spectrum, such as the ones shown in this dissertation.

Appendix B

Essentials of Metabolism

B.1 Overview of the TCA cycle

The TCA cycle is the central hub of eukaryotic metabolism. The reactions and structures of the intermediates are shown in Figure B.1.

The logical place to begin describing the cycle is with the substrates that may enter. Pyruvate (derived from glucose or three carbon metabolites such as lactate or alanine) may enter the TCA cycle in the oxidative pathway via pyruvate dehydrogenase (PDH), or via the anapleurotic pathway via pyruvate carboxylase. Many biochemistry textbooks emphasize only the oxidative pathway. However, if TCA cycle intermediates are used for net synthesis of other compounds (e.g. α -ketoglutarate is used to produce glutamate which is exported from the cell), flux through PC is the only way to replenish intermediates that are lost. Thus the name anapleurosis, derived from Greek: 'filling up', is an apt name. Acetate may enter the TCA cycle only as acetyl-CoA via a reaction catalyzed by acetyl-CoA synthetase (ACoAS).

The citrate synthase (CS) reaction involves the stereospecific condensation of acetyl-CoA and oxaloacetate to form citrate. Though citrate appears at first glance to be a symmetrical molecule, it is in fact pro-chiral. The structure of CS determines its reaction with the asymmetrical substrates

B.2 Metabolite Structures

With hundreds of compounds potentially detectable by NMR, it becomes useful to have a reference showing the exact chemical structure (with protons drawn explicitly), together with the trivial name.

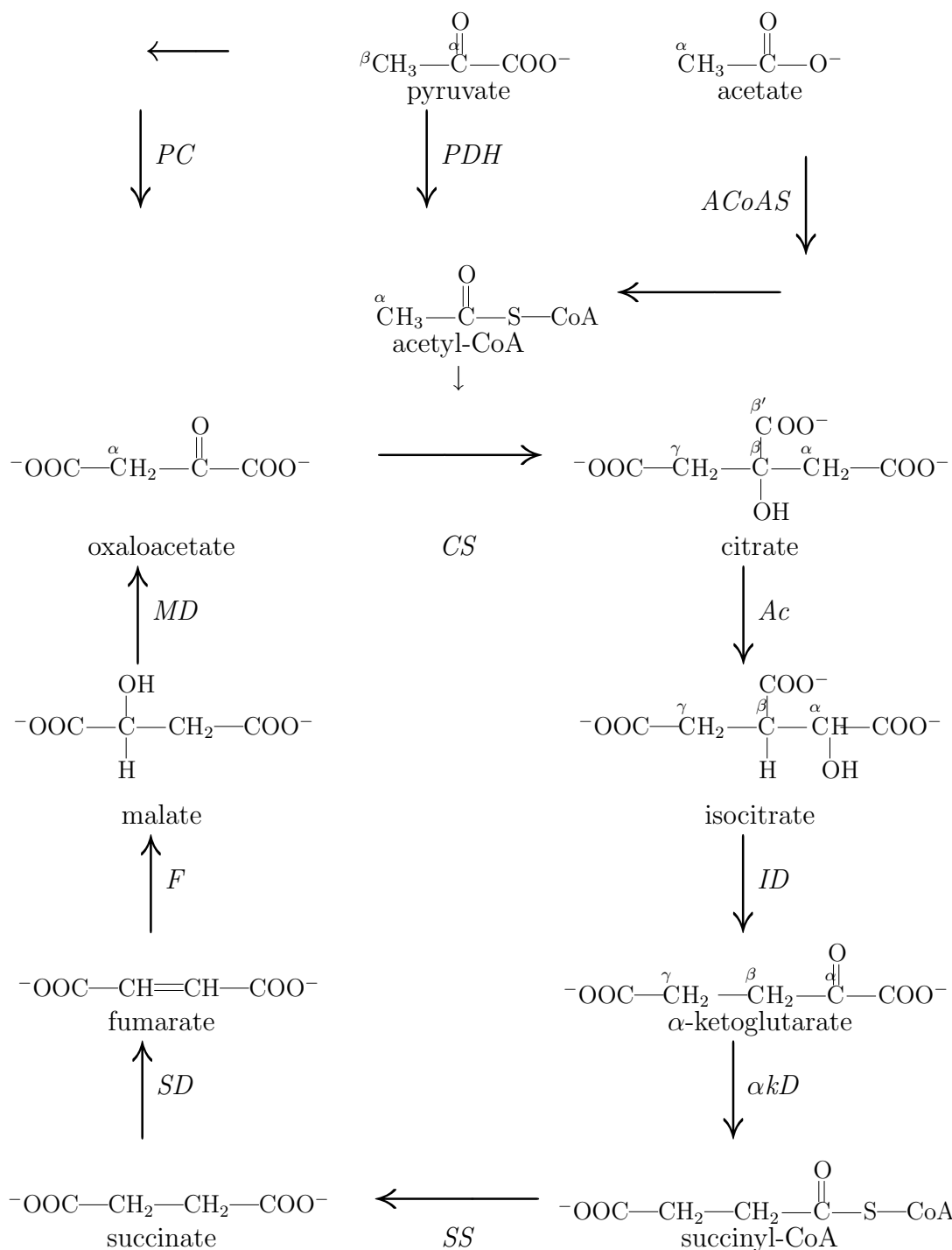
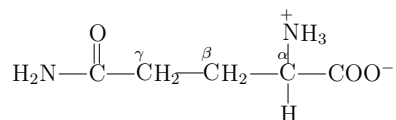
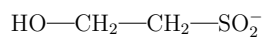
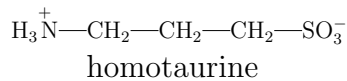


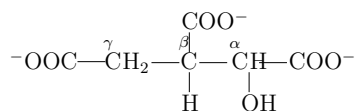
Figure B.1: Reactions of the TCA cycle. Key: *Ac*, Aconitase; *αkD* , α -ketoglutarate Dehydrogenase; *CS*, citrate synthase; *F*, Fumarase; *ID*, Isocitrate dehydrogenase; *MD*, Malate Dehydrogenase; *PC*, pyruvate dehydrogenase; *PDH*, pyruvate dehydrogenase; *SD*, Succinate Dehydrogenase; *SS*, succinyl-CoA synthetase;



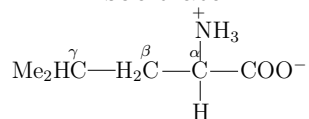
glutamine



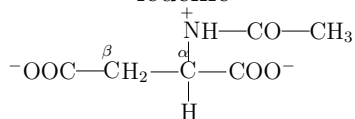
isethionate



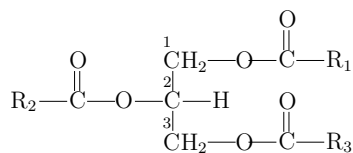
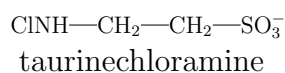
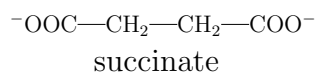
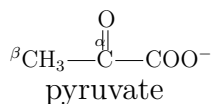
isocitrate



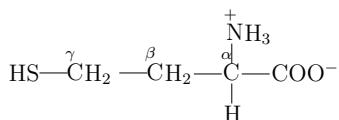
leucine



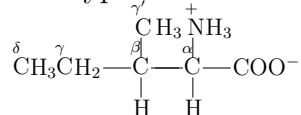
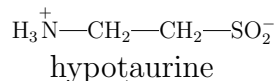
Nacetylaspartate



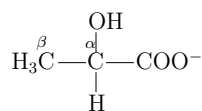
triacylglycerol



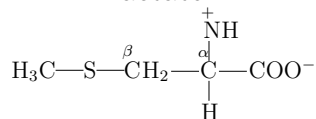
homocysteine



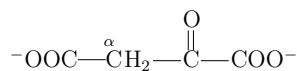
isoleucine



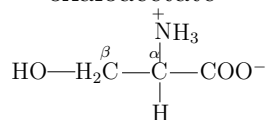
lactate



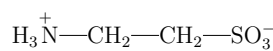
methionine



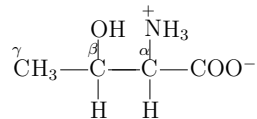
oxaloacetate



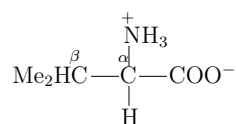
serine



taurine



threonine



valine

Table B.1: Metabolite structures

Appendix C

Mathematical description of principal components analysis

Mathematically, PCA can be accomplished in the following way. The first step is to collect the data into matrix form where each row corresponds to an individual, and each column a parameter measured on that individual.

$$\vec{\vec{D}} = \begin{bmatrix} meas_1(I_1) & meas_2(I_1) & \dots & meas_n(I_1) \\ meas_1(I_2) & meas_2(I_2) & \dots & meas_n(I_2) \\ \vdots & & \ddots & \vdots \\ meas_1(I_m) & meas_2(I_m) & \dots & meas_n(I_m) \end{bmatrix} \quad (C.1)$$

The next step is to compute the covariance matrix (see §C.1):

$$\vec{\vec{C}} = cov(\vec{\vec{D}}) \quad (C.2)$$

Finally, we obtain the principal component vectors by computing the eigenvectors of the covariance matrix $\vec{\vec{C}}$, and sorting them according to their eigenvalues.

C.1 Covariance and the covariance matrix

The covariance between two random variables X and Y is defined as

$$Cov(X, Y) = \langle (X - \bar{X})(Y - \bar{Y}) \rangle \quad (C.3)$$

where the angled brackets denote the expected value of the quantity they enclose, and the bars indicate the means of the random variables. In the case of discrete random

variables, the formula for computing the covariance is:

$$Cov(X, Y) = \frac{1}{(n-1)} \sum_{i=1}^N (x_i - \bar{x})(y_i - \bar{y}) = \frac{n \sum_{i=1}^n x_i y_i - \sum_{i=1}^n x_i \sum_{i=1}^n y_i}{n(n-1)} \quad (C.4)$$

where the n individual elements of X and Y are the x_i and y_i . The second form is preferred for computation. Note that $Cov(X, X)$ is equal to the variance of X .

The discussion of covariance has focused thus far only on a single pair of variables. However for a collection of data organized into a matrix \vec{C} of n rows (observations) and m columns (variables), all possible covariances can be computed in matrix form:

$$\vec{C} = \begin{bmatrix} c_1^2 & c_{12} & \dots & c_{1m} \\ c_{21} & c_2^2 & \dots & c_{2m} \\ \vdots & & \ddots & \vdots \\ c_{m1} & c_{m2} & \dots & c_m^2 \end{bmatrix} \quad (C.5)$$

where the elements c_{ij} of \vec{C} are given by

$$c_{ij} = \frac{1}{(n-1)} \left(\sum_{k=1}^n x_{ik} y_{jk} - \frac{1}{n} \sum_{k=1}^n x_{ik} \sum_{k=1}^n y_{jk} \right) \quad (C.6)$$

Bibliography

- Albrecht, U. and Eichele, G. (2003). The mammalian circadian clock. *Curr Opin Genet Dev*, 13(3):271–7.
- Allen, T. M. and Hardin, C. D. (1998). Pattern of substrate utilization in vascular smooth muscle using ^{13}C isotopomer analysis of glutamate. *Am J Physiol*, 275(6 Pt 2):H2227–35.
- Anderson, C. M. and Swanson, R. A. (2000). Astrocyte glutamate transport: review of properties, regulation, and physiological functions. *Glia*, 32(1):1–14.
- Badar-Goffer, R. S., Bachelard, H. S., and Morris, P. G. (1990). Cerebral metabolism of acetate and glucose studied by ^{13}C -n.m.r. spectroscopy. a technique for investigating metabolic compartmentation in the brain. *Biochem J*, 266(1):133–9.
- Bailey, M. S. and Shipley, M. T. (1993). Astrocyte subtypes in the rat olfactory bulb: morphological heterogeneity and differential laminar distribution. *J Comp Neurol*, 328(4):501–26.
- Ballenger, J. C. and Post, R. M. (1978). Kindling as a model for alcohol withdrawal syndromes. *Br J Psychiatry*, 133:1–14.
- Barak, A. J., Beckenhauer, H. C., Junnila, M., and Tuma, D. J. (1993). Dietary betaine promotes generation of hepatic s-adenosylmethionine and protects the liver from ethanol-induced fatty infiltration. *Alcohol Clin Exp Res*, 17(3):552–5.
- Barak, A. J., Beckenhauer, H. C., and Tuma, D. J. (1996). Betaine, ethanol, and the liver: a review. *Alcohol*, 13(4):395–8.
- Barker, S. B. and Summerson, W. H. (1941). The colorimetric determination of lactic acid in biological material. *J. biol. Chem.*, 138:535.
- Becker, H. C. (1996). The alcohol withdrawal "kindling" phenomenon: clinical and experimental findings. *Alcohol Clin Exp Res*, 20(8 Suppl):121A–124A.
- Bender, R. and Lange, S. (1999). Multiple test procedures other than bonferroni's deserve wider use. *Bmj*, 318(7183):600–1.

- Benjamin, A. M. and Quastel, J. H. (1972). Locations of amino acids in brain slices from the rat. tetrodotoxin-sensitive release of amino acids. *Biochem J*, 128(3):631–46.
- Bertocci, L. A. and Lujan, B. F. (1999). Incorporation and utilization of [3-13c]lactate and [1,2-13c]acetate by rat skeletal muscle. *J Appl Physiol*, 86(6):2077–89.
- Bland, J. M. and Altman, D. G. (1995). Multiple significance tests: the bonferroni method. *Bmj*, 310(6973):170.
- Bleich, S., Lenz, B., Ziegenbein, M., Beutler, S., Frieling, H., Kornhuber, J., and Bensch, D. (2006). Epigenetic dna hypermethylation of the herp gene promoter induces down-regulation of its mrna expression in patients with alcohol dependence. *Alcohol Clin Exp Res*, 30(4):587–91.
- Borges-Silva, C. N., Alonso-Vale, M. I., Franzoi-De-Moraes, S. M., Takada, J., Peres, S. B., Andreotti, S., Skorupa, A. L., Cipolla-Neto, J., Pithon-Curi, T. C., and Lima, F. B. (2005). Pinealectomy impairs adipose tissue adaptability to exercise in rats. *J Pineal Res*, 38(4):278–83.
- Brainard, J. R., Kyner, E., and Rosenberg, G. A. (1989). 13c nuclear magnetic resonance evidence for gamma-aminobutyric acid formation via pyruvate carboxylase in rat brain: a metabolic basis for compartmentation. *J Neurochem*, 53(4):1285–92.
- Braunova, Z., Kasparova, S., Mlynarik, V., Mierisova, S., Liptaj, T., Tkac, I., and Gvozdzakova, A. (2000). Metabolic changes in rat brain after prolonged ethanol consumption measured by 1h and 31p mrs experiments. *Cell Mol Neurobiol*, 20(6):703–15.
- Brindle, J. T., Antti, H., Holmes, E., Tranter, G., Nicholson, J. K., Bethell, H. W., Clarke, S., Schofield, P. M., McKilligin, E., Mosedale, D. E., and Grainger, D. J. (2002). Rapid and noninvasive diagnosis of the presence and severity of coronary heart disease using 1h-nmr-based metabonomics. *Nat Med*, 8(12):1439–44.
- Bushong, E. A., Martone, M. E., Jones, Y. Z., and Ellisman, M. H. (2002). Protoplasmic astrocytes in cal stratum radiatum occupy separate anatomical domains. *J Neurosci*, 22(1):183–92.
- Butt, A. M., Hamilton, N., Hubbard, P., Pugh, M., and Ibrahim, M. (2005). Synantocytes: the fifth element. *J Anat*, 207(6):695–706.

- Carmichael, F. J., Israel, Y., Crawford, M., Minhas, K., Saldivia, V., Sandrin, S., Campisi, P., and Orrego, H. (1991). Central nervous system effects of acetate: contribution to the central effects of ethanol. *J Pharmacol Exp Ther*, 259(1):403–8.
- Cerdan, S., Kunnecke, B., and Seelig, J. (1990). Cerebral metabolism of [1,2-¹³C₂]acetate as detected by in vivo and in vitro ¹³C nmr. *J Biol Chem*, 265(22):12916–26.
- Chandler, L. J., Newsom, H., Sumners, C., and Crews, F. (1993). Chronic ethanol exposure potentiates nmda excitotoxicity in cerebral cortical neurons. *J Neurochem*, 60(4):1578–81.
- Chateil, J., Biran, M., Thiaudiere, E., Canioni, P., and Merle, M. (2001). Metabolism of [1-(¹³C)glucose and [2-(¹³C]acetate in the hypoxic rat brain. *Neurochem Int*, 38(5):399–407.
- Chauvin, M. F., Megnin-Chanet, F., Martin, G., Mispelter, J., and Baverel, G. (1997). The rabbit kidney tubule simultaneously degrades and synthesizes glutamate. a ¹³C nmr study. *J Biol Chem*, 272(8):4705–16.
- Coen, M., Lenz, E. M., Nicholson, J. K., Wilson, I. D., Pognan, F., and Lindon, J. C. (2003). An integrated metabonomic investigation of acetaminophen toxicity in the mouse using nmr spectroscopy. *Chem Res Toxicol*, 16(3):295–303.
- Cohen, S. A. and Michaud, D. P. (1993). Synthesis of a fluorescent derivatizing reagent, 6-aminoquinolyl-n-hydroxysuccinimidyl carbamate, and its application for the analysis of hydrolysate amino acids via high-performance liquid chromatography. *Anal Biochem*, 211(2):279–87.
- Cohen, S. M. (1983). Simultaneous ¹³C and ³¹P nmr studies of perfused rat liver. effects of insulin and glucagon and a ¹³C nmr assay of free Mg²⁺. *J Biol Chem*, 258(23):14294–308.
- Cohen, S. M., Shulman, R. G., and McLaughlin, A. C. (1979). Effects of ethanol on alanine metabolism in perfused mouse liver studied by ¹³C nmr. *Proc Natl Acad Sci U S A*, 76(10):4808–12.

- Cornell-Bell, A. H., Finkbeiner, S. M., Cooper, M. S., and Smith, S. J. (1990). Glutamate induces calcium waves in cultured astrocytes: long-range glial signaling. *Science*, 247(4941):470–3.
- Craig, A., Cloarec, O., Holmes, E., Nicholson, J. K., and Lindon, J. C. (2006). Scaling and normalization effects in nmr spectroscopic metabonomic data sets. *Anal Chem*, 78(7):2262–7.
- Crockford, D. J., Holmes, E., Lindon, J. C., Plumb, R. S., Zirah, S., Bruce, S. J., Rainville, P., Stumpf, C. L., and Nicholson, J. K. (2006). Statistical heterospectroscopy, an approach to the integrated analysis of nmr and uplc-ms data sets: application in metabonomic toxicology studies. *Anal Chem*, 78(2):363–71.
- Dahchour, A., De Witte, P., Bolo, N., Nedelec, J. F., Muzet, M., Durbin, P., and Macher, J. P. (1998). Central effects of acamprosate: part 1. acamprosate blocks the glutamate increase in the nucleus accumbens microdialysate in ethanol withdrawn rats. *Psychiatry Res*, 82(2):107–14.
- Danbolt, N. C. (2001). Glutamate uptake. *Prog Neurobiol*, 65(1):1–105.
- De Witte, P. (2004). Imbalance between neuroexcitatory and neuroinhibitory amino acids causes craving for ethanol. *Addict Behav*, 29(7):1325–39.
- De Witte, P., Pinto, E., Ansseau, M., and Verbanck, P. (2003). Alcohol and withdrawal: from animal research to clinical issues. *Neurosci Biobehav Rev*, 27(3):189–97.
- Derr, R. F., Draves, K., and Derr, M. (1981). Abatement by acetate of an ethanol withdrawal syndrome. *Life Sci*, 29(17):1787–90.
- Devaud, L. L., Fritschy, J. M., Sieghart, W., and Morrow, A. L. (1997). Bidirectional alterations of gaba(a) receptor subunit peptide levels in rat cortex during chronic ethanol consumption and withdrawal. *J Neurochem*, 69(1):126–30.
- Devlin, N. J., Scuffham, P. A., and Bunt, L. J. (1997). The social costs of alcohol abuse in new zealand. *Addiction*, 92(11):1491–505.
- Dringen, R., Pfeiffer, B., and Hamprecht, B. (1999). Synthesis of the antioxidant glutathione in neurons: supply by astrocytes of cysgly as precursor for neuronal glutathione. *J Neurosci*, 19(2):562–9.

- Droenner, P., Schmitt, G., Aderjan, R., and Zimmer, H. (2002). A kinetic model describing the pharmacokinetics of ethyl glucuronide in humans. *Forensic Sci Int*, 126(1):24–9.
- Dumas, M. E., Debrauwer, L., Beyet, L., Lesage, D., Andre, F., Paris, A., and Tabet, J. C. (2002). Analyzing the physiological signature of anabolic steroids in cattle urine using pyrolysis/metastable atom bombardment mass spectrometry and pattern recognition. *Anal Chem*, 74(20):5393–404.
- Dumas, M. E., Maibaum, E. C., Teague, C., Ueshima, H., Zhou, B., Lindon, J. C., Nicholson, J. K., Stamler, J., Elliott, P., Chan, Q., and Holmes, E. (2006). Assessment of analytical reproducibility of (1)h nmr spectroscopy based metabolomics for large-scale epidemiological research: the intermap study. *Anal Chem*, 78(7):2199–2208.
- Eckardt, M. J., File, S. E., Gessa, G. L., Grant, K. A., Guerri, C., Hoffman, P. L., Kalant, H., Koob, G. F., Li, T. K., and Tabakoff, B. (1998). Effects of moderate alcohol consumption on the central nervous system. *Alcohol Clin Exp Res*, 22(5):998–1040.
- Fan, T. W., Higashi, R. M., Lane, A. N., and Jardetzky, O. (1986). Combined use of 1h-nmr and gc-ms for metabolite monitoring and in vivo 1h-nmr assignments. *Biochim Biophys Acta*, 882(2):154–67.
- Fan, T. W. M. (1996). Metabolite profiling by one- and two-dimensional nmr analysis of complex mixtures. *Progress in Nuclear Magnetic Resonance Spectroscopy*, 28:161–219.
- Fenoglio, P., Parel, V., and Kopp, P. (2003). The social cost of alcohol, tobacco and illicit drugs in france, 1997. *Eur Addict Res*, 9(1):18–28.
- Fiehn, O., Kopka, J., Dormann, P., Altmann, T., Trethewey, R. N., and Willmitzer, L. (2000). Metabolite profiling for plant functional genomics. *Nat Biotechnol*, 18(11):1157–61.
- Garcia-Espinosa, M. A., Garcia-Martin, M. L., and Cerdan, S. (2003). Role of glial metabolism in diabetic encephalopathy as detected by high resolution ^{13}C nmr. *NMR Biomed*, 16(6-7):440–9.

- Gavaghan, C. L., Wilson, I. D., and Nicholson, J. K. (2002). Physiological variation in metabolic phenotyping and functional genomic studies: use of orthogonal signal correction and pls-da. *FEBS Lett*, 530(1-3):191–6.
- Govindaraju, V., Young, K., and Maudsley, A. A. (2000). Proton nmr chemical shifts and coupling constants for brain metabolites. *NMR Biomed*, 13(3):129–53.
- Griffin, J. L. (2003). Metabonomics: Nmr spectroscopy and pattern recognition analysis of body fluids and tissues for characterisation of xenobiotic toxicity and disease diagnosis. *Curr Opin Chem Biol*, 7(5):648–54.
- Gutmann, I. and Wahlefeld, A. (1974). L-(-)-malate determination with malate dehydrogenase and nad. In H.U., B., editor, *Methods of Enzymatic Analysis*, pages 1586–1587. Academic Press, New York.
- Haberg, A., Qu, H., Haraldseth, O., Unsgard, G., and Sonnewald, U. (1998). In vivo injection of [1-13c]glucose and [1,2-13c]acetate combined with ex vivo 13c nuclear magnetic resonance spectroscopy: a novel approach to the study of middle cerebral artery occlusion in the rat. *J Cereb Blood Flow Metab*, 18(11):1223–32.
- Hassel, B. and Sonnewald, U. (1995). Selective inhibition of the tricarboxylic acid cycle of gabaergic neurons with 3-nitropropionic acid in vivo. *J Neurochem*, 65(3):1184–91.
- Hassel, B., Sonnewald, U., and Fonnum, F. (1995). Glial-neuronal interactions as studied by cerebral metabolism of [2-13c]acetate and [1-13c]glucose: an ex vivo 13c nmr spectroscopic study. *J Neurochem*, 64(6):2773–82.
- Hatton, G. I. (1997). Function-related plasticity in hypothalamus. *Annu Rev Neurosci*, 20:375–97.
- Hawkins, R. A., DeJoseph, M. R., and Hawkins, P. A. (1995). Regional brain glutamate transport in rats at normal and raised concentrations of circulating glutamate. *Cell Tissue Res*, 281(2):207–14.
- Hayakawa, K., Ando, K., Yoshida, N., Yamamoto, A., Matsunaga, A., Nishimura, M., Kitaoka, M., and Matsui, K. (2000). Determination of saccharides in sake by high-performance liquid chromatography with polarized photometric detection. *Biomed Chromatogr*, 14(2):72–6.

- Heales, S. J., Lam, A. A., Duncan, A. J., and Land, J. M. (2004). Neurodegeneration or neuroprotection: the pivotal role of astrocytes. *Neurochem Res*, 29(3):513–9.
- Hertz, L., Gibbs, M. E., O’Dowd, B. S., Sedman, G. L., Robinson, S. R., Sykova, E., Hajek, I., Hertz, E., Peng, L., Huang, R., and Ng, K. T. (1996). Astrocyte-neuron interaction during one-trial aversive learning in the neonate chick. *Neurosci Biobehav Rev*, 20(3):537–51.
- Hertz, L., Yu, A. C., Kala, G., and Schousboe, A. (2000). Neuronal-astrocytic and cytosolic-mitochondrial metabolite trafficking during brain activation, hyperammonemia and energy deprivation. *Neurochem Int*, 37(2-3):83–102.
- Hertz, L. and Zielke, H. R. (2004). Astrocytic control of glutamatergic activity: astrocytes as stars of the show. *Trends Neurosci*, 27(12):735–43.
- Hirrlinger, J., Hulsman, S., and Kirchhoff, F. (2004). Astroglial processes show spontaneous motility at active synaptic terminals in situ. *Eur J Neurosci*, 20(8):2235–9.
- Holland, P. and Mushinski, M. (1999). Costs of alcohol and drug abuse in the united states, 1992. alcohol/drugs coi study team. *Stat Bull Metrop Insur Co*, 80(4):2–9.
- Imbenotte, M., Azaroual, N., Cartigny, B., Vermeersch, G., and Lhermitte, M. (2003). Identification and quantitation of xenobiotics by 1h nmr spectroscopy in poisoning cases. *Forensic Sci Int*, 133(1-2):132–5.
- Israel, Y., Orrego, H., and Carmichael, F. J. (1994). Acetate-mediated effects of ethanol. *Alcohol Clin Exp Res*, 18(1):144–8.
- Jabaudon, D., Scanziani, M., Gahwiler, B. H., and Gerber, U. (2000). Acute decrease in net glutamate uptake during energy deprivation. *Proc Natl Acad Sci U S A*, 97(10):5610–5.
- Jain, A., Martensson, J., Stole, E., Auld, P. A., and Meister, A. (1991). Glutathione deficiency leads to mitochondrial damage in brain. *Proc Natl Acad Sci U S A*, 88(5):1913–7.
- Joachims, T. (2002). *Learning to Classify Text Using Support Vector Machines (Dissertation)*. Kluwer Academic Publishers.
- Jucker, B. M., Lee, J. Y., and Shulman, R. G. (1998). In vivo ^{13}C nmr measurements of hepatocellular tricarboxylic acid cycle flux. *J Biol Chem*, 273(20):12187–94.

- Kanamatsu, T. and Tsukada, Y. (1999). Effects of ammonia on the anaplerotic pathway and amino acid metabolism in the brain: an ex vivo ^{13}C nmr spectroscopic study of rats after administering $[2-^{13}\text{C}]$ glucose with or without ammonium acetate. *Brain Res*, 841(1-2):11–9.
- Kanehisa, M., Goto, S., Hattori, M., Aoki-Kinoshita, K. F., Itoh, M., Kawashima, S., Katayama, T., Araki, M., and Hirakawa, M. (2006). From genomics to chemical genomics: new developments in kegg. *Nucleic Acids Res*, 34(Database issue):D354–7.
- Karan, D., David, J. R., and Capy, P. (2001). Molecular evolution of the amp-forming acetyl-coa synthetase. *Gene*, 265(1-2):95–101.
- Kaufman, M. J., Chiu, T. M., Mendelson, J. H., Woods, B. T., Mello, N. K., Lukas, S. E., Fivel, P. A., and Wighton, L. G. (1994). In vivo proton magnetic resonance spectroscopy of alcohol in rhesus monkey brain. *Magn Reson Imaging*, 12(8):1245–53.
- Khurgel, M. and Ivy, G. O. (1996). Astrocytes in kindling: relevance to epileptogenesis. *Epilepsy Res*, 26(1):163–75.
- Kiselevski, Y., Oganessian, N., Zimatkin, S., Szutowicz, A., Angielski, S., Niezabitowski, P., Uracz, W., and Gryglewski, R. J. (2003). Acetate metabolism in brain mechanisms of adaptation to ethanol. *Med Sci Monit*, 9(5):BR178–82.
- Koehler, R. C., Gebremedhin, D., and Harder, D. R. (2006). Role of astrocytes in cerebrovascular regulation. *J Appl Physiol*, 100(1):307–17.
- Korri, U. M., Nuutinen, H., and Salaspuro, M. (1985). Increased blood acetate: a new laboratory marker of alcoholism and heavy drinking. *Alcohol Clin Exp Res*, 9(5):468–71.
- Krebs, H. A., Freedland, R. A., Hems, R., and Stubbs, M. (1969). Inhibition of hepatic gluconeogenesis by ethanol. *Biochem J*, 112(1):117–24.
- Kriat, M., Confort-Gouny, S., Vion-Dury, J., Sciaky, M., Viout, P., and Cozzone, P. J. (1992). Quantitation of metabolites in human blood serum by proton magnetic resonance spectroscopy. a comparative study of the use of formate and tsp as concentration standards. *NMR Biomed*, 5(4):179–84.

- Lam, T. K., Gutierrez-Juarez, R., Pocai, A., and Rossetti, L. (2005). Regulation of blood glucose by hypothalamic pyruvate metabolism. *Science*, 309(5736):943–7.
- Lanigan, R. S. and Yamarik, T. A. (2002). Final report on the safety assessment of bht(1). *Int J Toxicol*, 21 Suppl 2:19–94.
- Learn, J. E., Smith, D. G., McBride, W. J., Lumeng, L., and Li, T. K. (2003). Ethanol effects on local cerebral glucose utilization in high-alcohol-drinking and low-alcohol-drinking rats. *Alcohol*, 29(1):1–9.
- Lebon, V., Petersen, K. F., Cline, G. W., Shen, J., Mason, G. F., Dufour, S., Behar, K. L., Shulman, G. I., and Rothman, D. L. (2002). Astroglial contribution to brain energy metabolism in humans revealed by ^{13}C nuclear magnetic resonance spectroscopy: elucidation of the dominant pathway for neurotransmitter glutamate repletion and measurement of astrocytic oxidative metabolism. *J Neurosci*, 22(5):1523–31.
- Lee, H., Holburn, G. H., and Price, R. R. (2003). Proton mr spectroscopic studies of chronic alcohol exposure on the rat brain. *J Magn Reson Imaging*, 18(2):147–51.
- Lieber, C. S. (1965). Hyperuricemia induced by alcohol. *Arthritis Rheum*, 8(5):786–98.
- Lieber, C. S. (1999). Microsomal ethanol-oxidizing system (meos): the first 30 years (1968-1998)—a review. *Alcohol Clin Exp Res*, 23(6):991–1007.
- Lieber, C. S. and DeCarli, L. M. (1970). Hepatic microsomal ethanol-oxidizing system. in vitro characteristics and adaptive properties in vivo. *J Biol Chem*, 245(10):2505–12.
- Lieber, C. S., Jones, D. P., Losowsky, M. S., and Davidson, C. S. (1962). Interrelation of uric acid and ethanol metabolism in man. *J Clin Invest*, 41:1863–70.
- Lindon, J. C., Holmes, E., Bollard, M. E., Stanley, E. G., and Nicholson, J. K. (2004). Metabonomics technologies and their applications in physiological monitoring, drug safety assessment and disease diagnosis. *Biomarkers*, 9(1):1–31.
- Ling, M. F. and Brauer, M. (1991). ^1H nmr analyses of methyl group-containing metabolites in rat liver extracts—effects of starvation, anoxia, acute glycerol and carbon tetrachloride treatment and chronic ethanol administration on hepatic metabolism. *Physiol Chem Phys Med NMR*, 23(4):229–38.

- Liu, H., Sanuda-Pena, M. C., Harvey-White, J. D., Kalra, S., and Cohen, S. A. (1998). Determination of submicromolar concentrations of neurotransmitter amino acids by fluorescence detection using a modification of the 6-aminoquinolyl-n-hydroxysuccinimidyl carbamate method for amino acid analysis. *J Chromatogr A*, 828(1-2):383–95.
- Llorente, P., Marco, R., and Sols, A. (1970). Regulation of liver pyruvate kinase and the phosphoenolpyruvate crossroads. *Eur J Biochem*, 13(1):45–54.
- Majchrowicz, E. (1975). Induction of physical dependence upon ethanol and the associated behavioral changes in rats. *Psychopharmacologia*, 43(3):245–54.
- Mayes, P. A. (2000). Chapter 27: Lipid transport and storage. In *Harper’s Biochemistry*. Appleton & Lange, New York, 25 edition.
- McGinnis, J. M. and Foege, W. H. (1993). Actual causes of death in the united states. *Jama*, 270(18):2207–12.
- Mendelson, J. H., Woods, B. T., Chiu, T. M., Mello, N. K., Lukas, S. E., Teoh, S. K., Sintavanarong, P., Cochin, J., Hopkins, M. A., and Dobrosielski, M. (1990). In vivo proton magnetic resonance spectroscopy of alcohol in human brain. *Alcohol*, 7(5):443–7.
- Mishima, T., Hayakawa, T., Ozeki, K., and Tsuge, H. (2005). Ethyl alpha-d-glucoside was absorbed in small intestine and excreted in urine as intact form. *Nutrition*, 21(4):525–9.
- Mokdad, A. H., Marks, J. S., Stroup, D. F., and Gerberding, J. L. (2004). Actual causes of death in the united states, 2000. *Jama*, 291(10):1238–45.
- Mokuda, O., Tanaka, H., Hayashi, T., Ooka, H., Okazaki, R., and Sakamoto, Y. (2004). Ethanol stimulates glycogenolysis and inhibits both glycogenesis via gluconeogenesis and from exogenous glucose in perfused rat liver. *Ann Nutr Metab*, 48(4):276–80.
- Mushahwar, I. K. and Koeppe, R. E. (1972). Incorporation of label from(1- 14 c)ethanol into the glutamate-glutamine pools of rat brain in vivo. *Biochem J*, 126(3):467–9.
- Newman, E. A. (2001). Propagation of intercellular calcium waves in retinal astrocytes and muller cells. *J Neurosci*, 21(7):2215–23.

- Newman, E. A. (2003). New roles for astrocytes: regulation of synaptic transmission. *Trends Neurosci*, 26(10):536–42.
- Nicholson, J. K., Foxall, P. J., Spraul, M., Farrant, R. D., and Lindon, J. C. (1995). 750 mhz ^1H and ^1H - ^{13}C nmr spectroscopy of human blood plasma. *Anal Chem*, 67(5):793–811.
- Nicholson, J. K., Lindon, J. C., and Holmes, E. (1999). 'metabonomics': understanding the metabolic responses of living systems to pathophysiological stimuli via multivariate statistical analysis of biological nmr spectroscopic data. *Xenobiotica*, 29(11):1181–9.
- Nishiyama, A., Yang, Z., and Butt, A. (2005). Astrocytes and ng2-glia: what's in a name? *J Anat*, 207(6):687–93.
- Norberg, A., Jones, A. W., Hahn, R. G., and Gabrielsson, J. L. (2003). Role of variability in explaining ethanol pharmacokinetics: research and forensic applications. *Clin Pharmacokinet*, 42(1):1–31.
- Norenberg, M. D. (1979). Distribution of glutamine synthetase in the rat central nervous system. *J Histochem Cytochem*, 27(3):756–62.
- Norenberg, M. D. and Martinez-Hernandez, A. (1979). Fine structural localization of glutamine synthetase in astrocytes of rat brain. *Brain Res*, 161(2):303–10.
- Obernier, J. A., Bouldin, T. W., and Crews, F. T. (2002a). Binge ethanol exposure in adult rats causes necrotic cell death. *Alcohol Clin Exp Res*, 26(4):547–57.
- Obernier, J. A., White, A. M., Swartzwelder, H. S., and Crews, F. T. (2002b). Cognitive deficits and cns damage after a 4-day binge ethanol exposure in rats. *Pharmacol Biochem Behav*, 72(3):521–32.
- O'Brien, R. W. and Stern, J. R. (1968). Stereospecificity of citrate synthetase in relation to glutamate biosynthesis by extracts of *chloropseudomonas ethylicum*. *J Bacteriol*, 95(2):385–8.
- Oliet, S. H., Piet, R., Poulain, D. A., and Theodosis, D. T. (2004). Glial modulation of synaptic transmission: Insights from the supraoptic nucleus of the hypothalamus. *Glia*, 47(3):258–67.

- Olsen, K. M., Gentry-Nielsen, M., Yue, M., Snitily, M. U., and Preheim, L. C. (2006). Effect of ethanol on fluoroquinolone efficacy in a rat model of pneumococcal pneumonia. *Antimicrob Agents Chemother*, 50(1):210–9.
- O’Neal, R. M. and Koeppe, R. E. (1966). Precursors in vivo of glutamate, aspartate and their derivatives of rat brain. *J Neurochem*, 13(9):835–47.
- Orrego, H., Carmichael, F. J., and Israel, Y. (1988). New insights on the mechanism of the alcohol-induced increase in portal blood flow. *Can J Physiol Pharmacol*, 66(1):1–9.
- Parri, H. R. and Crunelli, V. (2001). Pacemaker calcium oscillations in thalamic astrocytes in situ. *Neuroreport*, 12(18):3897–900.
- Pasti, L., Volterra, A., Pozzan, T., and Carmignoto, G. (1997). Intracellular calcium oscillations in astrocytes: a highly plastic, bidirectional form of communication between neurons and astrocytes in situ. *J Neurosci*, 17(20):7817–30.
- Paulson, O. B. and Newman, E. A. (1987). Does the release of potassium from astrocyte endfeet regulate cerebral blood flow? *Science*, 237(4817):896–8.
- Pellerin, L. and Magistretti, P. J. (1994). Glutamate uptake into astrocytes stimulates aerobic glycolysis: a mechanism coupling neuronal activity to glucose utilization. *Proc Natl Acad Sci U S A*, 91(22):10625–9.
- Petersen, K. F., Cline, G. W., Blair, J. B., and Shulman, G. I. (1994). Substrate cycling between pyruvate and oxaloacetate in awake normal and 3,3’-5-triiodo-L-thyronine-treated rats. *Am J Physiol*, 267(2 Pt 1):E273–7.
- Petroff, O. A., Errante, L. D., Rothman, D. L., Kim, J. H., and Spencer, D. D. (2002). Glutamate-glutamine cycling in the epileptic human hippocampus. *Epilepsia*, 43(7):703–10.
- Phillis, J. W., Ren, J., and O’Regan, M. H. (2000). Transporter reversal as a mechanism of glutamate release from the ischemic rat cerebral cortex: studies with dl-threo-beta-benzyloxyaspartate. *Brain Res*, 868(1):105–12.
- Porter, J. T. and McCarthy, K. D. (1997). Astrocytic neurotransmitter receptors in situ and in vivo. *Prog Neurobiol*, 51(4):439–55.

- Reo, N. V. (2002). Nmr-based metabolomics. *Drug Chem Toxicol*, 25(4):375–82.
- Roach, M. K. and Reese, W. N., J. (1971). Effect of ethanol on glucose and amino acid metabolism in brain. *Biochem Pharmacol*, 20(10):2805–12.
- Roach, M. K. and Resse, W. N., J. (1972). (2- 14 c) ethanol as a precursor of glutamine, glutamate, -aminobutyric acid and aspartate in hamster brain in vivo. *Biochem Pharmacol*, 21(15):2013–9.
- Roberto, M., Madamba, S. G., Stouffer, D. G., Parsons, L. H., and Siggins, G. R. (2004). Increased gaba release in the central amygdala of ethanol-dependent rats. *J Neurosci*, 24(45):10159–66.
- Rudolph, J. G., Walker, D. W., Iimuro, Y., Thurman, R. G., and Crews, F. T. (1997). Nmda receptor binding in adult rat brain after several chronic ethanol treatment protocols. *Alcohol Clin Exp Res*, 21(8):1508–19.
- Sankoh, A. J., Huque, M. F., and Dubey, S. D. (1997). Some comments on frequently used multiple endpoint adjustment methods in clinical trials. *Stat Med*, 16(22):2529–42.
- Sarkola, T., Iles, M. R., Kohlenberg-Mueller, K., and Eriksson, C. J. (2002). Ethanol, acetaldehyde, acetate, and lactate levels after alcohol intake in white men and women: effect of 4-methylpyrazole. *Alcohol Clin Exp Res*, 26(2):239–45.
- Scarfe, G. B., Nicholson, J. K., Lindon, J. C., Wilson, I. D., Taylor, S., Clayton, E., and Wright, B. (2002). Identification of the urinary metabolites of 4-bromoaniline and 4-bromo-[carbonyl- ^{13}C]-acetanilide in rat. *Xenobiotica*, 32(4):325–37.
- Schmitt, G., Aderjan, R., Keller, T., and Wu, M. (1995). Ethyl glucuronide: an unusual ethanol metabolite in humans. synthesis, analytical data, and determination in serum and urine. *J Anal Toxicol*, 19(2):91–4.
- Shank, R. P., Bennett, G. S., Freytag, S. O., and Campbell, G. L. (1985). Pyruvate carboxylase: an astrocyte-specific enzyme implicated in the replenishment of amino acid neurotransmitter pools. *Brain Res*, 329(1-2):364–7.
- Shen, J., Petersen, K. F., Behar, K. L., Brown, P., Nixon, T. W., Mason, G. F., Petroff, O. A., Shulman, G. I., Shulman, R. G., and Rothman, D. L. (1999).

- Determination of the rate of the glutamate/glutamine cycle in the human brain by in vivo ^{13}C nmr. *Proc Natl Acad Sci U S A*, 96(14):8235–40.
- Sibson, N. R., Dhankhar, A., Mason, G. F., Behar, K. L., Rothman, D. L., and Shulman, R. G. (1997). In vivo ^{13}C nmr measurements of cerebral glutamine synthesis as evidence for glutamate-glutamine cycling. *Proc Natl Acad Sci U S A*, 94(6):2699–704.
- Sibson, N. R., Dhankhar, A., Mason, G. F., Rothman, D. L., Behar, K. L., and Shulman, R. G. (1998). Stoichiometric coupling of brain glucose metabolism and glutamatergic neuronal activity. *Proc Natl Acad Sci U S A*, 95(1):316–21.
- Siesjo, B. K. (1978). *Brain Energy Metabolism*. Wiley, New York.
- Simard, M. and Nedergaard, M. (2004). The neurobiology of glia in the context of water and ion homeostasis. *Neuroscience*, 129(4):877–96.
- Skipper, G. E., Weinmann, W., Thierauf, A., Schaefer, P., Wiesbeck, G., Allen, J. P., Miller, M., and Wurst, F. M. (2004). Ethyl glucuronide: a biomarker to identify alcohol use by health professionals recovering from substance use disorders. *Alcohol Alcohol*, 39(5):445–9.
- Solanky, K. S., Bailey, N. J., Holmes, E., Lindon, J. C., Davis, A. L., Mulder, T. P., Van Duynhoven, J. P., and Nicholson, J. K. (2003). Nmr-based metabonomic studies on the biochemical effects of epicatechin in the rat. *J Agric Food Chem*, 51(14):4139–45.
- Spanagel, R., Pendyala, G., Abarca, C., Zghoul, T., Sanchis-Segura, C., Magnone, M. C., Lascorz, J., Depner, M., Holzberg, D., Soyka, M., Schreiber, S., Matsuda, F., Lathrop, M., Schumann, G., and Albrecht, U. (2005). The clock gene *per2* influences the glutamatergic system and modulates alcohol consumption. *Nat Med*, 11(1):35–42.
- Srere, P. A. (1975). The enzymology of the formation and breakdown of citrate. *Adv Enzymol Relat Areas Mol Biol*, 43:57–101.
- Stern, J. R., Hegre, C. S., and Bambers, G. (1966). Glutamate biosynthesis in anaerobic bacteria. ii. stereospecificity of aconitase and citrate synthetase of *Clostridium kluyveri*. *Biochemistry*, 5(4):1119–24.

- Sumegi, B., Sherry, A. D., and Malloy, C. R. (1990). Channeling of tca cycle intermediates in cultured *saccharomyces cerevisiae*. *Biochemistry*, 29(39):9106–10.
- Sumner, L. W., Mendes, P., and Dixon, R. A. (2003). Plant metabolomics: large-scale phytochemistry in the functional genomics era. *Phytochemistry*, 62(6):817–36.
- Tang, H., Wang, Y., Nicholson, J. K., and Lindon, J. C. (2004). Use of relaxation-edited one-dimensional and two dimensional nuclear magnetic resonance spectroscopy to improve detection of small metabolites in blood plasma. *Anal Biochem*, 325(2):260–72.
- Taylor, S. I. (1999). Deconstructing type 2 diabetes. *Cell*, 97(1):9–12.
- Teague, C., Holmes, E., Maibaum, E., Nicholson, J., Tang, H., Chan, Q., Elliott, P., Stamler, J., Ueshima, H., Zhou, B., and Wilson, I. (2004). Ethyl glucoside in human urine following dietary exposure: detection by 1h nmr spectroscopy as a result of metabonomic screening of humans. *Analyst*, 129(3):259–64.
- Tian, G. F., Azmi, H., Takano, T., Xu, Q., Peng, W., Lin, J., Oberheim, N., Lou, N., Wang, X., Zielke, H. R., Kang, J., and Nedergaard, M. (2005). An astrocytic basis of epilepsy. *Nat Med*, 11(9):973–81.
- Tran-Dinh, S., Hoerter, J. A., Mateo, P., Gyppaz, F., and Herve, M. (1998). ¹³c-nmr spectroscopic evaluation of the citric acid cycle flux in conditions of high aspartate transaminase activity in glucose-perfused rat hearts. *Biochimie*, 80(12):1013–24.
- Tsai, G. and Coyle, J. T. (1998). The role of glutamatergic neurotransmission in the pathophysiology of alcoholism. *Annu Rev Med*, 49:173–84.
- Tsai, G., Gastfriend, D. R., and Coyle, J. T. (1995). The glutamatergic basis of human alcoholism. *Am J Psychiatry*, 152(3):332–40.
- Vaag, A., Henriksen, J. E., Madsbad, S., Holm, N., and Beck-Nielsen, H. (1995). Insulin secretion, insulin action, and hepatic glucose production in identical twins discordant for non-insulin-dependent diabetes mellitus. *J Clin Invest*, 95(2):690–8.
- Van den Berg, C. J., Krzalic, L., Mela, P., and Waelsch, H. (1969). Compartmentation of glutamate metabolism in brain. evidence for the existence of two different tricarboxylic acid cycles in brain. *Biochem J*, 113(2):281–90.

- Viant, M. R. (2003). Improved methods for the acquisition and interpretation of nmr metabolomic data. *Biochem Biophys Res Commun*, 310(3):943–8.
- Viant, M. R., Rosenblum, E. S., and Tjeerdema, R. S. (2003). Nmr-based metabolomics: a powerful approach for characterizing the effects of environmental stressors on organism health. *Environ Sci Technol*, 37(21):4982–9.
- Volkow, N. D., Hitzemann, R., Wolf, A. P., Logan, J., Fowler, J. S., Christman, D., Dewey, S. L., Schlyer, D., Burr, G., Vitkun, S., and et al. (1990). Acute effects of ethanol on regional brain glucose metabolism and transport. *Psychiatry Res*, 35(1):39–48.
- Volkow, N. D., Wang, G. J., Franceschi, D., Fowler, J. S., Thanos, P. P., Maynard, L., Gatley, S. J., Wong, C., Veech, R. L., Kunos, G., and Kai Li, T. (2006). Low doses of alcohol substantially decrease glucose metabolism in the human brain. *Neuroimage*, 29(1):295–301.
- Volterra, A. and Meldolesi, J. (2005). Astrocytes, from brain glue to communication elements: the revolution continues. *Nat Rev Neurosci*, 6(8):626–40.
- Waniewski, R. A. and Martin, D. L. (1998). Preferential utilization of acetate by astrocytes is attributable to transport. *J Neurosci*, 18(14):5225–33.
- Waters, N. J., Waterfield, C. J., Farrant, R. D., Holmes, E., and Nicholson, J. K. (2005). Metabonomic deconvolution of embedded toxicity: application to thioacetamide hepato- and nephrotoxicity. *Chem Res Toxicol*, 18(4):639–54.
- Weinmann, W., Schaefer, P., Thierauf, A., Schreiber, A., and Wurst, F. M. (2004). Confirmatory analysis of ethylglucuronide in urine by liquid-chromatography/electrospray ionization/tandem mass spectrometry according to forensic guidelines. *J Am Soc Mass Spectrom*, 15(2):188–93.
- Westergaard, N., Sonnewald, U., and Schousboe, A. (1995). Metabolic trafficking between neurons and astrocytes: the glutamate/glutamine cycle revisited. *Dev Neurosci*, 17(4):203–11.
- Williamson, J. R., Scholz, R., Browning, E. T., Thurman, R. G., and Fukami, M. H. (1969). Metabolic effects of ethanol in perfused rat liver. *J Biol Chem*, 244(18):5044–54.

- Wurst, F. M., Kempter, C., Metzger, J., Seidl, S., and Alt, A. (2000). Ethyl glucuronide: a marker of recent alcohol consumption with clinical and forensic implications. *Alcohol*, 20(2):111–6.
- Wurst, F. M., Schuttler, R., Kempter, C., Seidl, S., Gilg, T., Jachau, K., and Alt, A. (1999). Can ethyl glucuronide be determined in post-mortem body fluids and tissues? *Alcohol Alcohol*, 34(2):262–3.
- Wurst, F. M., Seidl, S., Ladewig, D., Muller-Spahn, F., and Alt, A. (2002). Ethyl glucuronide: on the time course of excretion in urine during detoxification. *Addict Biol*, 7(4):427–34.
- Wurst, F. M., Skipper, G. E., and Weinmann, W. (2003). Ethyl glucuronide—the direct ethanol metabolite on the threshold from science to routine use. *Addiction*, 98 Suppl 2:51–61.
- Wurst, F. M., Wiesbeck, G. A., Metzger, J. W., and Weinmann, W. (2004). On sensitivity, specificity, and the influence of various parameters on ethyl glucuronide levels in urine—results from the who/isbra study. *Alcohol Clin Exp Res*, 28(8):1220–8.
- Yamamoto, T., Moriwaki, Y., and Takahashi, S. (2005). Effect of ethanol on metabolism of purine bases (hypoxanthine, xanthine, and uric acid). *Clin Chim Acta*, 356(1-2):35–57.
- Yu, A. C., Drejer, J., Hertz, L., and Schousboe, A. (1983). Pyruvate carboxylase activity in primary cultures of astrocytes and neurons. *J Neurochem*, 41(5):1484–7.
- Yuferov, V., Bart, G., and Kreek, M. J. (2005). Clock reset for alcoholism. *Nat Med*, 11(1):23–4.
- Zimmer, H., Schmitt, G., and Aderjan, R. (2002). Preliminary immunochemical test for the determination of ethyl glucuronide in serum and urine: comparison of screening method results with gas chromatography-mass spectrometry. *J Anal Toxicol*, 26(1):11–6.
- Zwingmann, C. and Leibfritz, D. (2003). Regulation of glial metabolism studied by ¹³c-nmr. *NMR Biomed*, 16(6-7):370–99.